

THE USE OF GEOLOGICAL METHODS FOR THE CHARACTERIZATION OF
ROMAN METALLURGICAL SLAG FROM THE EXCAVATIONS OF THE
YASMINA CEMETERY IN CARTHAGE, TUNISIA

by

NICHOLE MARON LYLE

(Under the direction of Samuel E. Swanson)

ABSTRACT

The fill material excavated from the Yasmina Cemetery in Carthage is comprised of a significant amount of metallurgical slag, but there have been no studies conducted on the slag to determine its chemical and mineralogical character or its relevance to Roman Carthaginian metallurgy. In order to do so, the slag was sampled from storage at the Museum of Carthage to assess the amount and types of metallurgical slag excavated from the site and to select representative samples for return to the University of Georgia Geology Department for petrographic and electron microprobe analyses. Based on the initial characterization, the slags indicate the presence of a small scale metals workshop skilled in a variety of metallurgical techniques consistent with those found elsewhere in the Roman Empire between the 2nd and 7th centuries AD, including the smelting and smithing of iron and copper and the use of lead in secondary metal refining processes.

INDEX WORDS: Metallurgical slag, Carthage, Roman, Iron, Copper, Lead,
Yasmina Cemetery

THE USE OF GEOLOGICAL METHODS FOR THE CHARACTERIZATION OF
ROMAN METALLURGICAL SLAG FROM THE EXCAVATIONS OF THE
YASMINA CEMETERY IN CARTHAGE, TUNISIA

by

NICHOLE MARON LYLE

A.B., The University of Georgia, 1998

A Thesis Submitted to the Graduate Faculty of The University of Georgia in Partial
Fulfillment of the Requirements for the Degree

MASTER OF SCIENCE

ATHENS, GEORGIA

2002

© 2002

Nichole Maron Lyle

All Rights Reserved.

THE USE OF GEOLOGICAL METHODS FOR THE CHARACTERIZATION OF
ROMAN METALLURGICAL SLAG FROM THE EXCAVATIONS OF THE
YASMINA CEMETERY IN CARTHAGE, TUNISIA

by

NICHOLE MARON LYLE

Approved:

Major Professor: Samuel E. Swanson

Committee: Ervan Garrison
Naomi J. Norman
David B. Wenner

Electronic Version Approved:

Gordhan L. Patel
Dean of the Graduate School
The University of Georgia
August 2002

DEDICATION

This thesis is dedicated to my family, who has always encouraged me to be better than I thought I was capable, and to David Tardif, whose memory reminds me to be thankful for every day I have to experience life.

ACKNOWLEDGEMENTS

I would first like to thank Sam – I could not have made it here without you. Thank you for your willingness to take an anthropology student and design a project out of your field of expertise; it is inspiring to know that professors are willing to take a chance and learn along with their students – you have certainly made me a life-long learner!!!! Thank you for all the many hours of slag discussions and probe time and for teaching me all I know about slag chemistry. I hope one day to work with you again on metallurgical slags!

Thank you to my committee for your support and advice and for making my defense such a pleasant experience. I have enjoyed working with each of you! I am especially thankful to Naomi for suggesting the project and the opportunity to travel to Tunisia – it was one of the greatest experiences of my life.

I would also like to thank the following people for their contributions to the completion of this thesis: Dr. Ennabali of the Museum of Carthage for allowing me to remove my samples for study, Dr. Mark Farmer for providing photographic equipment and expertise, Chris Fleischer for help and advice with the electron microprobe – I would have been completely lost without your help!, and Colleen Stapleton – without your encouragement and assistance I would not have ever completed this project – I hope to work with you again in the future!!!!

Finally, and most importantly, I would like to thank Joe for all of his support – I certainly would not have been able to finish this without you! I am so grateful to have you in my life and I am looking forward to spending the rest of my life with you!

TABLE OF CONTENTS

	Page
ACKNOWLEDGEMENTS	v
CHAPTER	
1 INTRODUCTION	1
2 THE ROMAN IRON AGE	4
Iron Metallurgy	4
Copper/Bronze Metallurgy	14
Lead/Silver Metallurgy	16
3 ROMAN CARTHAGE	21
Historical Summary	21
City Plan.....	32
4 CREATING A CLEARER PICTURE OF CARTHAGINIAN METALLURGY	40
Site Description.....	41
Field Sampling Methodology	46
Slag Mineralogy and Petrology	63
5 CONCLUSIONS AND RECOMMENDATIONS	134
REFERENCES	143
APPENDICES	148

CHAPTER 1

INTRODUCTION

Archaeological excavation of the Roman Yasmina cemetery in Carthage, Tunisia produced a wide variety of artifacts from the site's fill material, in addition to several major funerary monuments and statues. These excavations were conducted by the University of Georgia Classics Department, under the direction of Dr. Naomi J. Norman, who took an interest not only in the major features of the site, but also the numerous artifacts that comprised the fill. The fill is interpreted as the result of several backfilling events that the Romans periodically performed to level the cemetery ground for another stage of use.

In this fill material, field archaeologists identified "slags" as part of the artifact assemblage and stored these artifacts together in the Museum of Carthage, located in the modern suburb of Carthage, Tunisia. Over the course of five excavation seasons, 15 crates of slag were accumulated, along with hundreds of other crates of artifacts categorized and stored from the fill sediments. As the excavations at Yasmina came to a close in 1997, focus turned toward the analysis and interpretation of the excavated artifact assemblages.

In order to better interpret the archaeology of the Yasmina cemetery, as well as that of Roman Carthage as a whole, a basic characterization of the various artifact assemblages was necessary. The metallurgical slags, in particular, were a mystery, as very little work in Carthage has been done on metallurgical slags. It is in an effort to

characterize the metallurgical slags from the Yasmina cemetery and to produce some preliminary interpretation of the metallurgical processes they represent, that this thesis is written.

Metallurgical slags are essentially the by-products of the smelting or smithing processes used to produce metals. That is, as a metallic ore is heated and reduced in a furnace, the ore gangue, fluxes, and furnace linings become molten and form a slag. The formation of a slag is an essential step in the smelting process as it serves as a vehicle for the removal of impurities from the metal. Typically, slags are periodically removed from the furnace by a process called “tapping” in which the molten slag is poured or allowed to run out of the furnace and onto the ground. Slags are generally composed primarily of silicate mineral phases, with other compounds, such as oxides and metals, more often present than absent (Bachmann, 1982). Metallurgical slags, although they are essentially waste products, were very closely monitored by ancient, and modern, metallurgists because they serve as indicators of the activity within the furnace and the efficiency of the process.

For the archaeometallurgist, slags are particularly useful remnants of the metallurgical process(es) in question. Slags are typically abundant in the archaeological record at metallurgical sites, as they are resistant to weathering and were generally considered waste material and therefore not generally removed from the site (Craddock, 1995). Utilizing a variety of analytical techniques on slags, information such as the reducing conditions of the furnace, the chemistry of the metallurgical process, the metal smelted, and the efficiency of the separation of the metal from its gangue, can be estimated (Craddock, 1995). Many of these techniques, such as Atomic Absorption

Spectroscopy (AAS), X-Ray Diffraction (XRD), and micro-analytical spectroscopy (includes the electron microprobe), are familiar instruments to the geologist and geoarchaeologist. These techniques, in combination with the basic field identification and characterization, can provide a great deal of information about archaeometallurgical slags.

For the purposes of this thesis, characterization of the slags was done in several stages. First, the slags were preliminarily characterized in the field using common geological techniques for petrographic and mineral identification. Then, representative samples were selected for micro-analysis using both transmitted and reflected light microscopy and an electron microprobe. These micro-analytical techniques provide qualitative and quantitative data about the phase assemblages in the slags. From this data, the slags can be characterized mineralogically and petrographically. The quantitative data, in particular, is used to determine details of the metallurgical processes represented by the slags, including the metals processed and process temperatures and chemistries. Based on hand sample and petrographic/mineralogical characterization of the Yasmina slags, preliminary interpretations can be made about the metal processing in Roman Carthage.

CHAPTER TWO

THE ROMAN IRON AGE

The metallurgical slag recovered from the Roman Yasmina Cemetery in Carthage, Tunisia is from fill layers that have been closely dated on the basis of numanistic and ceramic evidence. The slag was excavated from these fill layers, dated between the 2nd and 6th centuries AD (Norman and Haeckl, 1992), placing these slags firmly within the Roman Iron Age. Therefore, interpretations made about the slags from this site must take into account the technological sophistication and organization of Roman metallurgy during this time. The metals of the Roman Iron Age most relevant to these interpretations, specifically iron, copper/bronze, and lead/silver metallurgy, are each discussed in this section.

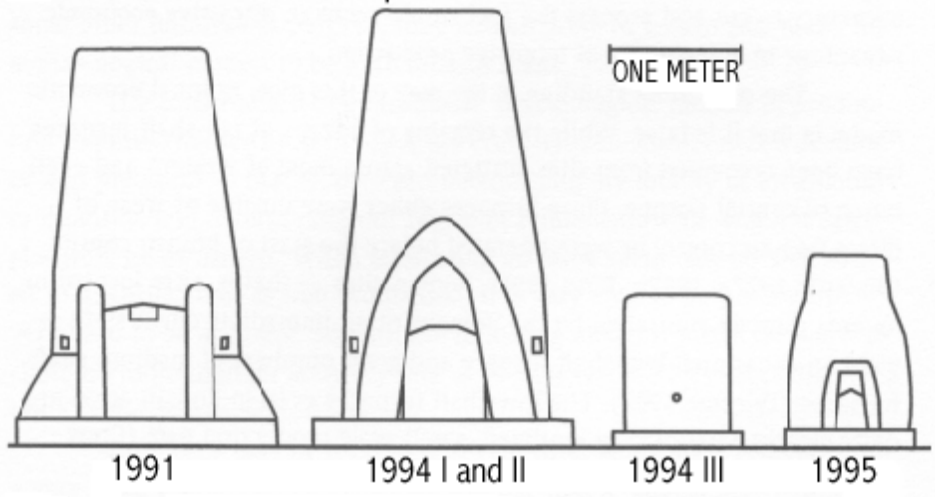
Iron Metallurgy

The iron smelting technology utilized by the Romans was the bloomery process, which produced a nearly pure form of metallic iron (wrought iron) in a furnace by the solid-state reduction of an iron ore (Blair, 1999). The Romans utilized a wide variety of iron ores, but generally preferred limonitic and carbonate ores, which required the minimum amount of heat and reductant for successful smelting (Cleere, 1976). In many cases, ores were roasted before smelting to reduce the stress on the furnace (Cleere, 1976); roasting removed the water and/or sulfides from the ores and made them more friable. Whatever the ore, the smelting process was designed to reduce the iron oxide to metal by the removal of the oxygen (Blair, 1999). In order to facilitate this reduction,

charcoal was used to heat the furnaces and silicate fluxes were added to promote slag formation to remove impurities from the forming metal. The product was not metallic iron, however, but a bloom of metallic iron in physical association with slag, a largely silicate waste product (Blair, 1999). This mix of iron, slag, and other impurities, such as charcoal, partially reduced ore, and cinder, made up the bloom. As the bloom formed in the furnace, the bulk of the liquid slag was tapped off and allowed to collect outside the furnace. The slag that remained as part of the bloom bound the metallic iron together and prevented reoxidation from the blast entering the furnace (Blair, 1999). At the end of the smelt, the cooled bloom was removed and then worked (forged) to separate the metallic iron from the rest of the bloom constituents.

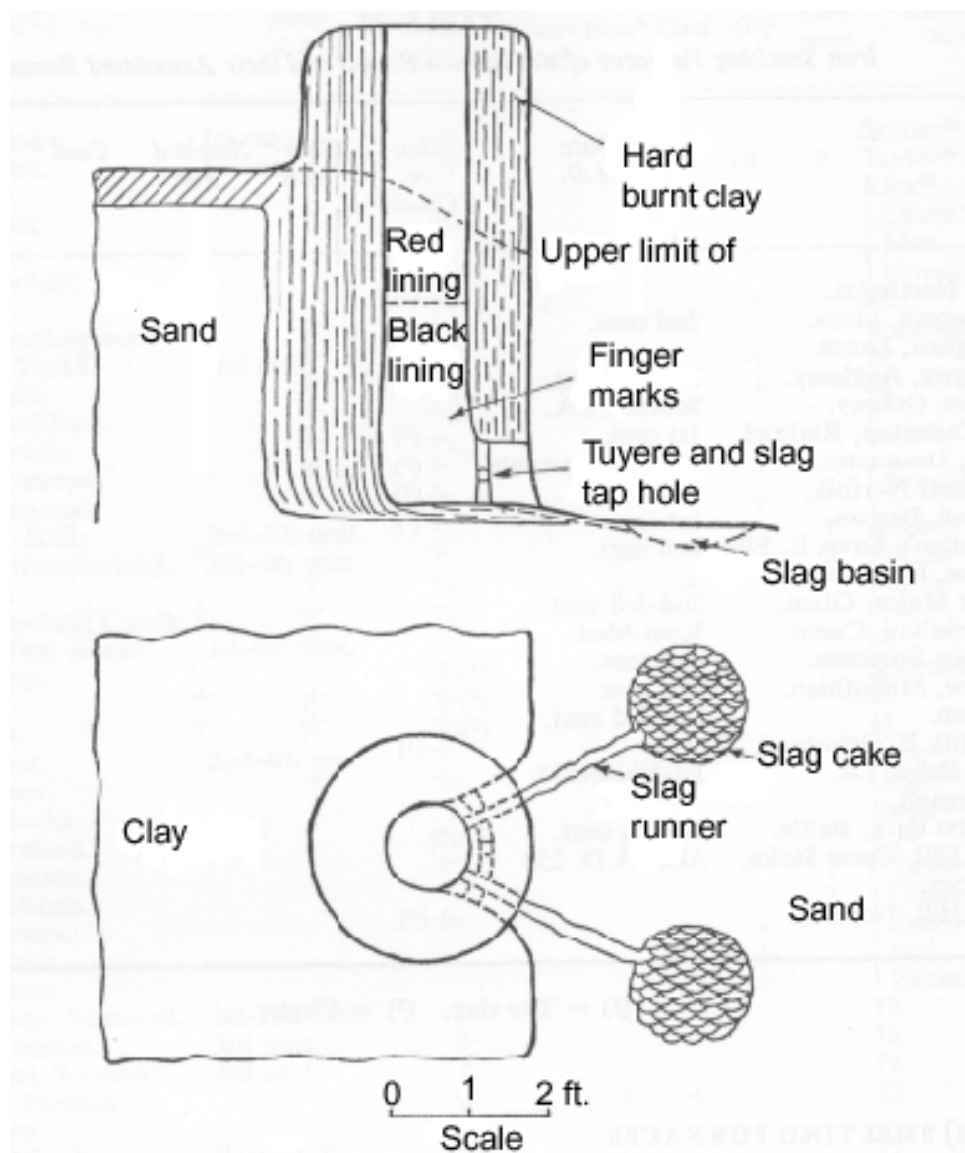
There were hundreds of local varieties of the three main furnaces types Romans used for bloomery iron production, namely, the tall, medium, and low shaft furnaces (Blair, 1999). Figure 2.1 shows Blair's depiction of four shaft furnaces of varying sizes built as part of the SMELT project and designed based on Roman archaeological evidence (Blair, 1999). Tylecote also depicts a Roman shaft furnace based on a reconstruction of a second century CE furnace excavated at Ashwicken, Norfolk (Tylecote, 1962) (Figure 2.2). All furnaces were top-charging (Blair, 1999), that is, the charcoal, iron ore and fluxes were added through the top of the furnace. Furnaces walls were generally made of thick, unfired sand and clay mixtures and the air blasts to heat the systems were provided by human-powered bellows and in some cases, natural convection (Blair, 1999). Although experimental evidence demonstrates that the tall shaft furnace would have been the most efficient means of smelting iron, archaeological evidence indicates that medium-shaft furnaces were the most widely used (Blair, 1999). At large

The SMELT furnaces in profile.



The four SMELT furnaces in profile. Although they are fundamentally quite similar in design, their differences in size may be clearly seen.

Figure 2.1
(after Blair, 1999)



Reconstruction of Roman shaft furnace found at Ashwicken, Norfolk. (2nd century AD). courtesy of Norfolk Archaeology.

Figure 2.2
(after Tylecote, 1962)

production centers, tall-shaft furnaces would have been preferred, for the abundant local smelters throughout the empire, low and medium shaft furnaces would have been easier to operate and more suitable for local iron production (Blair, 1999). Once the iron bloom was obtained, it was often transported from the production site, often near the mines from which the ore came, to a Roman workshop located nearer to settlements for smithing (Tylecote, 1976).

Smithing, or working, the iron bloom is the second crucial step in the production of useable iron metal. Roman smiths worked the wrought iron from the blooms to produce irons with different properties. Quench hardening and carburization were more widely used in the Roman Iron Age than before, to produce irons that were harder than the wrought iron that came from the bloom (Tylecote, 1976). Depending on the desired product, varying amounts of carbon were added; for cast iron, the carbon content was increased to between two and five percent, creating a brittle iron, but one appropriate for casting (Craddock, 1995). The smiths of the Roman Iron Age made it possible for iron to be used for virtually every purpose that we use iron today (Healy, 1978).

The Romans, while they cannot be credited with the invention of many new techniques for metal smelting, were certainly the first to produce, import and consume iron in large quantities (Blair, 1999). They achieved this distinction primarily through their ability to industrialize metal production, especially that of iron, on a scale never before imagined. Tylecote notes that “the main contribution of the Roman Empire to world technology was not one of originality but one of organization” (Tylecote, 1976). It is not until the Roman Iron Age that the archaeological record in Europe and the Mediterranean reveals enormous slag heaps and extensive mining and production centers

associated with metallurgy. While metals from earlier ages, like copper, bronze, gold, silver and lead, were still important economic metals, as the Roman Empire expanded iron became the preferred metal for tools, weapons, and all types of other practical implements.

There is no consensus among archaeometallurgists as to precisely where or how iron metallurgical technology began, but its spread seems to have been generally from Anatolia to Asia to Greece and the Aegean and then into the rest of Europe (Wilson, 1994). Forbes suggested that iron metallurgy reached Italy by around 1100 BCE from the Hittite culture of the Armenian region in eastern Europe (Forbes, 1955). The bloomery process, to extract iron from its ores, was already established, and it was the wrought iron from this process that Romans eventually became so proficient at producing (Tylecote, 1976). For another 100 years or so, bronze remained the dominant metal produced in Italy, but by 900 BCE, the Villanovan civilization, which appears in early levels at Rome, began producing abundant iron for use in making agricultural implements. Rome was founded in 753 BCE and by around 510 BCE, iron production in the region had become industrial in scale (Forbes, 1955). Iron mines were centered on the island of Elba and between Rome and Capua at Ertruria, where the iron was smelted into blooms (Snodgrass, 1980). Then, the blooms were shipped to Puteoli, where there was abundant wood, for smithing into military weaponry and agricultural tools. From Puteoli, a port city, these items were shipped to wherever they were needed. In some cases, the entire bloom was shipped for working by hired smiths commissioned to produce whatever the owner requested. Over time, the whole smelting industry moved nearer the mines and blooms or ingots were exported from there to trade centers

throughout the growing empire (Forbes, 1955). The size of the bloom varied from the more common 5 or 6 kg spindle-shaped currency bars to 10 kg blooms (Tylecote, 1976). Blooms supplied to Roman workshops and prepared by locals were likely smaller than the standard currency bars. This method of creating the bloom and then trading it continued throughout the Roman Iron Age.

The Roman Empire was virtually self-sufficient in terms of metal production. As their territory expanded, the Romans acquired more iron mines, particularly the high grade bog and limestone ores of Britain, as well as numerous other copper, tin, lead, gold, and silver ore bodies scattered throughout Europe and the Mediterranean basin. The largest of these deposits were state organized, but iron was still produced locally in many forest regions where abundant wood and ores were available (Forbes, 1955). Mines that the Romans found to be particularly lucrative were confiscated by the emperor and turned over to management by imperial lessees (Forbes, 1955). The locally produced iron blooms were often welded together and traded to the military, each outpost of which had a permanent smithy (Forbes, 1955). Slags from these operations are often found in Roman forts in England and in Roman villas, where ordinary tools were manufactured or repaired (Forbes, 1955). Forges have even been found in Rome itself, beneath the floor of a church, evidence that smithing was indeed a common skill among the populace of the Roman empire (Forbes, 1955).

The early empire had guilds of iron workers, *fabri* (Forbes, 1955), but slave labor became increasingly important to Rome's iron output, as the work was certainly difficult and required many unskilled workers to assist the several skilled smiths needed to oversee the operations (Blair, 1999). In general, the smithing of iron was divided

between two camps: the individual smiths who owned shops or worked in villas to accommodate the needs of the private sector, and the large firms which produced articles in large and consistent amounts. For example, in Capua, iron utensils were made in small shops by iron workers specializing in that particular tool, alongside other specialists smithing helmets, shields, swords, knives, locks, and nails (Forbes, 1955). In contrast, there is evidence from the time of Diocletian (245-313 CE) that all arms for the imperial forces were made in their own workshops, some of which specialized in swords or spearheads and others in more general military items (Tylecote, 1976). Large firms, like those of the military, reached levels of efficiency that were never before seen, and it is this efficiency with which the Roman Iron Age is credited. Enormous hoards of nails, nearly 900,000 of them in a single hoard, have been found in Scotland at a fort built in 83 CE (Tylecote, 1976).

Romans understood the differences between steels and showed preferences for iron produced in certain regions for certain items. Rome exploited Spanish iron, for example, for arms and cutlery and there are records of societies, officials, and private individuals who were connected with the extraction, manufacture, distribution of that iron (Forbes, 1955). Rome also imported iron from outside the empire (Forbes, 1955). Roman smiths also demonstrated their preference for the particular parts of an ore body that were to be exploited. At Noricum, the Romans preferred to use the yellow and white ores over the spathic (high manganese) iron ores that had been the focus of earlier iron workings. It turns out that non-spathic ores contained titanium, which imparts an excellent quality to steel: hardness. At another site in the Hallstatt region, native smelting furnaces reveal the working of spathic iron ores, with characteristic high manganese

content, while the slags from the Roman settlements there show they were smelting hematite, with low manganese and high lime and magnesium contents (Forbes, 1955).

Rome exploited the mineral resources in every area of its empire. East and Central Europe and Britain provide much of the archaeological information about the Roman Iron Age (Tylecote, 1976), for it is there that the famous iron ores of the Forest of Dean and the Weald are found. Roman Gaul has evidence of enormous masses of iron metallurgical slags, some of which date to the pre-Roman Iron Age. Tylecote also asserts that, “Undoubtedly, North African deposits were exploited, and recent work at Sbeitla in Tunisia has shown that local iron was being worked between the 2nd and the 6th centuries CE” (Tylecote, 1976). Iron continued to be exploited in Elba and Tuscany, near Rome, and ore deposits in Macedonia and modern Turkey were mined by the Romans as well. Another good source of iron ore was near Rudki in the Holy Cross Mountains of Poland, where there is no doubt that ironworking was very active during the Roman period (Tylecote, 1976).

As noted earlier, the qualities of the iron the Romans produced did not vary greatly from other bloomery irons produced before them. In general, the blooms the Roman Iron Age produced are no less heterogeneous than those of the Early Iron Age, especially with respect to the carbon content which can vary according to where the bloom was located relative to the tuyere during the reheating process (Tylecote, 1976). Additionally, iron tools from Roman Iron Age sites in Poland reveal that a varied technology was used in their production; some knives and chisels show evidence of having been quench-hardened, while others show no sign of quenching (Tylecote, 1976). So, it seems that just as Romans mined Early Iron Age sites for iron ores, they also

continued to use Early Iron Age technologies with an increasing number of smiths capable of carburizing and quenching to obtain high quality tools (Tylecote, 1976).

Some Roman iron does contain significantly less phosphorous than earlier iron, suggesting that the Romans knew low-phosphorous iron was easier to carburize, however, there are plenty of examples of high-phosphorous iron in the Roman period as well (Tylecote, 1976). Most of the iron used by the Romans was of low carbon content and therefore never carburized, but the techniques of quench-hardening and carburizing were more widely used than ever before. For implements, like the chisels found on two British sites, Wall and Chesterholm, there is clear evidence of the edges being successfully hardened using heat treatments (Tylecote, 1976).

Roman swords, the principal weapon of the legions, tend to show the best Roman craftsmanship. Pattern welding, which is the welding together of strips, rods, or wires to make a weapon of complex structure, was the “hallmark” of Roman Iron Age swords and first appears in the Rhineland and at Nydam in Schleswig-Holstein early in the third century CE (Tylecote, 1976). The wires are welded together and heated and forged and usually welded onto a “core” of iron, although there are many variations on this process. It is not clear that this technique increased the strength of the weapon any more than piling did, but it is evidence of the craftsmanship involved. The use of techniques like pattern welding demonstrate the Roman mastery of the more traditional smithing techniques.

Romans used iron for virtually as many products as we do today. Indeed, the Romans knew all the types of hand tools in existence today, with the possible exception of the wood screw (Tylecote, 1976). Metallurgical production during the Roman Iron

Age was controlled by the economy of the empire and the needs of its citizens. The demand for iron came from both the civilian and military sections of society, creating the expansive iron industry for which the Roman Iron Age is famous.

Despite the Roman preference for iron for implements and tools, there was still a demand for other metals and thus a reliance on earlier metals technologies to produce them. Romans, just as we do today, valued gold, silver, copper, and lead for a variety of purposes, though after the introduction of iron, their uses changed dramatically. Various alloys of these metals were important economically, as well as aesthetically for the Romans. Bronze, for example, once the preferred alloy for weaponry was replaced in that regard by iron, but was still popular for artistic vases, tableware, and coinage (Healy, 1978). Romans continued producing metals other than iron, and the metallurgy of some of those metals, in particular copper/bronze and lead/silver because of their occurrence at the Yasmina site, will be addressed briefly here.

Copper/Bronze Metallurgy

Copper smelting is generally a simpler process than that of iron. From the primary smelt, the metallurgist obtains a workable metal, without the necessity of smithing. Roman copper metallurgy relied on the same processes developed over the centuries, which involved the smelting of a copper ore in a reducing furnace with the production of a slag to remove the impurities (Craddock, 1995). Either oxidic or sulphidic copper ores were exploited, the latter requiring preliminary roasting to remove the sulphur before smelting began. The temperatures and reducing conditions necessary for smelting copper were less rigorous than those for iron production. There is abundant evidence throughout the Roman empire, particularly in Britain and northern Europe, for

the Roman extraction and smelting of copper ores (Healy, 1978). In general, copper ores were smelted at the mine site and in some cases were alloyed there as well (Tylecote, 1978). Copper was in greatest demand for its use in coinage, but was also used widely in general construction and adornment (Healy, 1978). Copper was exploited primarily in Spain, but it was during the Roman Iron Age that copper deposits were re-opened in the Palestinian Arabah (Negev) after a nearly 1000 year lapse (Tylecote, 1976). Romans, however, rarely made pure copper; they preferred to alloy it with a wide variety of other metals. Not only did they produce large amounts of bronze and brass, the Romans also made ternary alloys of copper, zinc, lead, and tin for casting (Tylecote, 1976).

Alloying metals was the job of the metal smith and occurred in one of several ways, depending on the alloy desired and the ore types available. One method was that of smelting an ore already containing more than one metal, as in the case of smelting auriferous ores which contain silver, to produce “white gold” (Healy, 1978). Another was the smelting of two different metallic ores simultaneously, a process often used to create bronzes of variable quality (Healy, 1978). Still another was the mixing of pure metal with an ore, as is the case with brass; zinc melts at 419°C and thus would vaporize if placed in a furnace hot enough to melt copper at 1083°C. Therefore calamine, zinc carbonate/silicate, was used instead to alloy zinc and copper into brass. Alloying metals imparted qualities, such as hardness and strength that the Romans found more desirable than many pure metals.

The importance of bronze, the alloy of copper and tin, in the Roman world is best indicated by its wide variety of uses (Cleere, 1976). From everyday items like pots and pans to figurines and statuary, bronze is ubiquitous throughout the Roman era. All

bronzes were not, however, the same. Varying amounts of tin, up to 13% increased the hardness of copper to suit various purposes (Cleere, 1976). For bronze that was intended to be cast, lead was often added as well to lower the melting point of the bronze and increase its ability to flow easily into moulds (Cleere, 1976). The Romans obtained tin primarily from ores in southern Spain and Britain (Healy, 1978). Lead came from Spain as well as Britain throughout the Roman Iron Age (Healy, 1978).

Brass was an alloy that had little widespread use until the Romans introduced it on a large scale, principally for coinage, around 45 BCE (Tylecote, 1976). Tin was costly and scarce, but zinc was widely available and brass, an alloy of copper and zinc, would have certainly been an appealing option for the Romans. For the first time, true brasses were made with the only intentional alloying element being up to 20-30% zinc. (Zinc is present in earlier bronzes in trace amounts suggesting that its presence was due to the mineral composition of the ore, rather than it having been added on purpose). Brass was used primarily for coinage, while another copper-zinc-tin alloy, gunmetal, was preferred for most other uses since it was easier to cast than bronze (Tylecote, 1976). Brass was produced in a crucible by adding calamine, $ZnCO_3$, to copper under reducing conditions. The zinc was obtained from ores in Britain, Belgium, and the East (Healy, 1978).

Lead/Silver Metallurgy

While the Greek production of lead was by and large a by-product of their silver production, the Romans greatly increased the exploitation of lead ores, simply to produce lead (Tylecote, 1976). Lead is a particularly easy metal to smelt since its ores are abundant, it is easy to beneficiate, and it only requires moderate reduction to liberate lead

metal from the ore (Craddock, 1995). Galena is by far the most common lead ore, and was widely utilized by the Romans for both the lead and the silver it contained. Lead furnaces, called boles, were large, open furnaces that allowed the molten lead to collect at the bottom and produced a very pure lead, because the temperatures and reducing conditions were such that other metal phases, present as impurities in the ores, were not reduced (Craddock, 1995). Lead was particularly important for the manufacture of plumbing (Tylecote, 1976) which Romans used extensively in their elaborate bath-houses and fountains.

Lead smelting was a dangerous enterprise due to the toxicity of the fumes, and so often the smelter was located outside urban areas and the bellows operators were separated from the furnace by a wall (Craddock, 1995). As with copper/bronze and iron, lead was smelted at the mine sites into a transportable form, in this case 'pigs,' and then shipped throughout the empire for remelting and working into the desired form (Nriagu, 1983). Romans obtained lead from ores in Spain, Italy, Sardinia, Sicily, and Britain (Healy, 1978).

Although lead itself was an important metal to the Romans, the common association of lead with silver, was also an important reason the Romans exploited so many lead ores. Silver occurs very commonly in galena in amounts economic for Romans to extract for use in coinage, jewelry, and silverware (Sherlock, 1976). Romans not only smelted silver out of lead ores, but out of previously smelted lead ingots and even out of other smelted metals which contained silver, such as copper, using a variety of different techniques (Craddock, 1995).

From lead ores, such as galena, silver was obtained by smelting the lead at much higher temperatures and more reducing conditions than was typical when just the lead was the metal sought (Craddock, 1995). This more rigorous smelting insured that all the silver present in the ore would be absorbed by the lead. After the lead was collected from the smelting furnace, the silver was extracted by a process called cupellation, during which the lead metal is heated to roughly 1000° C in an open crucible while a stream of air is blown over its surface, oxidizing the lead to litharge, PbO. The silver, which is not oxidized, collects at the bottom of the crucible. The other metallic impurities, such as zinc, that might have been present in the lead, are oxidized along with the lead, leaving a pure silver behind (Craddock, 1995). Cupellation occurred in a variety of receptacles, called cupels, but were generally lined with bone ash, chosen for its ability to combine with silica in the cupels and melt to produce a glass; this glass absorbs lead, keeping it in the cupel for recovery.

The Romans did not just exploit galena as a source of silver. Rio Tinto, in southern Spain, is famous for its jarosite ores that the Romans used extensively for silver production (Craddock, 1995). Indeed, the Punic Carthaginians, who occupied Rio Tinto area prior to the Roman occupation, mined these same ores for their silver (Craddock, 1995). These ores did not provide the requisite lead for removing silver from the ore, so imported lead was added to the jarosite ores during smelting and removed the silver (Craddock, 1995). The smelting process comprises several stages, which involve the additions of various fluxes and removal of slags, indicating not only the technological sophistication of the Roman metallurgists, but also the importance of silver as a metal for the Roman empire. The Rio Tinto ores caused additional difficulties because the arsenic

and antimony present in the ores, formed a speiss, a dense silvery mixture of arsenides and antimonides (Craddock, 1989), which absorbed the silver. The Romans, however, were able to overcome this, apparently using lead, as litharge was found there in large quantities associated with the speiss and other slag products (Craddock, 1995). Once the silver was isolated in the lead, cupellation was repeated until all the silver was removed (Craddock, 1995).

A final method used by the Romans to recover silver involves the recycling of other metals, specifically copper and copper mattes (Craddock, 1995). During initial copper smelting, silver and other elements present in the ore, like arsenic and antimony, collect as impurities in the copper metal. Silver, being highly valued by the Romans (Wilson, 1994), utilized a melting technique to remove it. The process is called liquation and silver is removed from the metal by mixing the molten copper with lead. Lead, which is immiscible with copper, will infiltrate the copper and remove the silver from it. As the mixture cools, the lead with the silver in it sinks to the crucible bottom and the copper floats on top. The lead is then separated and cupelled to remove the silver (Craddock, 1989). At Roman Corinth, in the third century CE, liquation debris apparently from the separation of silver from base alloys, is believed to be the result of recycling debased coinage for its silver (Craddock, 1995). The variety of methods the Romans used for the acquisition of silver clearly suggests its value in Roman society.

Roman Iron Age metallurgy, while historically significant primarily for its expansion and organization of iron production, is also significant metallurgically for the variety of metals exploited and the various techniques utilized to achieve those ends. While smelting centers generally remained near the ore sources, the smithing and refining

of metals occurred nearly everywhere there were concentrations of people, indicating the widespread knowledge of metallurgy at the time. Indeed, a wide variety of metals were often worked at the same site (Salter and Northover, 1992) – the Roman metal smith was apparently well-versed in a wide variety of techniques. The scope of metallurgical production and the commonality of its remains in archaeological contexts throughout the Roman Iron Age provide a means by which to interpret the metallurgical slags from the Yasmina Cemetery and enhance the understanding of Carthaginian metallurgy in terms of the greater Roman empire.

CHAPTER THREE
ROMAN CARTHAGE
Historical Summary

In order to make meaningful and relevant interpretations of archaeological materials, it is necessary first to understand something of the history of the site from which the material came. The Yasmina necropolis, used for roughly five centuries by the inhabitants of Carthage, certainly played a significant role in the city's history; it is in an effort to interpret the material from this cemetery, particularly that of the metallurgical slag, that the following description of Punic and Roman Carthage is written.

The city of Carthage lies in central North Africa, in modern Tunisia, on the Mediterranean coast (See Figure 3.1, after Soren, et al., 1990). Carthage is a port city, situated on the calm Gulf of Tunis, protected by the Cape Bon peninsula to the east. Although the majority of north Africa is technically desert, the land along the coast is strongly influenced by the Mediterranean Sea. Stratigraphic evidence from archaeological excavations at the Late Punic port of Carthage indicates the coastal area was successively dry land, submerged land in lagoonal conditions, a marsh, and finally dry land again (Hurst & Stager, 1978). Vegetation records from the Sergermes Valley, located approximately 100 km south of Carthage, indicate that during Roman times the landscape in northern Africa was generally poor in trees and dominated by shrubs, grasses, and herbs. Only moderate vegetation changes have taken place in coastal north Africa from the pre-Roman period to the present, with most of these changes attributable

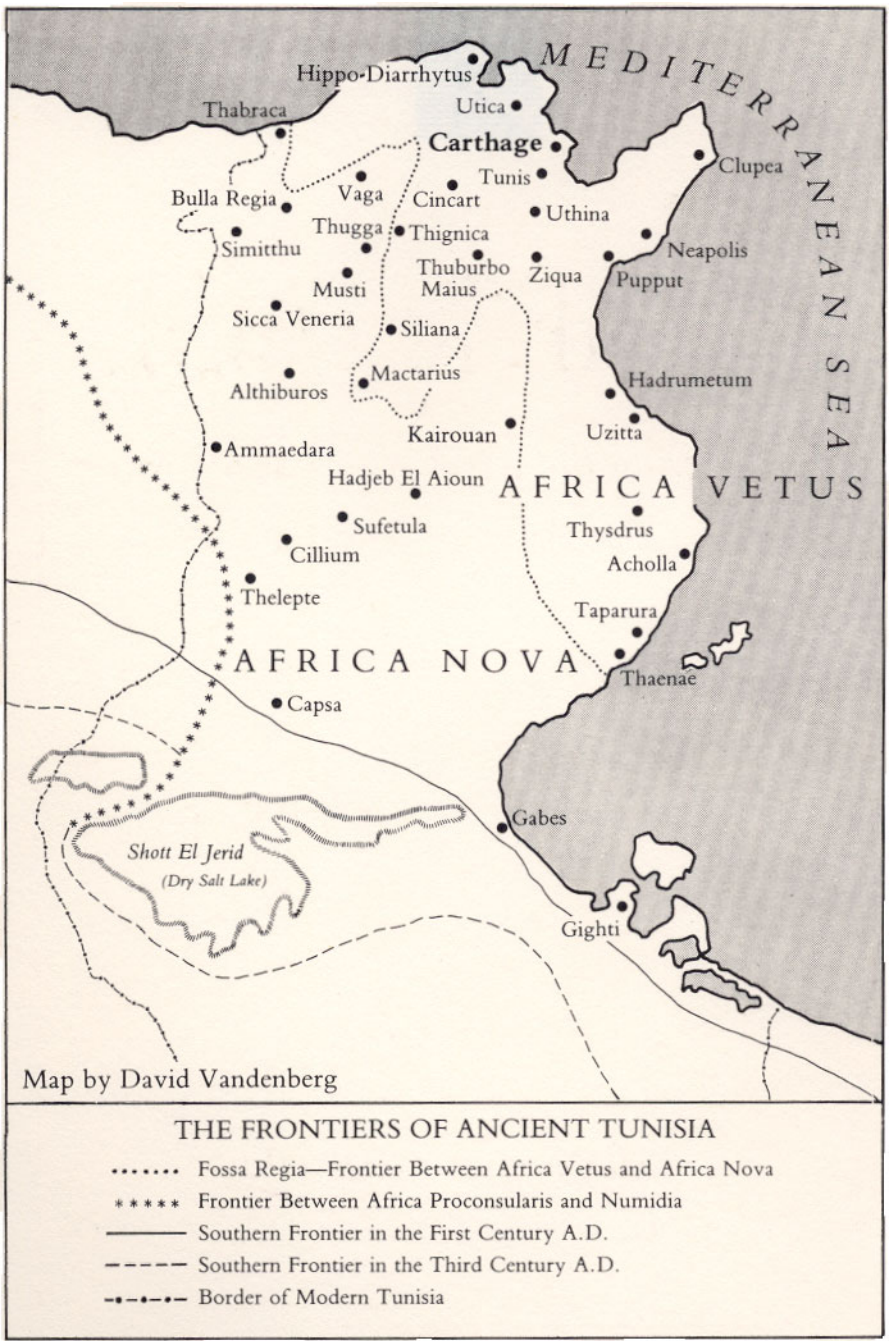


Figure 3.1
Map of the Frontiers of Ancient Tunisia (Soren, 1990).

to the introduction of cultivated plants, such as cereals and olive trees (Kolstrup, 1995). At the time Punic Carthage begins, the lands on which the city is settled are fertile for agricultural production and ideally situated for the seafaring Phoenicians, who, according to literary tradition, founded the city in 814 BCE (Niemeyer, 1990). Carthage quickly became the most important port of the growing Phoenician trade route along Africa's north coast, as the Phoenicians focused both on the sea and the resources of the hinterlands. From the beginning, Punic Carthage, situated very near the earlier Phoenician settlement of Utica, was in a strong geopolitical position in the midpoint of Mediterranean Africa as a "target territory" for Phoenician commercial and artisanal civilization (Lancel, 1995). And as her economic power grew over the centuries, Carthage was forced to face the other political power growing in the western Mediterranean – the Romans.

Roman and Carthaginian history became intimately linked at the time of the Roman Republic which began in 510 BCE. By 508 BCE, Rome entered into the first of many trade agreements with Carthage (Polybius, III, 22). Over the course of the next four centuries, the relationship between the two cities became more and more difficult as each struggled for political and economic dominance in the western Mediterranean. The complex relationship between these two intellectual and cultural centers is the subject of many scholarly works that seek to define the "aggressor" and the "defender" in their many conflicts over the centuries (Gruen, 1970).

For the purposes of this study, it must suffice to note that, after many years of war, the Romans did eventually destroy Carthage in 146 BCE and thus eliminate the Phoenician dominance of trade and politics along the southern Mediterranean coast.

Although the intentions of the Roman decision to destroy Carthage are still debated (Gruen, 1970), it is clear that the Roman sentiments against the Carthaginians were strong; the city was literally burned to the ground (Appian, *Libyca*, 134), formally cursed, and the roughly 50,000 surviving Carthaginians were sold into slavery or worse (Lancel, 1995). Roman distaste for Carthage, especially in the Senate, was such that its policy for a hundred years was that Carthage could not be resettled for fear that another power would arise to threaten Rome (Raven, 1984). So, it is not until the mid-first century BCE that Rome founds a city on the spot and the Roman phase of the city begins. Roman Carthage grows to exert tremendous influence in the western Mediterranean basin.

With the fall of Punic Carthage in 146 BCE, Rome annexed not only Carthage, but all of the Punic territories in North Africa, which comprised nearly 16,000 square miles (Soren, et al, 1990). Rome immediately sent a governor to Utica, a formerly Punic colony, who had complete authority over the new territory, which the Romans called *Africa Nova*. Rome, however, was not well equipped to administer the area in addition to the other territories that aggressive military campaigns brought under their control in the second and first centuries BCE (Raven 1984).

In order to institute some control over *Africa Nova*, Scipio Aemilianus, a Roman war hero, supervised the digging of a *fossa regia* (royal ditch) around the lands claimed for Rome. Within the confines of the ditch, Rome allowed the original landowners, whether Punic or Berber, to continue to work their land, but they were now charged a tax as rent. The entire territory was then surveyed and divided into square lots, called *centuria* (“centuries”) to be awarded to Roman or friendly native settlers. A proconsul and a senator who employed various legates and assistants to collect taxes and oversee

the exploitation of the various resources of the region governed the new province, *Africa Nova*. Utica was made capital (Soren, 1990) and was quickly populated by Roman merchants (Khader, 1987).

Carthage herself remained abandoned, at least by any new Roman settlers, who had been warned away by threats of cursed lands and mysterious happenings, and the African lands that had been assigned to Roman administrators were sold to investors, many of whom sold them back to wealthy Punic locals (Khader, 1987).

Meanwhile, the hinterlands of the new province were much like the “Wild West” (Soren, 1990) in that the native Libyan tribes were seriously threatening the newly placed Roman legions. The Battle of Jugurtha (112-107 BCE) and the attack of Cato and the Numidians on Utica in the mid-first century BCE kept Roman citizens from populating the territory despite Rome’s offer of free lands. The populace of the province consisted primarily of poor Romans, Italians, hostile and Romanized Libyans, disenfranchised but enterprising survivors of Punic Carthage, Roman merchants and speculators of the Roman middle classes (Soren, 1990).

After Caesar defeated the Numidians at Utica, the Roman Senate began to see the opportunities in *Africa Nova* and began to use it as a place to carve out new empires for themselves and to make money off of local tributes. Earlier colonization efforts that met with little success were forgotten as moneylenders and traders moved in and were given land under Caesar’s encouragement (Khader, 1987). It was Caesar’s wish that Carthage be rebuilt in order to provide land for his veterans, to exploit the vast economic potential of the region and to symbolize Caesar’s political power (Wightman, 1980). Although he was assassinated in 44 BCE, settlement began around that same year in Carthage under

Statilius Taurus who initiated some building, although to what extent is not known (Wightman, 1980). Caesar's nephew, Augustus, officially refounded Carthage in 29 BCE and oversaw the rebuilding of the city amid the Punic ruins (Rakob, 1998). It was Augustus who eventually realized Caesar's dream in creating *Africa Proconsularis* with Carthage as the new capital. Augustus' plan included the placement of needy veterans and locals on the fertile lands near Cape Bon so Rome could keep a close watch. Attempts were made to unify the disparate Roman provinces through development and material progress, and the Roman legion ensured peace by establishing control centers further from the coast (Soren, 1990). By the close of the first century CE, *Africa Proconsularis* enjoyed the *pax Romana* delivered by Augustus and economic prosperity with Carthage again at the helm of its success.

Veterans were encouraged to move to the new city, and Carthage drew them in, along with various urban and agrarian people (Phoenicians, Italians, Numidians) in need of economic gain and Punic people who still lived in the hinterlands of the newly populated city (Khader, 1987). These "settlers" were employed in the production of grain and olive oil in the fertile lands outside of Carthage proper and received land allotments to grow whatever Rome required. These goods were then exported from Carthage to Rome. Emanating from Carthage, the Romans built an immense system of roads, which ignited some conflicts with the Berbers who were still allowed to graze in *Africa Proconsularis*, but in general, Rome disturbed the local traditions as little as possible. Overall, "Carthage was a shining example of Romanization" (Khader, 1987).

Carthaginian society, and by extension, that of *Africa Proconsularis*, was highly integrated into Roman culture as evidenced by the presence in the city of bilingual

inscriptions (Latin and Phoenician), Punico-Roman architecture, and the syncretization of the religious beliefs of the once mortal enemies (Khader, 1987). The Libyans, who were local tribal peoples, were also included in the new society of *Africa Proconsularis*: Punicized Libyans made up a large portion of the middle class and the urban proletariat. Berbers were slaves or migrant worker (Soren, 1990). City life, although made up of people of various cultural backgrounds, was not egalitarian; the Romans did impose their laws, their language, and their customs onto the non-Roman populace and remained firmly in control of the finances of the new province. Wealth, however, generally increased for everyone in *Africa Proconsularis* and even the poorest were allowed the luxury of the use of the palatial baths and theaters that were built for the city's entertainment (Soren, 1990). Outside of Carthage, towns grew and became *municipia* and in some cases even *colonia*, which had full Latin rights and Roman citizenship (Khader, 1987), allowing more freedoms to the indigenous people than perhaps they had had under Punic rule. Carthage had entered her *Golden Age*.

By the end of the second and beginning of the third centuries CE, Carthage was at the height of her power as a Roman city. It is during this time that the city was extensively remodeled. The wealthy added water to their homes with indoor fountains fed by lead pipes, an amphitheater and circus were built to entertain Carthage's over 100,000 citizens, and city life was soon considered the only "civilized" way to live (Soren, 1990). Other, smaller urban centers sprang up throughout the province, often each with its own bath complex, theater or amphitheater, circus, and forum. In all, there were some 200 Roman cities throughout *Africa Proconsularis*, many of which were built right on top of the former Punic settlements that had been carefully chosen and laid out

centuries before. Water was important in these population centers too, just as it was in Carthage, and the Romans built dams and reservoirs throughout the countryside; the most extraordinary example of the Roman quest for water is the monumental 75 mile long aqueduct built by Hadrian in 128 CE from the Temple of the Waters to Carthage (Soren, 1990).

But how did Roman Africa fund all this city building and the extravagant lifestyle of its citizenry? The answer is quite simple: wheat. The tremendous economic development through the end of the first century CE was based primarily on Africa's designation as "the granary of Rome," (Khader, 1987). Wheat was the king of the crops, as olive oil and wine were avoided in the early imperial period because of Italy's dominance of those markets. *Africa Proconsularis* provided much of Rome's grain and fed 200,000 Roman citizens on the dole for eight months out of every year. It was not until the second century CE that Africa diversified its crops to include olives and grapes, due in large part to crises in Italian production (Soren, 1990). Olive oil became so abundant that in the fourth century CE St. Augustine, who lived, studied, and taught in Roman Carthage, noted that Carthaginians could keep their lamps lit all night for the abundance of oil they had for fuel (Soren, 1990). But, olive oil was not all that Roman Africa had to offer the Mediterranean economy; the citizenry of the *Africa Proconsularis* participated fully in the exchange of goods and ideas with the rest of the Roman world, most notably through the establishment of universities that drew students not only from all over Africa, but from other parts of the empire to learn (Raven, 1984).

In addition to scholarly and intellectual pursuits, and agricultural production, Roman Africa was involved in several other important industries. Ceramic production,

which had stopped with the fall of Carthage, was revitalized at the end of the first century CE and production of amphorae for transporting grain, oil, and wine began in earnest. Vases, cups, plates, statues, and most appropriately, oil lamps, were exported throughout the Mediterranean from the workshops in the area (Soren, 1990). Production centers were located near abundant clay deposits in Kairouan, Hajeb-Al Aiouan, El Aouja and El Jem in Tunisia, which roughly corresponds to *Africa Proconsularis*, (Khader, 1987) and contributed to those towns' prosperity. African Red Slip Ware was the most successful type of African pottery production and was made up until the time of the Islamic invasions in the sixth century CE and exported throughout the Roman world (Soren, 1990).

Other exports during the Roman era included garum (dried fish used as a condiment) from production centers in Neapolis, Sullectum, and Kelibia in Tunisia, yellow and dark rose marbles mined from the quarry at Chemtou near the Algerian border, and luxury items like mosaics, rugs, wool clothing, and leather goods (Soren, 1990; Khader, 1987). There was also some mining of copper, iron, and lead, but these industries remained a minor part of economic life at the time (Raven, 1984), although there is evidence that modest manufacture of these metals occurred in Carthage, for example (Hurst, 1984). All these products were shipped through Carthage on their way elsewhere and in exchange, Carthage imported gold, ivory, slaves, precious stones, and wild beasts (Soren, 1990), which can be seen depicted on the elaborate Roman mosaics of the era. Carthage became increasingly independent from Rome and by the end of the second century CE, her prosperity again equaled that of Rome. Her good fortunes were not to last.

Beginning at the end of the third century CE, with the death of emperor Septimius Severus, Rome entered a period of political unrest. Her emperors were overthrown at an alarming rate creating economic instability and erupting in civil unrest and rebellion. El Jem, ancient Thyrsdus, the great olive production center of Africa, along with other Roman African cities, began to express dissatisfaction with taxation and imperial administration in *Africa Proconsularis*. In El Jem, this dissatisfaction led to the murder of the Roman procurator and a bid for one of their own, Gordian, to become emperor. Carthage, and other cities in *Africa Proconsularis*, enthusiastically supported this movement. The Roman Senate, of which Gordian was a member, confirmed El Jem's choice and a North African became emperor of Rome.

By the end of the third century, non-Italians were playing major roles in Roman politics and barbarians encroached on the far-flung Roman empire. Emperor Diocletian, a Yugoslav, realizing the Roman Empire was too large to be controlled from Rome alone, divided it up between his loyal colleagues, forming what became known as the *tetrarchy*. *Africa Proconsularis* (approximately northern Tunisia) and Byzacenia (southern Tunisia) stayed within the orbit of Rome, however (Khader, 1987). Throughout the fourth century, Carthage still prospered and trade boomed, but the political stability of North Africa was severely threatened.

Amid the political upheaval, the traditional Roman religions began to fade, and Christianity attracted many converts in North Africa. The religious transition was certainly not an easy one, as intellectuals and church officials argued as to how the new religion should be practiced, while Rome persecuted Christians periodically for their unwillingness to sacrifice to the Roman pantheon. Christianity continued to grow in

Africa Proconsularis, but not on a unified front. During the fourth century CE, many Roman Africans felt Carthaginian bishops responded too softly to Roman persecutions and a rift developed, commonly referred to as the Donatist Controversy. The Edict of Milan, issued in AD 312 by the new Emperor Constantine, attempted to put an end to the bickering by proclaiming religious tolerance (Khader, 1987). But the edict was only marginally successful as the religious arguing had already become a class war between poor Christians and rich pagans; many Christians were forced to flee Africa (Soren, 1990). Eventually the Donatists were forced out of Africa and the Roman Catholic Church was firmly established there by an assembly in Carthage in AD 411.

During this time, Constantine also moved the seat of the empire from Rome to Constantinople, continuing the effort begun by Diocletian to diversify power in the empire. Berber chiefs, who had grown powerful during Carthage's renewal in the third century, now found themselves in control both of North Africa's official Roman troops and of Rome's grain supply. Rebellions ensued in the increasing power vacuum in North Africa. Rome fell to the Visigoths in 410 CE, and the Vandals devastated Gaul. Then, the Vandals headed for Carthage (Khader, 1987).

It is uncertain what Roman Carthage was like shortly before the Vandal invasion; many of the buildings from this latter Roman period were destroyed and subsequently reconstructed during the Vandal period (Humphrey, 1980). There is, however, some evidence indicating there was a cultural and economic revival in the latter part of the fourth century in Roman Carthage. A new harbor was built in 380, suggesting trade was still flourishing. Mosaics continued to be of high quality and adorned many of the new churches built in the city during this time (Khader, 1987). Nevertheless, when the

Vandals invaded in 429 CE, Carthage fortified herself and fought, only to be taken over in AD 439 (Raven, 1984). A treaty signed shortly thereafter in Constantinople turned all of *Africa Proconsularis* over to the Vandals (Khader, 1987), bringing an official end to Roman rule in North Africa.

City Plan

In addition to historical perspective, it is also important to have a clear picture of how Roman Carthage was spatially organized in order to interpret archaeological sites such as the Yasmina Cemetery. The city plan of Roman Carthage reflects, at its most basic interpretation, the intentions of Caesar in recolonizing the city in the first place. He intended the new city not only as a practical solution for landless veteran soldiers and poor citizens, nor as simply a potential economic boon for Rome, but also to serve as a symbol of the power of politics over religious ritual and his own political superiority over his rival Pompey. The extraordinary adherence of Augustus' city plan to Roman centuriation symbolizes the grandeur of Rome and a city reborn on accursed soil (Wightman, 1980). Additionally, as Carthage grew in population and cultural and economic importance, the infrastructure of the city changed as well with the addition and modification of industrial areas and public works, etc. The Yasmina Cemetery must be placed in this context so that its remains can be better understood.

More than 100 years after its destruction by Rome, Carthage was officially founded in 29 BCE by Rome as part of Augustus' plan to recolonize and rebuild the city. The city plan that he envisioned has been recreated through extensive archaeological and epigraphic evidence and is shown here in Figure 3.2. Although city buildings were occasionally remodeled during the Roman period, the original city plan with which

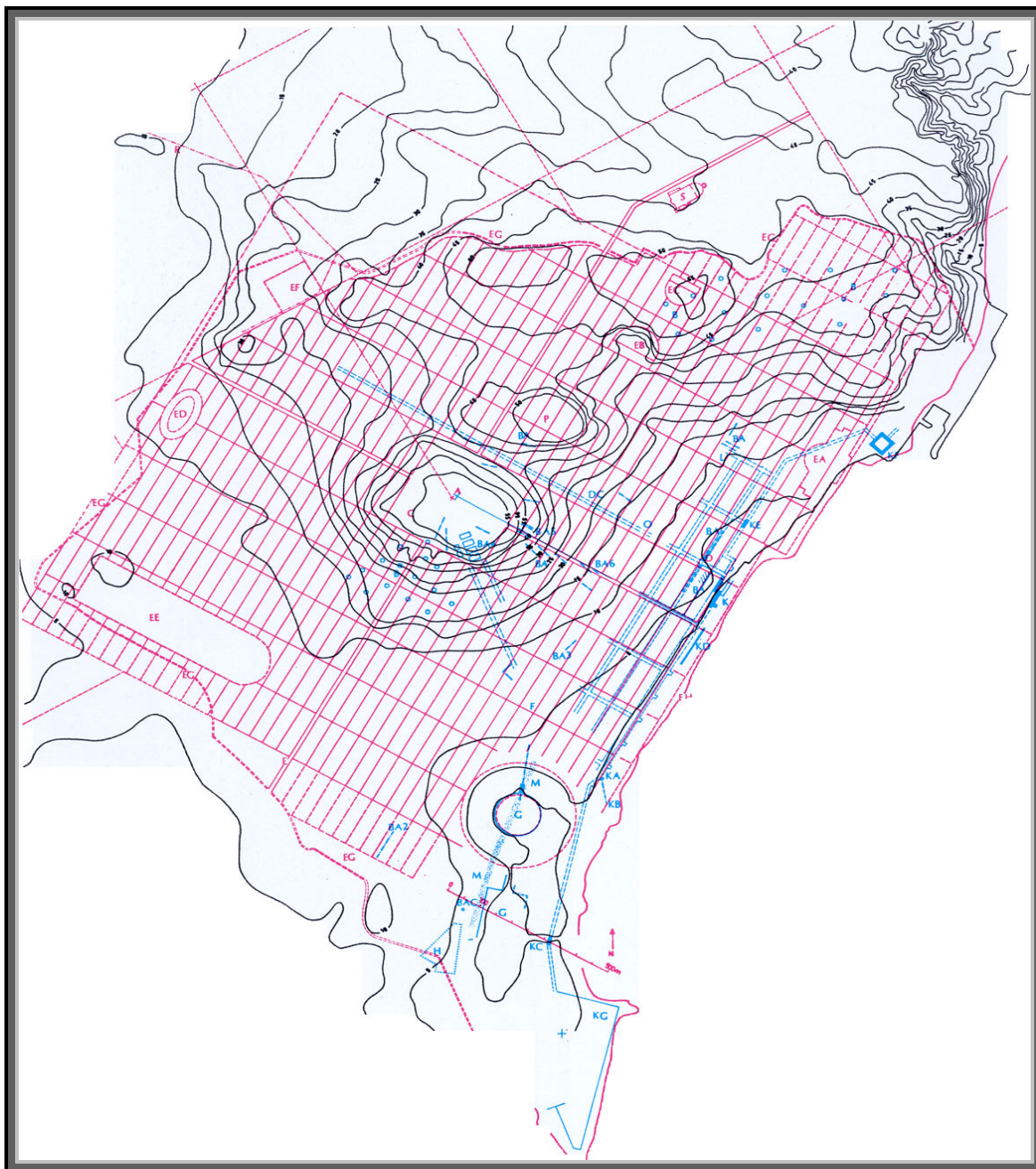


Figure 3.2

Carthage. Punic building alignments (blue) and the plan of the Roman colony (red). Scale 1:10,000 (from *Karthago* I, plan 34 and Hurst and Roskams [supra n.7] fig. 11).

The Yasmina Cemetery is located to the south of the Roman Circus (EE), just outside of the grid.

Augustus is credited (Wightman, 1980) was never abandoned (Rakob, 1998). Roman Carthage was laid out from the beginning in a structured and uniform way and without regard for topography or even traffic flow. The extreme regularity of the grid system is remarkable, considering the dramatic changes in elevation from the coast to the top of the Byrsa hill and the placement of the Roman city on the same site as that of the Punic city. It is not unusual, however, for Roman urbanization to adhere to rational order in the face of uneven terrain (Rakob, 1998).

The city plan of Augustan Carthage was based on a center point or *groma* located at the summit of the Byrsa hill. This was also the *groma* of the Punic city and it appears that Gracchus, who made an unsuccessful attempt at resettling Carthage around 44 BCE, laid some preliminary measurements and assignations and chose this site for the *groma*. Augustus left this part of Gracchus' plan intact and it was from this highest point in the city that he laid out the grid system. At the *groma*, the intersection of the two major roads in Carthage, the *decumanus maximus*, running roughly east/west, and the *cardo maximus*, running north/south, were set. The width of these two main streets were roughly 40 Roman feet, setting them apart from the rest of the city roads (Wightman, 1980). From these axes, *insulae*, or city blocks with dimensions of 480 x 120 Roman feet (Wightman, 1980), were laid out creating a symmetrical grid that spread in four directions away from the Byrsa. All buildings within the city were to fit into these city blocks. The edges of this grid were dictated to the east by the Mediterranean Sea and to the north, south and west, by the rural *centuriation*, or grid, that was established simultaneously with urban *centuriation* (Rakob, 1998). The cisterns of La Malga, located outside the urban *centuriation*, but aligned with the rural *centuriation* as well as with the

groma, suggest that the grid were established simultaneously (Rakob, 1998). Although there was a recognized boundary between the urban and rural areas, no city wall was built, reflecting the peaceful living conditions (Rakob, 1998). The entire extent of Roman Carthage was laid out from the start and as the population grew, private homes and businesses filled in the city blocks.

The Augustan building program dictated that in each of the four sectors of the city there should be a monumental public building to frame the Byrsa hill (Rakob, 1998). The theater, amphitheater, circus, and *platea maritime* appear in Figure 3.2 along with other major buildings from the Augustan plan. Despite the locations of these major public buildings and other popular venues, like the harbor or the agora, the roads built to connect these areas were not made any wider than the average street. The Roman adherence to the orthogonal grid plan was not deviated from for any traffic circulation issues or topographic difficulties. Often streets had to be terraced and stepped, in some cases to the point that they were no longer useful for the traffic of carts and carriages (Rakob, 1998). The *cardo maximus* and *decumanus maximus* remained the only major, widened roads in the city even though they did not provide access to important public areas.

The Byrsa hill, once the heart of the Punic city, was again made the political and economic center of the Roman city, but not without significant modifications. The Romans removed the entire top of the hill, obliterating any trace of Punic construction, and erected a monumental platform (Rakob, 1998) supported by massive vaulted structures. On this terrace they placed a Temple to Jupiter and numerous public buildings (Khader, 1987) that would serve as the commercial and cultural center of the city. The

buildings were constructed using a central-Italian building technique, *opus reticulum*, that was reserved here, and elsewhere in the city, for monumental architecture and official monuments (Rakob, 1998). Also, the building materials used for these public buildings were imported from nearby Cape Bon and not recycled from the Punic city ruins as was typical of Roman buildings elsewhere in Carthage (Rakob, 1998). The Byrsa was the focus of the earliest construction efforts in Carthage and was to serve as the centerpiece for the growing city around it.

Throughout the rest of Carthage, the Romans reused much of the Punic rubble for private buildings, the evidence for which includes the appearance in Roman walls of the red bricks burned in the 146 BCE destruction (Rakob, 1998). A variety of architectural styles were used for buildings, in many cases dictated by the shape and size of the Punic stone blocks the Romans recycled. According to Rakob, there was a great deal of removal, sorting, and reuse of the Punic rubble for construction after the surveying had been completed for the uniform *insulae* (Rakob, 1998). Despite their willingness to reuse Punic materials, the Romans were decidedly unwilling to reuse Punic structures; they may have followed the path of a Punic wall, but they completely tore down the original and rebuilt it from the remaining materials (Rakob, 1998). The Roman city was clearly not a copy of the former Punic one, but rather a true Roman city built, in large part, from the recycled remains of Punic Carthage.

The changes in the buildings of Carthage over the next 500 years are extremely complex as well as site specific and beyond the scope of this paper. It is important to note, however, that virtually nothing of the original centuriation was modified, even though the buildings themselves underwent periods of major reconstruction (Rakob,

1998). There were additions of new buildings as the city grew and reconstructions of some the Augustan monumental public buildings, most extensively by Antonius Pius in the second century CE (Rakob, 1998). Antonine construction primarily embellished what had already been established by Augustus as, for example, in the addition of a colonnade to the *decumanus* running from the Byrsa to the sea (Rakob, 1998). As industry and trade grew, the ports and workshops along the shore were reestablished and modified to accommodate the Roman shipping industry (Hurst, 1984). Carthage gradually expanded to fill the urban centuriation established by Augustus and, indeed, never did reach the limits of the urban grid, especially to the north (Wightman, 1980).

Perhaps the most extensive change to the original city plan was the addition of a fortification wall between 423 and 425 CE by Theodosius II (Soren, 1990). The wall, called the Theodosian Wall, was built as a defensive measure against the impending threat of Vandal invasion. The historical source for the establishment of this wall appears in the Gallic Chronicles, which states that in 425 CE Carthage was surrounded by a wall, although it had been unfortified since the second century BCE for fear of rebellion (*Chronica Gallica*, a. ccccxxv). The 3.5 meter-wide wall, constructed of a core of grey charcoal-flecked mortar rubble and faced with large square blocks, was set in place adjacent to buildings that were still in use at the time of the wall's construction (Hurst, 1974). The city wall was approximately 9.5 kilometers in length and surrounded the entire *pomoerium*, or formal urban area, of Carthage along the landward sides and also along the coast (Hurst and Roskams, 1984). Ancient sources state that Carthage had nine gates at the time of the governorship of John Troglitas (546-c.563 CE) (Corippus, VI, 60) and several of these gates have been identified archaeologically as the result of

excavations throughout Carthage. The theoretical course of the wall is outlined in Figure 3.2 (Rakob, 1998). The course of the wall suggests that it was intended to only enclose the *pomoerium* and not all the areas that were in use around Carthage in the fifth century. Roman cities are typically organized so that the cemeteries are located outside the city proper (Hurst and Roskams, 1984). Fifth century Roman Carthage follows this tradition as the course of the Theodosian Wall clearly excludes cemeteries from the space it encloses; indeed, in places where the course of the wall is not discernable by excavation or geophysics, the location of cemeteries are used to reconstruct the theoretical course of the wall (Hurst and Roskams, 1984).

So, where does the Yasmina cemetery fit into this Augustan city plan with all of its modifications? The Yasmina cemetery lies in the southwest quadrant of the ancient city, just outside the south gate of the Theodosian Wall and c. 100 meters from the south *cavea* of the Roman circus (Norman and Haeckl, 1992). The necropolis was in use from roughly the second through the sixth centuries CE, so was clearly in place before the wall was constructed and deliberately left out of its enclosure. The cemetery contains a variety of grave types, ranging from modest inhumation burials to more elaborate ashlar funerary monuments and there seems to be a general decrease in the status of the burials as time progressed (Norman and Haeckl, 1992). Interestingly, the cemetery contained a statue of a Roman charioteer which, given the close proximity of the Roman circus, suggests that there was some relationship between the two sites; the Yasmina cemetery would certainly have been a prominent topographical feature as people entered the south gate on racing days (Norman and Haeckl, 1992). The Yasmina necropolis, because of its

long history of use and its proximity to such an important public building, was an important cemetery for Carthage.

A more detailed description of the excavated material remains associated with the site will be discussed in the next chapter. The history of Roman Carthage and the plan of the Roman city, together with the synopsis of Roman Iron Age metallurgy in the previous section, are intended to provide the framework for the interpretation of the metallurgical remains excavated from the necropolis' fill material. The details of the field sampling and analytical methods used to characterize the slag, as well an interpretation of those results, are the topics for Chapter Four and Chapter Five.

CHAPTER 4

CREATING A CLEARER PICTURE OF CARTHAGINIAN METALLURGY

The metallurgical slags excavated from the fill layers of the Yasmina cemetery in Carthage indicate that some sort of metallurgy was indeed being practiced in the vicinity of the cemetery. But what sort of metallurgical site did the slags come from? What type of metals were being smelted or worked? What was the extent of the metallurgical operation from which these slags came? What specific metallurgical processes do the Yasmina slags represent? In order to begin answering these questions, a general characterization of the various slags recovered from the Yasmina excavations is necessary.

Slag characterization begins first with a description of the site from which the material was excavated followed by a discussion of the sampling methodology and descriptions of the various slags in hand sample. Representative samples from slag types identified in the field are then analyzed with a petrographic microscope to identify and characterize the major phases of the slags. Characterization of the slags concludes with electron microprobe analyses of slag phases. With these data and the historical contexts described in the previous chapters, some suggestions can be made about Carthaginian metallurgical practices during the Roman Iron Age. The first two sections of this chapter address each level of characterization performed for this thesis; the final section is devoted to a discussion of the results and interpretations.

Site Description

Geologic Setting

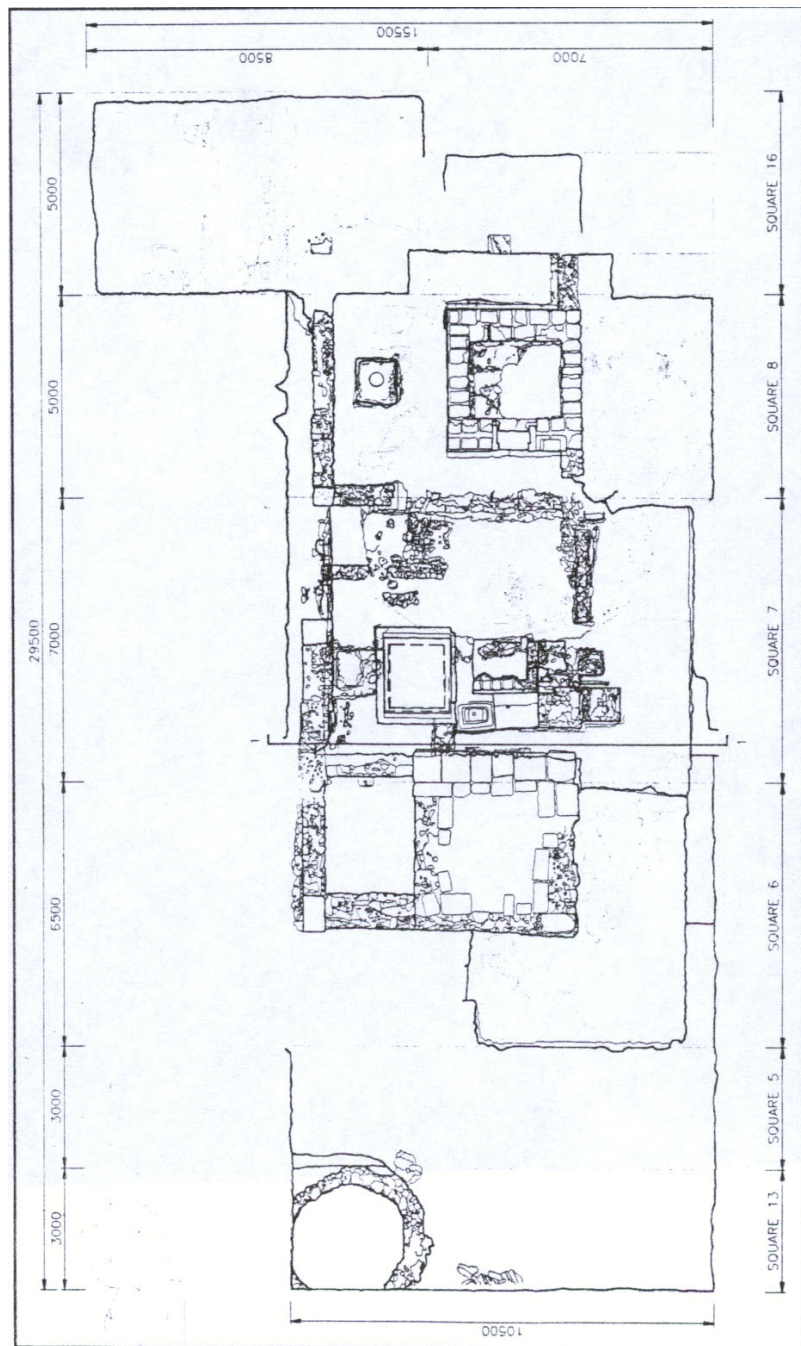
The geologic setting of northern Tunisia is relatively uniform, composed of sedimentary rock, primarily carbonate rocks that have been deposited and subsequently metamorphosed as a result of the Atlas Mountain orogeny which began in the Miocene (Girgis, 1987). The lithologies in the area consist of clay beds, quartz sandstones, conglomerates, and shore-zone, shell fragment sands in the low-lying areas; limestones, dolomites, and sandstones form resistant topographic highs and numerous outcrops throughout the region (Bullard, 1975).

These local materials were utilized widely by the inhabitants of the region. The local limestones and sandstones provided the Phoenicians, as well as the Romans, with abundant architectural building materials (Bullard, 1975). For example, Romans quarried sandstone blocks for use in the construction of the rectangular harbor (Bullard, 1975). Archaeological evidence from ceramic kiln excavations also indicates that the local sedimentary lithologies were used in the making of amphorae near Carthage during the Roman era (Peacock and Tomber, 1991).

Associated with the dominantly carbonate lithologies of the region are localized areas of metalliferous deposits concentrated by hydrothermal activity in the strongly folded rocks in the northern part of Tunisia (Sainfeld, 1955). The principal deposits are associations of lead and zinc (Sainfeld, 1955). Lack of epigraphic evidence and the historical exploitation of these lead-zinc mines has made it difficult to determine if these ores were exploited by the Romans (Sainfeld, 1955), though lead was certainly of major



Figure 4.1
Photograph of Yasmina cemetery excavation (courtesy of Nina Serman).



E. M. R. S T U D I O S
jhr@emrstudios.com
119-10 Angus Road, Vaughan, Ontario L4R 6K3
(905) 881-5353, 533-1888 fax

SITE NORTH

Client/Project
University of Georgia
Excavations
The Yasmina Necropolis
Carthage, Tunisia 1992-1997

Drawing Title
SITE PLAN
Yasmina Necropolis

Date: July 1997	PROJECT NO: 97100
Scale: 1:150	Drawn By:
Checked By:	Drawing no: A-1.04
Total Drawings:	File: 97YBASE.dwg

Figure 4.2
Plan view of Yasmina cemetery

importance to Roman society, particularly for its widespread use in plumbing (Healy, 1978). Tylecote also notes the presence of iron ores in northern Africa, although he does not give any detailed locations or evidence of exploitation (1976).

Archaeological Setting

The site from which the metallurgical slag for this characterization study was obtained is a Roman cemetery, in use from the second to the sixth centuries CE, located on the outskirts of the modern town of Carthage, Tunisia (Figure 4.1, Figure 4.2). The Yasmina Cemetery is named after the neighborhood in which it is located, having been discovered during Tunisian bull-dozing for a road; full-scale scientific excavations did not begin until 1992 by the University of Georgia (Norman and Roby, web site). Conservation work aimed at emergency stabilization began immediately at the site in 1992 and is being continued today as the site is intermittently excavated and conserved (Norman and Roby, web site). The metallurgical slags used in this study represent the material that has been excavated over five excavation seasons in 1992, 1993, 1994, 1995, and 1997.

The Yasmina cemetery was used by some of the wealthiest and most prominent families of Roman Carthage (Norman, web site). Fine stucco reliefs decorate several multi-storied monuments for cremation burials and two life-size marble funerary statues adorn a larger ashlar tomb monument dating from the early third century CE (Norman, web site). In addition to funerary monuments, coins, pottery, glass bowls, cremation urns, funerary inscriptions and skeletons have been excavated (Purdy, 1995) along with a variety of fill materials, including metallurgical slag. The fill materials occur throughout the cemetery at several different levels. It appears the Romans placed the fill sediments

around older monuments and burials to level and raise the cemetery ground level for later stages of use. The cemetery continued in use into late antiquity when inhumation burials began to appear. It went out of use in the seventh century CE (Norman, web site).

The location of the cemetery relative to ancient Carthage is significant as well. Roman citizens tended to put their cemeteries in conspicuous places outside the city gates (Purdy, 1995). The Yasmina cemetery is located on the route to the Roman Circus where passersby could see the funerary monuments and marvel at the lives of the deceased (Norman, Purdy, 1995). The Yasmina cemetery is clearly an important cemetery for Carthage: it was in use for nearly six centuries, periodically back filled for re-use and its monuments repaired after natural disasters, like an earthquake in the seventh century (Purdy, 1995).

The Yasmina cemetery has only been partially excavated; its extent is as yet unknown. The excavations, completed over the course of five field seasons, were recorded using a Harris matrix. While most of the fill material was catalogued by the archaeologists, the recording of the locations of the major funerary monuments and large, intact artifacts were the focus of the excavations efforts. The site was excavated so as to preserve the integrity of the major finds, rather than as a study of the site's stratigraphic layers. Therefore, reconstructing the stratigraphy of the fill layers from which the metallurgical slag came would be difficult without further excavation of the site.

The archaeological material excavated from the fills at Yasmina includes a wide variety of artifacts, such as abundant ceramic sherds, brick fragments, metallurgical slag, bone fragments, rock fragments, and coins. It is unlikely that all of this fill material has any direct association with the activity at the cemetery site. For example, the

metallurgical slag excavated there is not a typical cemetery find; its presence at Yasmina is more likely a result of its transport from a nearby (and yet undiscovered) metallurgical site as part of a collection of sediments to fill in the cemetery for another phase of use. Nevertheless, the presence of metallurgical slag indicates that some form of metallurgy was indeed going on in Roman Carthage or its immediate environs. It is the purpose of this study to characterize the metallurgical slag and provide some initial interpretations about the processes the slags represent.

It is important to note that none of the features or artifacts typically found at metallurgical sites, such as hearths, furnace remains, or tuyeres, were excavated and stored in association with the metallurgical slags from Yasmina. Essentially, there is no real contextual evidence that could be used to interpret the metallurgical processes other than the slags themselves. The importance of excavating and analyzing all metallurgical remains, especially ceramic remains that can provide evidence for the furnace structure, is stressed by most archaeometallurgists (Craddock, 1995, Kassianidou, 1995, Bachmann, 1982). Although this contextual evidence is not available at Yasmina, the slags can still provide a great deal of information about the metallurgical processes they represent.

Field Sampling Methodology

Methodology

A trip to Carthage, Tunisia was made in May of 2000 to obtain slag samples for analyses and characterization. The artifacts from the Yasmina Cemetery excavated by the University of Georgia Classics Department under the direction of Naomi J. Norman, are housed at the Museum of Carthage located on the Byrsa in the modern city of Carthage. During the excavations, the archeologists had separated what they identified in

the field as metallurgical slag from the other artifacts recovered from the fill material, such as ceramics sherds, bone fragments, and charcoal. These archaeological samples labeled “slag” were collected over the course of the five excavation field seasons (1992, 1993, 1994, 1995, and 1997) and stored in 15 crates with approximate dimensions of 30cm x 30cm x 61cm. These crates, along with hundreds of others from the Yasmina excavations are stored in a back room off the rear courtyard of the Museum of Carthage. The hundreds of crates were stacked two and four deep and in some cases, 15 or 20 high in this small, unventilated, storage room (Figure 4.3). As there was no central location for crates related to metallurgical finds, a day was taken, with the aid of a field assistant, to locate crates labeled “slag,” “metals/other,” and “charcoals/metals” that had been identified by the field archaeologists as they excavated. In total, only 15 crates were labeled to contain metallurgical or possibly metallurgical remains.

The 15 crates labeled as associated with metallurgical technology were located and removed from the storage room at the Museum of Carthage with the permission of Dr. Abdelmajid Ennabali, the Conservator of the Site of Carthage and the Director of the Museum. The metallurgical crates contained plastic bags filled with anywhere from a single, fingernail-size piece of slag to bags consisting of several large slag chunks. Furthermore, as these bags were opened and their contents identified, it became apparent that many of the artifacts identified in the field as related to metallurgy were, in fact, not metallurgical in origin at all. For example, along with metallurgical slag, the bags and crates contained great quantities of fragments of charred bone, flecks of charcoal, rock fragments, a variety of glass slags and fragments and clods of sediment. In order to sample adequately the metallurgical slag present in these crates (and perhaps any



Figure 4.3
Storage room at the Museum of Carthage, Tunisia.

associated refractories, like furnace fragments or ore pieces), each bag was opened and its contents categorized according to its morphology. Those artifacts identified as metallurgical slag were separated from the rest of the various materials in the bags and set aside for further classification. The criteria used to identify metallurgical slag versus other materials are outlined in the table and discussion below:

The metallurgical slag was identified using Hans-Gert Bachmann's criteria from *The Identification of Slags From Archeological Sites* (1982). The criteria used to separate the metallurgical slag from the other archeological samples were similar to those used in the identification of geological samples in the field, such as color, porosity, streak, texture, specific gravity, inclusions, and magnetism. In addition to these criteria, the presence of metallurgical indications like green surface crusts, flow textures and plano-convex shapes were used to separate metallurgical slags from the other materials in the crates. When the metallurgical slag was finally separated from the rest of the archaeological material, the number of crates of slag was reduced from 15 to five, with approximately one full crate from each excavation year. The identifying labels on each bag were preserved from both the metallurgical samples and the other material from the fill.

Once all the metallurgical slag had been separated from the other material remains in the crates, roughly five crates of slag remained. Within these five crates there was still a great deal of variety in the textures, specific gravities, colors, etc. of the slags. To ensure a representative sample of all the varieties of slags present, the contents of the five crates were again laid out and categorized using a combination of Bachmann's criteria discussed above and morphological observations made in the field. Bachmann's criteria

provide a basis on which to distinguish metallurgical slags from non-metallurgical slags, while observations of the variety of slags present provided a basis for distinguishing slag types.

Through the course of separating the metallurgical slag from the other artifacts, it was observed that there were various types of slag morphologies represented in the bags and crates. Each piece of slag from the five crates was analyzed and placed into a category based on its morphology. The names of the slag types used in the field highlight their morphological differences, rather than indicating their association with a specific metallurgical process. The four basic types observed are outlined in Table 4.1. The slags that comprised these categories were labeled as iron slags, as this was the type of metallurgical activity to be expected from a Roman site.

Additionally, approximately 60% of the total volume of slag in the five crates exhibited the characteristic green coloring that is diagnostic of slags associated with copper metallurgy (Bachmann, 1982). Therefore, in each of the above categories, slags were sampled that had the diagnostic green coloring, as well as those that did not, creating a total of eight categories of slag: iron tap slag, iron cake slag, iron furnace slag, iron frothy slag, copper tap slag, copper cake slag, copper furnace slag, copper frothy slag.

Once the categories and slag types were established, it was necessary to obtain a representative sample from the wide variety of slags recovered from the Yasmina fill. In order to do so, the locus number associated with the slag (the locus number identifies the archaeological feature, the excavation of which revealed the slag – see “Site Description” section) was kept in mind to see if there was still some chance for acquiring

Table 4.1

Slag Morphologies based on preliminary field characterization	
<i>Slag Type</i>	<i>Properties</i>
tap slag	exhibits flow texture, high specific gravity, silvery metallic in color, weakly magnetic, may have large vesicles near edges
cake slag	similar to tap slag in appearance, but without flow texture, plano-concave or convex in shape, weakly magnetic
furnace fragments	slag adhering to furnace fragment characterized by fusion with a vitrified or partially vitrified ceramic
frothy slag	highly variable in color and texture, lower specific gravity and smaller vesicles than tap or cake slag, highly vesicular

representative samples from each category over time. However, in order to sample the slag chronologically, it would be necessary to obtain samples from the same square from a number of seasons. The Harris matrices, which depict the stratigraphic sequence of the site, indicated that this would only be possible for squares numbered 6, 7, and 8. These excavation units did not generally produce more than one sample of each slag type from each of the stratigraphic layers. Without a sizeable or consistent sample suite for comparison across stratigraphic units, observing technological changes over time would be impossible. Therefore, sampling methods would have to focus on obtaining a suite of samples representative of the entire assemblage of metallurgical slag morphologies over the extent of the cemetery fill.

A sampling strategy was devised to obtain a sample suite of slags for return to the University of Georgia Geology Department for analyses and further characterization. This strategy was to sample one of each slag type (e.g. iron tap slag, copper tap slag) from each square (e.g., 6, 7, and 8) when possible and from each excavation season. This would ensure several samples of each morphological type, as well as ensuring those samples came from all portions of the excavated material, both spatially and chronologically. See Table 4.2 for a summary of sampling strategy used at Yasmina. For each excavation year, bags were divided into four iron morphologies and four copper morphologies according to what had been observed in the entire sample suit. Then, from each category of bags, a piece of slag was removed that was at least 2.5 centimeters in diameter. No smaller samples were chosen, because they were too small to thin section easily for further analyses. Samples larger than a dinar (local currency coins about 2 cm in diameter) were taken when available, so that a significant portion of the sample would

remain intact after thin sections were made. Each of the five crates were sampled in the same manner. In some cases, a piece of slag that did not clearly fit into a category was also sampled to insure a representative sample suite and not one limited by initial field identification and characterization. These five samples were labeled “other.”

In total, 87 samples of metallurgical slag and associated finds were removed from the Museum of Carthage and returned to the University of Georgia for further study. Table 4.2 displays the loci numbers of the samples removed from the field as well as those samples eventually chosen for further characterization using petrographic and electron microprobe techniques.

Discussion

From field observations and preliminary categorization of the slags excavated from the Yasmina cemetery, it is apparent that there are at least two distinct metallurgical processes represented by these samples. The presence of green weathering minerals on the surfaces of approximately 60% by volume of the excavated slag and absent on the other 40%, suggests that the slags represent the presence of copper metallurgy and another unidentified metallurgy, presumably related to iron metallurgy.

From the variety of slag morphologies, for example, copper tap slags and copper cake slags, it seems that the slags are representative of different steps in the metallurgical process or of different locations in the smelting/smithing furnace.

The small volume and wide variety of slag is not conducive to random sampling methods to obtain a representative sample suite. Therefore, a strategy was devised in the field based on the morphological variety observed and the excavation records to acquire representative samples for further study.

Table 4.2

Chart of Slag Samples removed from the Museum of Carthage for Analysis					
Refer to site plan for square locations					
Excavation	1992	1993	1994	1995	1997
Square	4, ?	5,6,7,8,10	6,12,13,15	6,7,8,13,16	6,7,8
Slag type	# of Samples of each type removed from storage				
iron tap	3	1	1	4	2
iron cake	2	3	1	3	1
iron furnace	1	0	2	3	0
iron frothy	3	7	2	2	0
copper tap	1	4	2	2	0
copper cake	0	2	1	3	1
copper furnace	1	1	1	2	3
copper frothy	2	0	0	1	2
other/ores?	6	3	0	4	2
Total # of samples removed from Carthage					87
Excavation	1992	1993	1994	1995	1997
Square	4, ?	5,6,7,8,10	6,12,13,15	6,7,8,13,16	6,7,8
Slag type	Sample #s of each sample analyzed				
iron tap	1, 2		4	3, 5	
iron cake	6	9	10	7	8
iron furnace	14		12, 15	11, 13	
iron frothy	18, 19, 20	16,17,21,23			22
copper tap	28	25, 26	24	27	
copper cake		30, 32	31	33	29
copper furnace			36	37	34, 35, 38
copper frothy	39, 43			41	40, 42
other/ores?	44, 45, 47				46, 48
Total # of samples analyzed					48

The variation in size of the slag samples, from less than a few millimeters in length to fist-sized chunks, made representative sampling difficult as well. The smallest pieces of slag were difficult to identify and did not constitute more than 10% of the total volume of excavated slag. Since only samples roughly the size of a dinar could be reasonably thin sectioned with any success, the smaller size fraction of slag pieces were ignored for sampling.

Hand sample characterization using Bachmann's techniques indicated that there were eight categories of slag morphology, four associated with iron metallurgy and four associated with copper metallurgy. The petrology of each slag type is significantly different from the others in terms of morphology, grain size (visible in hand sample), and vesicularity. Each type is briefly described below and illustrated in figures.

Iron tap slag: In hand sample, these slags appear ropey on their surface and are the characteristic dark metallic grey of tap slags that Bachmann describes (1982). This ropey texture is generally considered to be diagnostic of slags that have been tapped out of the furnace; the finger-like runners represent droplets of slag as they emerged from the furnace and cooled as they flowed (Bachmann, 1982; Tylecote, 1980). Figure 4.4 shows a representative iron tap slag. These slags have a relatively high specific gravity and are magnetic. The slag appears homogeneous based on the appearance of smooth, black, metallic surfaces and no visible grains embedded in the slag matrix. Weathering products, in the form of rust colored residues on the surface, are minimal. While the bottom surfaces of the slags are "pocked," that is, they appear to have cooled on a grainy surface, uneven surface, the number of vesicles is small. What few vesicles are evident,



Figure 4.4
Image of iron tap slag showing ropey texture



Figure 4.5
Image of iron cake slag, sample #7

are several millimeters in diameter and well-rounded. Sample sizes range from five to 30 cm in diameter.

Iron cake slags: These slags are similar in terms of color, vesicularity, and specific gravity to the iron tap slags. The surfaces do not exhibit the ropey texture of the tap slags, but are irregular and bumpy with large vesicles open onto the surface. Figure 4.5 show a typical iron cake slag from Yasmina. There is very little evidence for weathering of these slags; virtually no rust appears on the slag surfaces. Two of the samples belonging to this category are bowl-shaped, that is, the bottom surface of the slag is rounded as if it cooled in a rounded mold approximately 10cm in diameter. On these two samples, one of which is pictured in Figure 4.5, crystals are visible in hand sample on the broken surfaces of the slag. These slags are magnetic. Sample sizes range from 10 cm to 15 cm in diameter.

Iron furnace fragments: This slag category includes those slags that clearly had ceramic pieces fused to the slag proper. The morphology of the slag portion of the sample was generally like the tap and cake slags described above in terms of specific gravity, metallic grey color, and low vesicularity. Figure 4.6 shows a representative sample of this type; the curvature of the slag on top likely represents the curve of the inside of a furnace. There is some variation in the colors and textures of the ceramics attached to the slags. Colors range from reddish-orange to black, presumably a function of the amount of oxygen present during the heating of the ceramic. In some samples, the ceramics vary in color from black near the surface attached to the slag, to reddish on the broken surface furthest from the slag/ceramic boundary. Some of the white, rounded grains in the ceramic matrix fizzed in HCl, indicating that at least some of the temper



Figure 4.6
Image of iron furnace fragment, sample #14



Figure 4.7
Image of iron frothy slag, sample #17

used in these ceramics was calcite (CaCO_3). These slags do not appear weathered, i.e. rust-colored weathering rinds are not present. The slag portion of these samples is magnetic. Sample sizes range in diameter from five to eight centimeters.

Iron frothy slags: This category of slag is the most variable in terms of slag color and visible inclusions, but all samples are highly vesicular. Figure 4.7 shows a particularly large and homogeneous iron frothy slag. It is greenish-grey in color; other slags in this category range in color from black to a deep reddish-purple. Vesicles are consistently abundant in the frothy slags, are generally less than two millimeters in diameter, and appear on all surfaces of the slag pieces. White sand-size and larger grains were often visible on the surfaces of the frothy slags; many of the grains fizzed in HCl, again indicative of calcite. Iron frothy slags do not have rust-colored weathering rinds on their surfaces. These samples are weakly magnetic. The sizes of these slag pieces range in diameter from five to 15 centimeters.

Copper tap slag: These slags exhibit the flow texture indicative of tap slags, although this texture does not appear as dramatically as in the iron tap slags on the surface. Figure 4.8 shows a sample representative of this slag type. As with all the copper slags from Yasmina, the surfaces are highly weathered; they are covered in crusts of green and blue copper oxides, hydroxides and carbonates which mask much of the underlying morphology of the slags. Inclusions are not visible from the surfaces due to extensive weathering. These copper tap slags vary in specific gravity, but are generally lighter than the iron tap slags. Despite lower specific gravities, vesicles are rare and no larger than a few millimeters. These samples are non-magnetic and range in diameter from five to 10 centimeters.



Figure 4.8
Image of copper tap slag, sample #25



Figure 4.9
Image of copper cake slag, sample #30

Copper cake slag: Samples in this category exhibit a blockier texture and a higher specific gravity than the copper tap slags. Figure 4.9 shows a typical copper tap slag. Again, much of the actual morphology of the slag is masked by the green weathering products on the slag's surface, so that no inclusions are visible. (The grains visible in Figure 4.9 are sediments adhering as the result of burial). Vesicles are generally absent. These slags range in diameter from five to 15 centimeters and are non-magnetic.

Copper furnace fragments: This category of copper slag morphology was the easiest to recognize in the field. All samples of this type are characterized by the obvious attachment of ceramic fragments to the surfaces of the slag. Figure 4.10 shows a typical copper furnace fragment. Like the iron furnace slags, the slag portions of these samples are denser than the furnace fragments attached. Ceramics are generally reddish-orange in color. Again, green corrosion products mask much of the other features of the slag. Vesicles are not evident. Samples are non-magnetic and range in size from seven to 15 cm in diameter.

Copper frothy slags: This slag morphology is characterized by its high vesicularity. Vesicles range from roughly one to five millimeters in size. These slags are very light (low density) and exhibit a range of colors. Figure 4.11 shows a copper frothy slag; the color varies from greenish to black across the sample. The surfaces of the frothy slags were generally less weathered, revealing more details of the original slag surface. Some of the white grains included in the slag matrix were calcite minerals; others are quartz grains. These samples are non-magnetic and range in size from four to 10 cm in diameter.



Figure 4.10
Image of copper furnace fragment, sample #37



Figure 4.11
Image of copper frothy slag, sample #40

In summary, the categories of slag based on morphological characteristics observed in the field were more readily applied to the iron slags than the copper slags, primarily due to the highly weathered surfaces of the copper slags. Nevertheless, the slag categories allowed for the wide variety of both iron and copper slags to be systematically sampled, ensuring that all slag morphologies were represented in the samples suite returned to the University of Georgia for analysis. As characterization studies continued in a laboratory setting, the field classifications showed variable degrees of success in terms of their applicability. In most cases, each discussed below, observing the mineralogy and petrology of the slags in cross section and thin section, changed the field interpretation of the slag type.

Slag Mineralogy and Petrology

Methodology

While the preliminary field characterization of the metallurgical slag excavated from the fill at the Yasmina Cemetery provided some clues as to the metallurgical processes going on in Roman Carthage, chemical and mineralogical analysis was necessary to verify and interpret the nature of the processes involved in the production of metals. Because of the small number and size of the slag samples, micro-analytical techniques were used, rather than bulk chemical analyses, to obtain the most information possible about the numerous phases in the slags. This was accomplished utilizing both reflected and transmitted light microscopy and an electron microprobe.

From the eight categories of slag established in the field based on textural and morphological differences observable in hand sample, five samples from each category, iron tap, iron cake, iron frothy, iron furnace, copper tap, copper cake, copper frothy, and

copper furnace were selected for analysis along with several additional samples that were unidentified and initially labeled “other.” Samples were cut and sent to a commercial firm (Vancouver Petrographic) for preparation of a polished thin section for each sample. Over half (48) of the 87 slag samples removed from Carthage, were cut sectioned. See the Appendix for a complete list of the samples thin-sectioned and their corresponding sample numbers.

Petrographic analysis on the thin sections used both transmitted and reflected light to determine the mineralogical composition of the slags and to confirm the types of metals being smelted. As each sample was analyzed, photomicrographs were made of diagnostic and interesting portions of the thin sections to produce a photographic data set of the mineral compositions of the slags. Petrographic examination provided another technique to characterize the Yasmina slags, allowing comparison to classifications based on hand sample morphology.

As the petrographic analyses proceeded, the sample suite was again sub-divided in order to analyze chemically each of the four subsets of iron and copper slags. For the iron slags, the microprobe was used primarily to confirm the mineral identifications made from the petrographic work and to obtain quantitative data for the chemistry of the mineral phases. For the copper slags, which proved to be much more difficult to interpret due to their mineralogical complexity, the microprobe served as another analytical tool to characterize and determine the processes associated with copper metallurgy at the site.

The electron microprobe used was a JEOL JXA-8600 available in the University of Georgia Geology Department. Both Energy Dispersive (EDS) and Wavelength Dispersive (WDS) techniques were used to identify phases in the slag samples. EDS

provided qualitative compositional data for mineral identification/verification, while WDS provided a means to quantitatively analyze slag phases of particular significance.

The EDS technique provided a framework for the design of analytical routines to analyze quantitatively specific mineral phases. (The EDS capability of the electron microprobe used for this study was compromised during the spring of 2001, during which time many of the probe analyses were made. Without the EDS, it was difficult to establish the appropriate analytical routines to analyze quantitatively many of the samples. Therefore, a decision was made not to focus on the more complex mineralogical phases, such as those associated with the weathering of the slags).

Analytical standards that most closely approximated the expected composition of the slag phases were run prior to each WDS analytical session. For example, hematite and magnetite standards were run prior to the analyses of iron oxide phases, such as wüstite, in the slags. The beam diameter varied depending on the particular phases to be analyzed during an analytical routine. For oxides, silicates and glass analyses, beam diameters were on the order of 10-20 μm to obtain analytical data over the extent of the phase. For metals (pure, alloys, and mixtures), spot beams (3–5 mm) were used for analyses of these minute and closely associated phases. An accelerating voltage of 15.0 kV was used for all analyses. All petrographic and electron microprobe analyses were performed by this researcher using the University of Georgia Geology Department facilities.

Due to the mineralogical differences between the slags, the iron and copper slag sample suites are treated separately in two sections below. For each type of metallurgy,

iron and copper, the various mineral phases associated with that particular metallurgy are described and discussed.

Iron Slags

Twenty-three of the 48 samples selected for petrographic analysis were from the set labeled “iron slags” in the field from hand sample characterization. The slags are a mixture of formerly molten material and grains of quartz sand. The sand was presumably added to the metal-bearing material to act as a flux, facilitating the production of slag to remove impurities (Tylecote, 1980). The presence of vesicles (former gas bubbles) attests to the previously molten character of the slags. Major mineral phases vary to some extent between the four iron slag morphologies identified in the field, but generally include: iron silicates and oxides, metallic iron, glass, quartz, iron hydroxides, residual ceramics fused or adhering to the slag phases, and rare titanium-iron-oxide (ilmenite) phases. The degree of vesicularity is highly variable between different groups of slags. Table 4.3 summarizes the analytical data from the electron microprobe phase analyses of olivines, pyroxenes, oxides, and metals in the iron slags.

Iron silicates: These minerals generally comprise the major phases in ferrous metallurgical smelting slags (Bachmann, 1982); in the Yasmina slags, the major iron silicate present is the Fe-olivine (fayalite) and Fe-rich pyroxene, hedenbergite.

Fayalite is commonly the most abundant mineral constituent in the slags with crystal sizes ranging from several microns to several millimeters in length. It occurs in a variety of shapes ranging from euhedral crystals to elongate feathery dendritic crystals, depending on the cooling regime of the slag (Donaldson, 1976). Fayalite grain size and shape allow identification of different droplets of slag (different cooling regimes) within

Table 4.3

Iron Slag Phases: Quantitative Data from Electron Microprobe												
PHASE	SAMPLE #											
OLIVINES		SiO2	Al2O3	MgO	FeO	CaO	NiO	MnO	Cr2O3	TiO2	Total	
<i>olivine 5 std large grain</i>		39.4	0.0	44.3	17.0	0.0	0.0	0.2	0.0	0.0	100.9	
fayalite	9	28.9	0.1	1.0	68.5	0.3	0.0	0.2	0.0	0.0	99.0	
fayalite	9	28.8	0.1	1.0	68.8	0.3	0.0	0.2	0.0	0.0	99.2	
fayalite	7	29.2	0.0	0.5	67.9	0.3	0.0	0.2	0.0	0.0	98.2	
		SiO2	TiO2	Al2O3	MgO	FeO	CaO	MnO	K2O	Na2O	Cr2O3	Total
<i>CR augite Std USNM</i>		50.4	0.5	7.8	17.9	4.4	17.8	0.3	0.0	0.8	1.0	100.9
fayalite	9	29.9	0.0	0.1	1.6	66.9	1.2	0.5	0.0	0.1	0.0	100.3
PYROXENES		SiO2	TiO2	Al2O3	MgO	FeO	CaO	MnO	K2O	Na2O	Cr2O3	Total
<i>CR augite Std USNM</i>		50.4	0.5	7.8	17.9	4.4	17.8	0.3	0.0	0.8	1.0	100.9
hedenbergite	13	49.3	0.1	0.1	2.9	28.1	16.1	2.7	0.1	0.0	0.0	99.2
hedenbergite	9	45.6	0.1	2.0	0.5	31.6	19.9	0.2	0.0	0.2	0.0	100.1
hedenbergite	9	44.8	0.1	2.4	0.9	29.6	21.0	0.2	0.0	0.1	0.0	99.1
pyroxene	17	45.6	0.8	6.5	11.7	10.3	24.2	0.2	0.1	0.4	0.1	100.0
OXIDES		Cu	Sn	Sb	Pb	As	Fe	Ag	S	Total		
<i>Hematite std (CMT)</i>		0.0	0.0	0.0	0.0	0.3	61.8	0.1	0.0	62.2		
<i>Magnetite std USNM</i>		0.0	0.0	0.0	0.0	0.2	64.5	0.0	0.0	64.8		
iron oxide	19	0.0	0.0	0.0	0.0	0.0	65.1	0.0	0.0	65.2		
iron oxide	18	0.0	0.0	0.0	0.0	0.0	65.0	0.0	0.2	65.2		
iron oxide	16	0.0	0.0	0.0	0.0	0.0	54.6	0.1	0.0	54.6		
iron oxide	17	0.0	0.0	0.0	0.0	0.0	55.0	0.0	0.0	55.0		
		SiO2	TiO2	Al2O3	MgO	FeO	CaO	MnO	Cr2O3	Total		
wustite	9	0.2	0.1	0.2	0.0	100.2	0.0	0.0	0.0	100.8		
magnetite	9	1.3	2.4	6.0	0.0	84.5	0.0	0.1	0.1	94.5		
magnetite	9	0.7	1.7	5.2	0.1	87.8	0.0	0.1	0.0	95.6		
		Fe	Mn	P	Ti	S	O	Total				
wustite	9	77.5	0	0	0.07	0.002	22.3	99.85				
METALS		Cu	Sn	Sb	Pb	As	Fe	Ag	S	Total		
<i>CMTaylor Pyrite Std.</i>		0.0	0.0	0.1	0.0	0.0	46.9	0.0	51.8	98.7		
iron prill	19	0.1	0.0	0.0	0.1	0.0	96.8	0.0	0.0	97.1		
iron prill	18	0.0	0.0	0.0	0.0	0.0	97.9	0.0	0.0	98.0		
iron prill	18	0.1	0.0	0.0	0.0	0.0	96.0	0.0	0.0	96.1		
GLASSES		SiO2	TiO2	Al2O3	MgO	FeO	CaO	MnO	K2O	Na2O	Cr2O3	Total
<i>CR augite Std USNM</i>		50.4	0.5	7.8	17.9	4.4	17.8	0.3	0.0	0.8	1.0	100.9
glass (cake)	9	48.8	0.2	4.2	1.4	31.4	11.4	0.3	1.4	0.6	0.0	99.7
glass (frothy)	17	43.1	0.0	35.0	0.0	1.7	19.7	0.0	0.0	0.6	0.0	100.1
glass (ceramic)	13	67.4	0.4	7.8	1.5	9.4	4.4	1.0	4.0	1.1	0.0	97.0
		SiO2	Al2O3	FeO	MnO	MgO	CaO	Na2O	K2O	Total		
<i>York 76-C-150 glass std.</i>		56.3	4.4	0.3	0.2	6.5	21.9	9.9	1.5	100.9		
<i>Arenal hornblende std.</i>		41.9	14.6	10.7	0.2	14.4	12.1	2.2	0.1	96.1		
<i>Fayalite Syn OL-11 std.</i>		30.4	0.0	72.4	0.0	0.0	0.0	0.0	0.0	102.8		
glass (cake)	9	52.4	14.4	16.4	0.0	0.0	8.0	1.5	3.5	96.2		
glass (cake)	9	55.1	14.8	11.2	0.2	0.0	10.2	1.8	3.6	96.9		

a single sample (Figure 4.12) suggesting amalgamation of droplets to form some types of slag. In the case of tap slags, the individual droplets are visible under the microscope and the fayalite crystal orientation and form vary between droplets. In Figure 4.12, the areas separated by the droplet boundary show both the euhedral and feathery fayalite textures observable in the slags. For cake slags, those that remained in the furnace during cooling, the fayalite crystals up to 10 mm in length are often visible even without a microscope. Larger crystals result from slower cooling rates.

Fayalite is relatively easy to identify in metallurgical slags. It is colorless to yellowish in plain light, with high relief and high birefringence visible in polarized light, as Figure 4.12 shows. Extinction is parallel to the crystal elongation for this orthorhombic mineral, a useful factor in discriminating fayalite from the other common iron silicate present in the slags: pyroxene.

Experimental olivine studies in the 1970's revealed that olivine crystal morphology changes systematically relative to the rate at which these crystals cooled from a melt (Donaldson, 1976). In general, the longer an olivine-producing melt has to cool, the more euhedral and complete an olivine crystal will be upon solidification. Comparisons of the shapes of olivine crystals from experimental melts with those found in rocks of similar composition, allow geologists to deduce the cooling rate of the rock. Figure 4.13 is a reproduction of Donaldson's summary of the change in shape of olivine crystals in cooling rate and isothermal crystallization experiments using Apollo 12 basalt. Based on a comparison of Figure 4.13 (and other photomicrographs available in Donaldson's work) and the various morphologies of olivine crystals in the iron slags, estimates of cooling rates for the slags can be made.

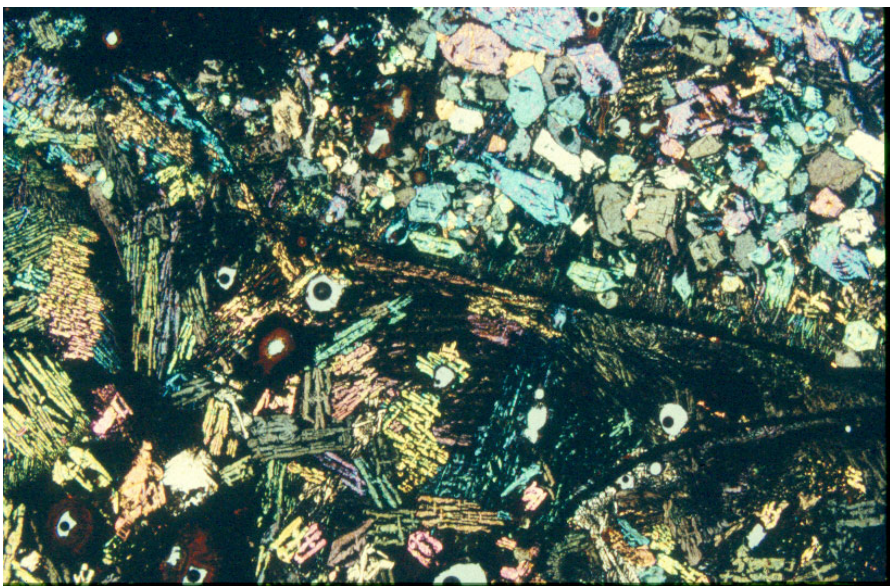


Figure 4.12
 Photomicrograph of fayalite from a tap slag – notice boundary between droplets (Magnification: 10X, transmitted polarized light), sample #5

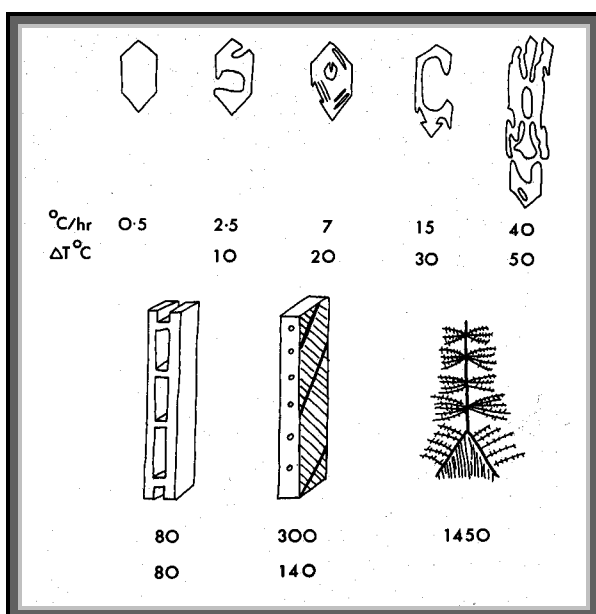


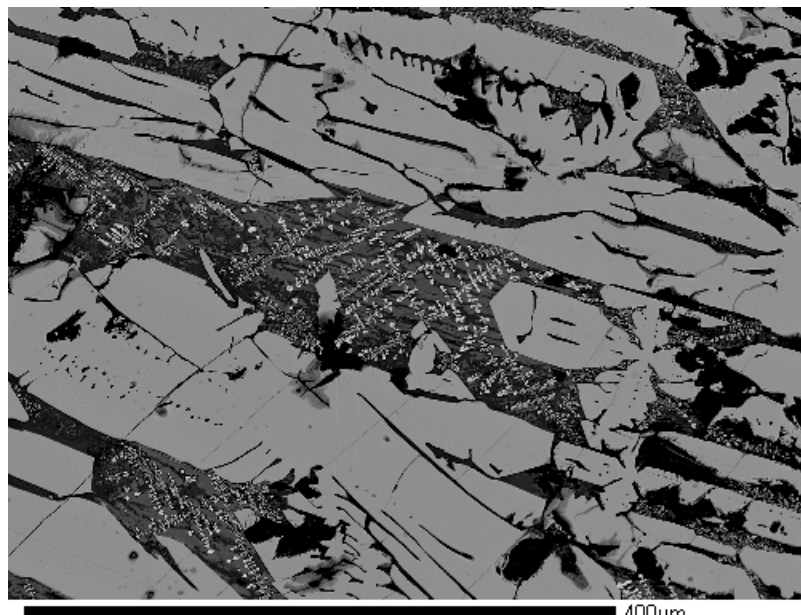
Figure 4.13
 Summary of the change in shape of olivine crystals in cooling rate and isothermal crystallization experiments on anhydrous rock compositions. Numbers refer to cooling rates and degrees supercooling at which particular shapes grew in runs on the Apollo 12 basalt (all crystals drawn with *c* vertical and *a* coming out of page), after Donaldson, 1976.

Figures 4.14 and 4.15 are backscattered electron images of fayalite in a tap slag (sample #4) and a cake slag (sample #9) from the Yasmina slag sample suite. Figure 4.15 shows olivine crystals that are more feathery, less cohesive or solid, and more elongated than those shown in Figure 4.14. Comparison with Donaldson's figure suggests that this particular piece of tap slag cooled in a range between 40°C/hour and 80°C/hour.

Donaldson describes these crystals as "elongate hoppers with marked edge growth" (1976). Figure 4.14 shows fayalite from a cake slag with more euhedral, less elongate and more solid than those from Figure 4.15; these fayalites likely cooled at a rate between 0.5°C/hour and 2.5°C/hour, according to Donaldson's calculations (Donaldson, 1976).

So, the morphology of the fayalites in the iron tap slags indicate they cooled more quickly than the fayalites in the cake slags. This can be explained easily if one considers the other morphological characteristics of these slag types in hand sample. The tap slags exhibit a ropey texture, indicative of having been "tapped" or poured out of the furnace while still molten and then left to cool outside the furnace, probably in a collection pit as illustrated by Tylecote (1976) (Figure 2.2). Cake slags, in some cases, show bowl shaped bottoms and display much larger, more euhedral fayalites, suggesting that they remained in the furnace proper during cooling and thus cooled at a much slower rate than the tap slags outside.

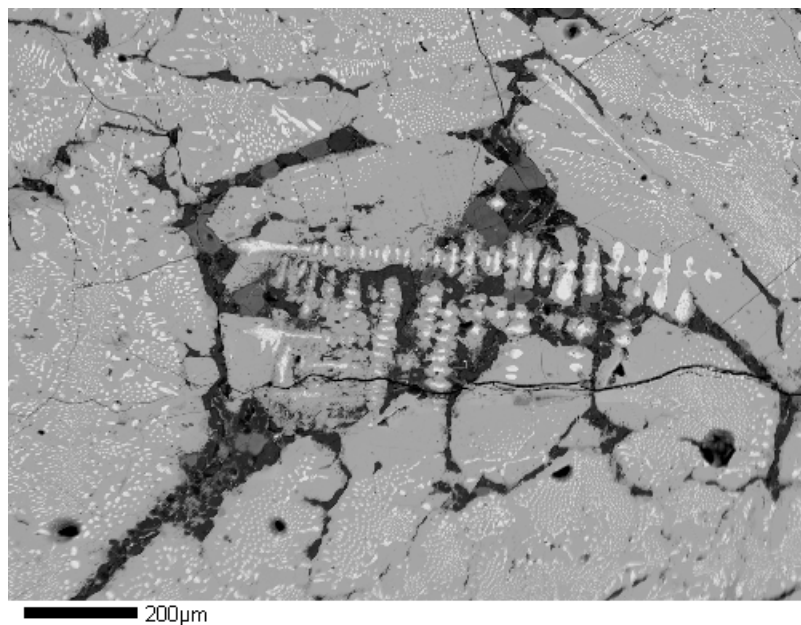
Pyroxene, $(\text{Fe, Mn, Mg})\text{O} \cdot \text{CaO} \cdot 2\text{SiO}_2$, also frequently occurs in the ferrous Yasmina slags, although in less abundance than fayalite. According to Bachmann (1982), pyroxene usually occurs in association with fayalite (Bachmann, 1982). The form of the crystals varies from euhedral to anhedral, depending on the cooling regime and general chemistry of the slag. When it occurs, pyroxene is generally finer-grained



BSI 4 wustite_olivine

Figure 4.14

Backscattered electron image of fayalite crystals (grey) from a tap slag; iron oxide dendrites and glass are interstitial, sample #4



BEI wustite - dendritic growth

Figure 4.15

Backscattered electron image of fayalite crystals (grey) from a cake slag; iron oxide dendrites and glass are interstitial, sample #9

than fayalite, on the order of several microns in length. This size difference indicates that the pyroxenes cooled more quickly out of the melt left behind after the olivines cooled, probably as the slag was removed from the furnace. Pyroxenes of two general types are found in the Yasmina slags: hedenbergite ($\text{CaFeSi}_2\text{O}_6$) is fairly common and wollastonite (CaSiO_3) is rare. Which pyroxene occurs in a slag depends on the elements locally available in the melt; elements in the melt are determined by the chemistry of the ore, the furnaces, the fluxes, and the fuel used during the smelting process.

Figure 4.16 shows the close association of pyroxenes (green, fine grained) adjacent to fayalite (higher birefringence, coarse-grained). The pyroxenes tend to be finer grained than the fayalites in the slags and appear in greater abundance in the presence of a silica source, such as the quartz grains incorporated into the slag in Figure 4.16 (lower left corner of photomicrograph).

Iron oxides: Next to silicates, iron oxides are the most important slag constituents (Bachmann, 1982) and occur in abundance in the Yasmina iron slags. The iron oxide, magnetite, Fe_3O_4 , is the most common oxide present in these slags and occurs as rare euhedral crystals, and more commonly as dendrites and as amorphous blebs. Morphology varies depending on location relative to other slag constituents, the type of iron slag, and the cooling history. The size of the iron oxide phases in the iron slags can be measured on the order of microns.

Magnetite is most easily visible in reflected light (see Figure 4.17); it is shown here in its dendritic form, which resulted from its relatively quick growth out of the residual glass upon cooling (Ettler, 2001). Also present in this image are fayalite (light grey) and interstitial glass (dark grey). Magnetite is present in nearly all metallurgical

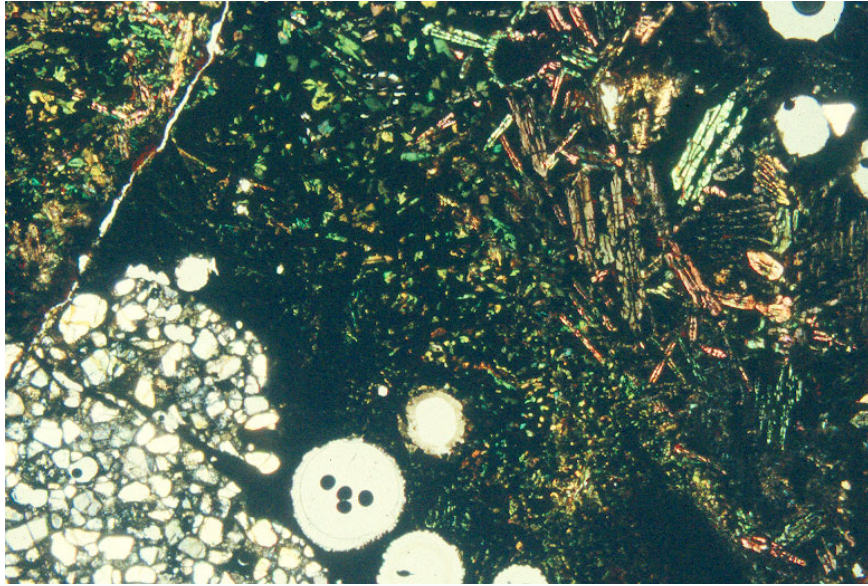


Figure 4.16

Photomicrograph of pyroxene, quartz inclusion, vesicles, and fayalite from a cake slag (Magnification: 10X, transmitted polarized light), sample #9

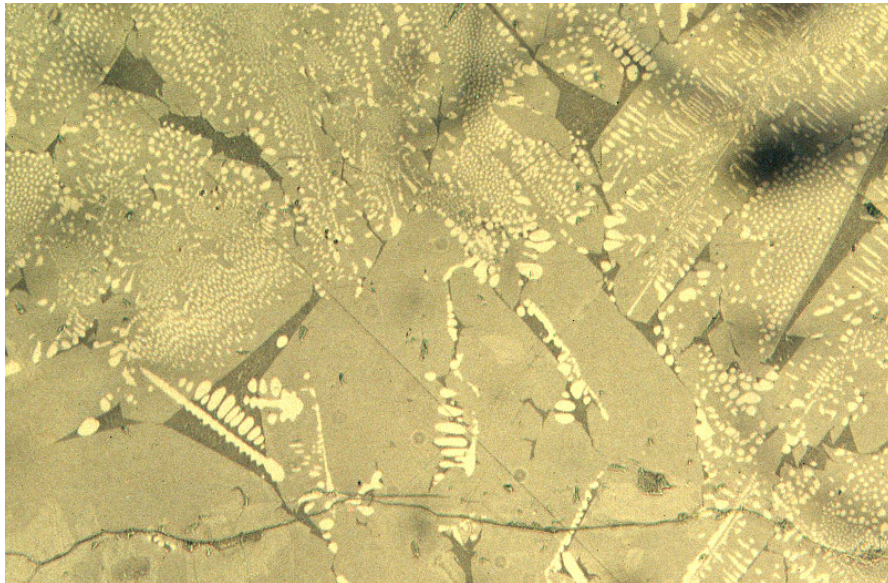


Figure 4.17

Photomicrograph of dendritic wüstite/magnetite with fayalite (large, grey crystals) and glass from a tap slag (Magnification: 10X, reflected light), sample #1

slags with high FeO contents; it is either embedded in the silicate matrix as small grains or crystal skeletons, or in idiomorphous crystals, sometimes of considerable size (Bachmann, 1982). The presence of magnetite is also easily detected with a small magnet.

Wüstite, FeO, is also occasionally found in these ferrous slags. Both magnetite and wüstite have dendritic crystal habits, crystallized out of glasses interstitial to the fayalite crystals and are most easily observable with backscattered electron images. In order to distinguish magnetite from wüstite chemically, elemental iron oxide analyses were subjected to a recalculation program that can account for the differences on the oxidation state of iron (Fe²⁺ versus Fe³⁺) (Carmichael, 1967). These recalculations indicated that the majority of iron in the dendrites was Fe³⁺ or magnetite. Some dendrites (rare) were also identified as hematite (Fe₂O₃) using this recalculation routine.

Iron-titanium-oxides (ilmenite) also occur rarely in the iron slag sample suite. They commonly appear as fine-grained, elongate or blocky oxide grains embedded in a glass matrix. In some samples, they are several microns in size, while in other they are too small and narrow for even the electron microprobe to analyze (less than several microns). The ilmenite is only distinguishable from the other iron oxides in the slags with analysis on the electron microprobe.

Obtaining sufficiently high analytical totals for elemental analysis of some of the iron oxides was difficult, suggesting that many of these phases are hydrated.

Metallic iron: At least two samples, #18 and #19, contained metallic iron; the results of the analyses of these metallic prills are shown in Table 4.3. The WDS analyses

show that the iron metal is essentially pure iron; none of the other metallic elements analyzed are above the detection limits of the electron microprobe.

Figure 4.18 shows a reflected light image of the iron metal prills surrounded by fayalite in the slag matrix. That the iron prill is surrounded by the fayalite suggests that the fayalite grew around the metallic iron as the slag cooled and that the iron prill was present in the melt. In reflected light the iron appears as a bright, rounded prill on the order of a few microns in diameter. The reflectivity of the iron is higher than the reflectivity of the iron oxides and the iron is brighter than the iron oxides in the back-scattered electron images. Quantitative analytical techniques were required to identify positively the metal as iron. Figure 4.19 shows the complexity of the iron prills; this prill is a mixture of metallic iron and oxidized iron.

The presence of metallic iron in bloomery slags is common, as the melting temperature of iron, at 1535°C, was not obtained in iron smelting furnaces until modern blast furnaces were developed (Bachmann, 1982). Bloomery slags typically contain wrought iron as spongy masses, isolated nodules, or flaky particles (Bachmann, 1982). In these two iron slags from Yasmina the metallic iron appears as isolated nodules or as multi-phase prills.

Glass: The amount of glass in the ferrous slags from Yasmina varies depending on the particular type of iron slag. For tap and cake slags, Figures 4.14 and 4.15 show that glass occurs primarily as interstitial pools between crystals of fayalite and iron oxide. The pools of glass are small, on the order of microns, and only rarely does a pool extend from the bottom to the top of the thin section. The glass thus appears opaque in plain and polarized light, despite its transparency, so it is best viewed in reflected light. For the

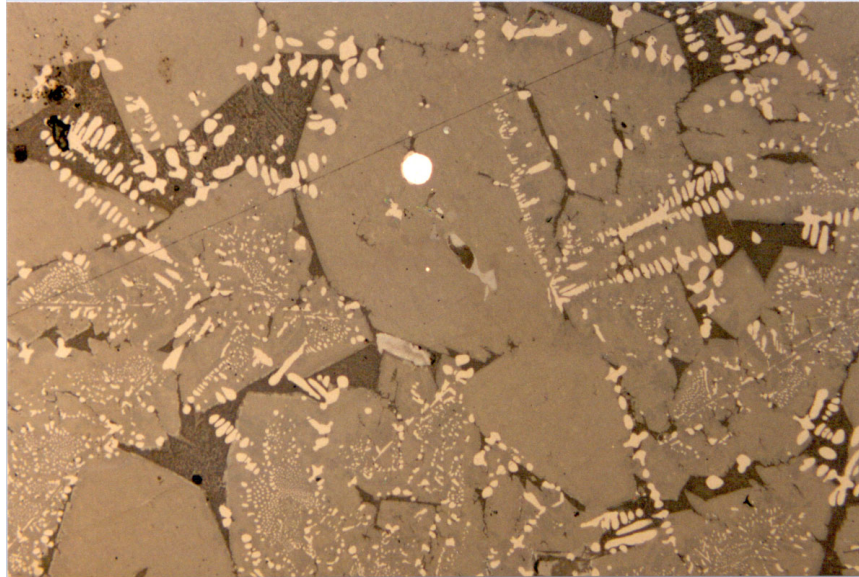
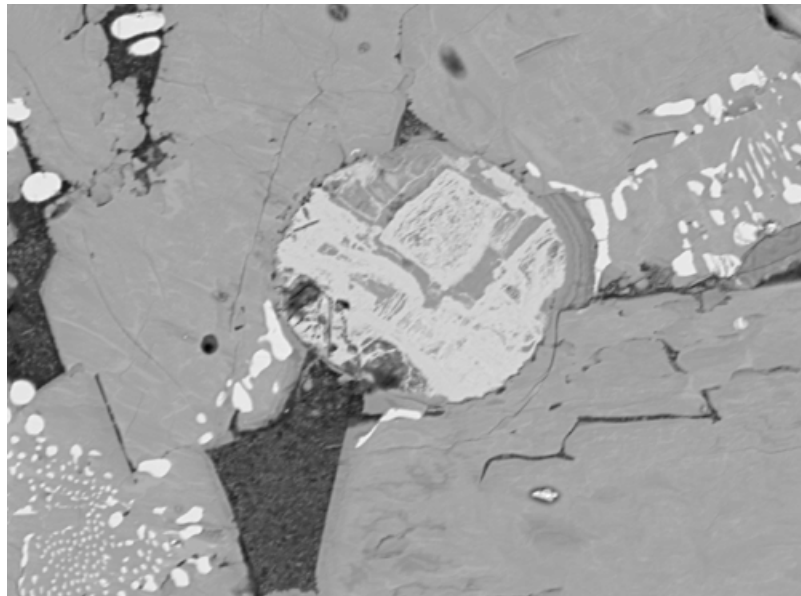


Figure 4.18

Photomicrograph of metallic iron prill (bright) with fayalite (grey) and iron oxides (dendritic, white), (Magnification: 20X, reflected light), sample #19



BEI #18, round multiphase iron prill

Figure 4.19

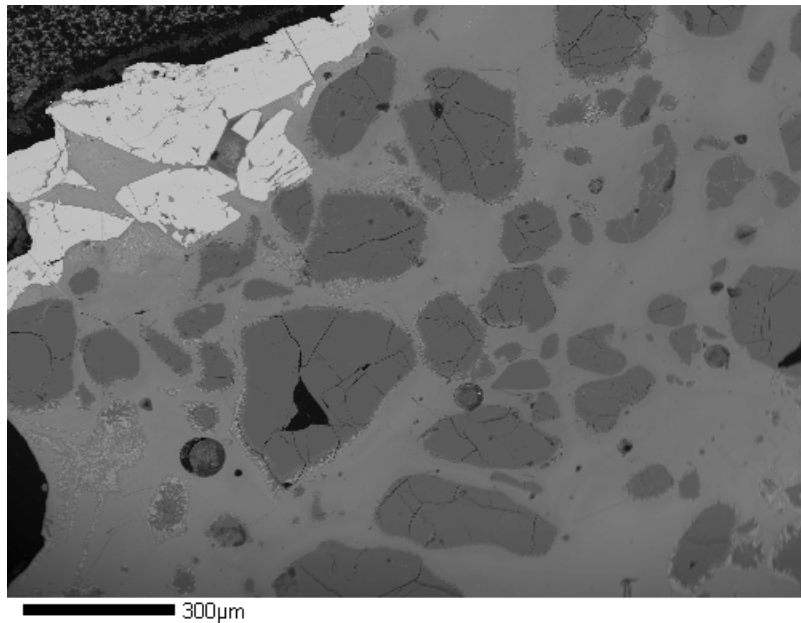
Backscattered electron image of multiphase iron-rich prill (center, light grey) surrounded by fayalite (grey) and dendritic iron oxides, sample #18

frothier samples, like Figure 4.20, glass is much more abundant and of variable composition relative to the other mineral constituents in the slag.

Figure 4.21 and Figure 4.22 show two more iron slags with glass interstitial to fayalite and wüstite. In the transmitted light photomicrograph, the black areas surrounding the large fayalite crystals are composed of glass and iron oxides. In reflected light, the glass appears dark grey.

Electron microprobe analyses of the glasses in the iron slags, shown in Table 4.3, indicate that the glasses are of variable composition, depending on specific type of iron slag from which it came. Many of the Yasmina slag glasses, particularly the frothier samples such as #17, are indeed anorthitic ($\text{CaO} \cdot \text{Al}_2\text{O}_3 \cdot 2\text{SiO}_2$) in composition as Bachmann suggests should be expected (1982). Alternatively, sample #9, a cake slag, contains glasses that are much higher in iron than an anorthitic glass and that vary considerably in their iron content throughout the sample.

Obtaining analytical data for iron slag glasses was difficult due to the interference of very fine-grained pyroxene minerals crystallizing in the melt and this explains some of the variability in composition. Sample #7, however, contained glass pools of sufficient size to obtain reproducible quantitative data. The result of the glass analyses performed on this sample are shown in Table 4.4 and are correlated with Figure 4.23 and 4.24, which show the location of these spot analyses. The figures show how small the glassy areas were in the iron slags. Figure 4.24 shows the fine-grained hedenbergite in the iron glasses; this is the source of the heterogeneity in the glass analyses. Nevertheless, the glass analyses in Table 4.4 show that the iron slag glasses are generally iron and silica-rich with variable amounts of calcium, aluminum, and potassium.



BEI 13-3 quartz, glass, Fe phase

Figure 4.20

Backscattered electron image of glass matrix (light grey), quartz (dark grey), and weathering product (white crystals) in an iron slag; glassy portion is indicative of a ceramic portion of the slag, sample #13

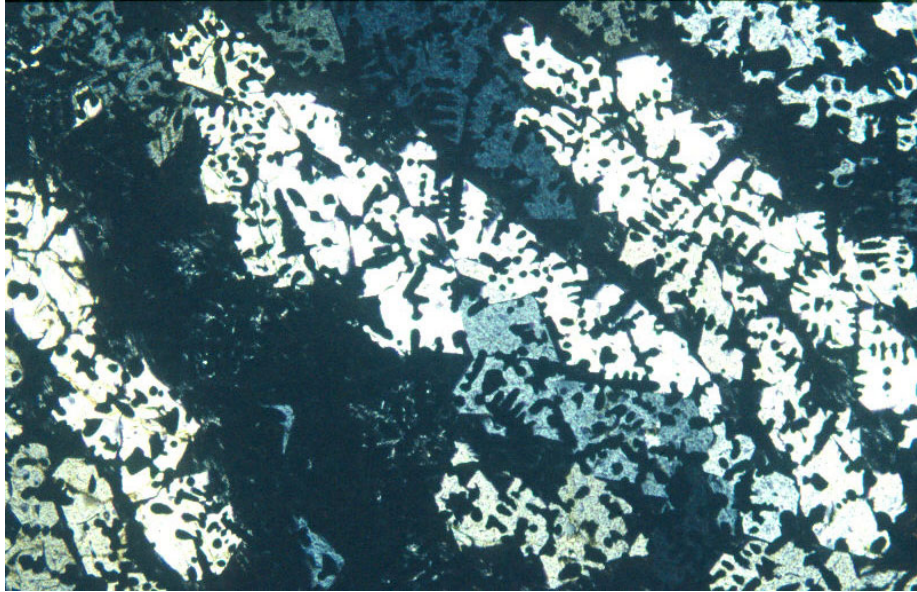


Figure 4.21

Photomicrograph of fayalite (white and blues), iron oxides (black dendrites) and glass (black interstices), (Magnification: 10X, transmitted light), sample #8

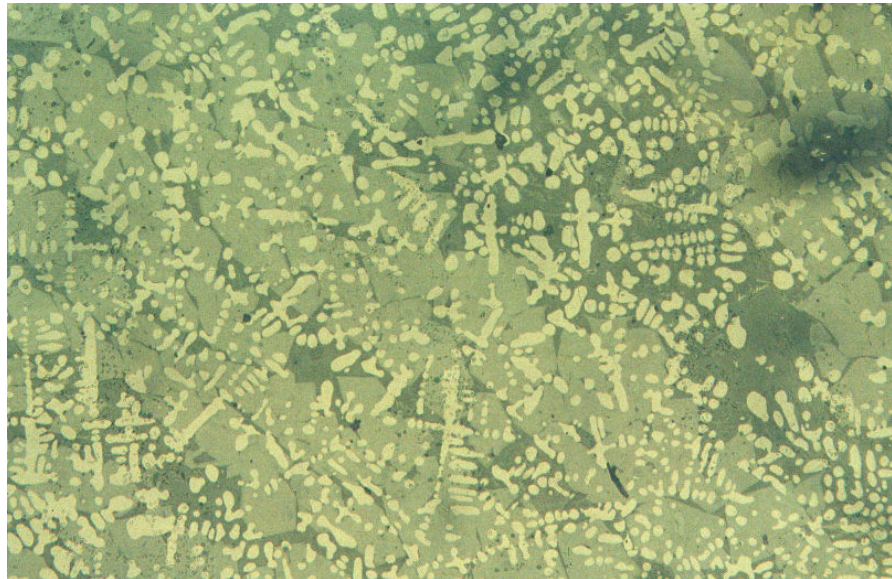
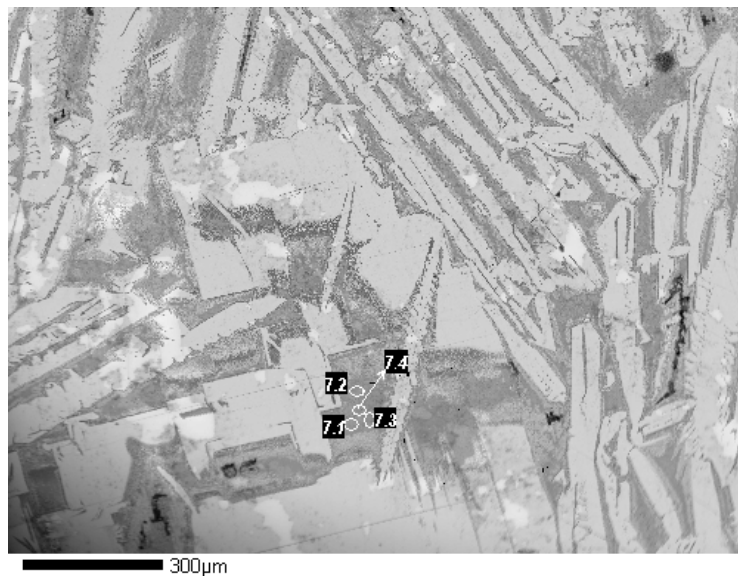


Figure 4.22

Photomicrograph of fayalite (light grey), iron oxides (white dendrites), and interstitial glass (dark grey), (Magnification: 10X, reflected light), sample #8

Table 4.4

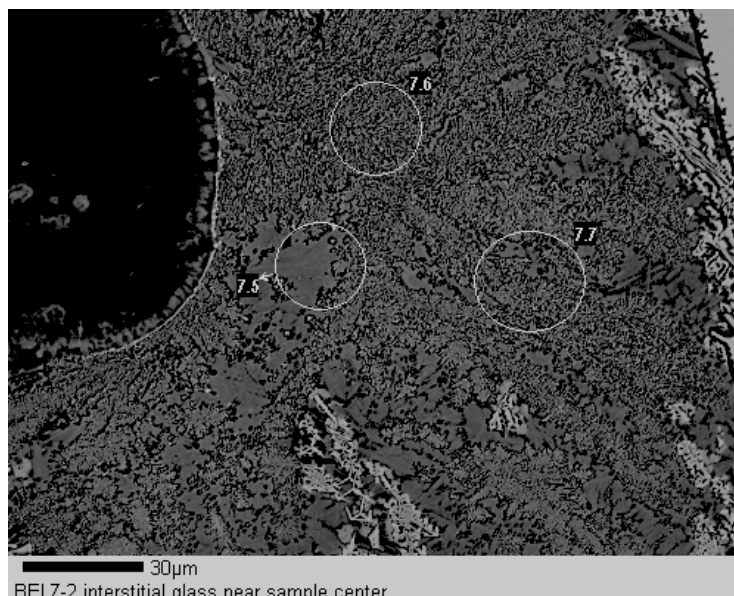
Iron Slag Glass Analyses						
Sample #7						
Oxide	Point 7.1	Point 7.2	Point 7.4	Point 7.6	Average	STDEV
SiO ₂	47.41	45.63	47.67	48.20	47.23	1.11
Al ₂ O ₃	5.96	6.17	5.97	6.25	6.09	0.15
FeO	37.60	36.26	36.42	36.21	36.62	0.66
MgO	0.00	0.00	0.01	0.00	0.00	0.01
CaO	3.09	1.75	3.43	2.73	2.75	0.73
Na ₂ O	0.54	0.92	0.22	0.44	0.53	0.29
K ₂ O	2.42	2.82	2.60	3.12	2.74	0.30
MnO ₂	0.10	0.00	0.07	0.13	0.05	0.07
Total	97.11	93.55	96.32	97.08	94.94	1.96



BEI 7-1 fayalite with interstitial glass

Figure 4.23

Backscattered electron image of point analyses of interstitial glass; fayalite (light grey), iron oxides (white), glass (dark grey), sample #7



BEI 7-2 interstitial glass near sample center

Figure 4.24

Backscattered electron image of spot analyses of interstitial glass; glass is partially re-crystallized, vesicle (black), sample #7

Thirty-three glass analyses were performed on various iron slags using several analytical routines. Glasses proved to be relatively heterogeneous throughout the iron slags, but generally fell within the chemical parameters shown on Table 4.3. Glass formation depends on the composition of the melt and the crystallizing minerals; if the stoichiometric proportions of elements promoting crystal formation are not present, these residual elements not taken by crystallizing minerals are concentrated in the remaining melts, creating highly variable melt compositions both between slag pieces and within the same sample. Rapid cooling of the molten slag quenches the melt to a glass (Bachmann, 1982).

Quartz: Fine-grained quartz is found in several of the Yasmina slag samples. It typically occurs as an occasional grain incorporated into the slag, adhering to the slag surface (the result of the molten slag having been poured onto the sandy ground), or as part of a vitrified ceramic that is fused to the slag. The grain size and shape varies from very fine-grained to coarse-grained from angular to sub-rounded. Often the quartz grains were fractured.

In one cake slag sample, fine-grained quartz was incorporated into the once molten slag as a localized mass (Figure 4.16). Here the quartz grains vary in size from fine grained to very fine grained and do not show extensive fracturing.

In general, the ferrous metallurgical slags contain only trace amounts of fine-grained quartz along sample edges. This is most likely due to incorporation of quartz into the molten slag as it was poured or, in the case of sample #9, the result of the addition of quartz as a flux during smelting. Quartz sand was commonly used as a flux in iron

smelting to combine with iron and impurities in the system to produce low-viscosity fayalitic slags (Bachmann, 1982).

Vesicles: The ferrous slags have variable proportions of vesicles. The tap and cake slags contain a few vesicles, generally only up to a few millimeters in diameter along the outer surface of the slag sample. The size and location of these vesicles indicates that they resulted from gas evolution as the slag cooled. Iron frothy samples and some of the iron furnace samples, however, are extremely vesicular (frothy), with abundant vesicles of varying size and shape throughout the slag. The abundance of vesicles suggests that these frothy slags formed in a more oxidizing environment than the iron slags with fewer vesicles.

Iron hydroxides: The aridity of ancient and modern Carthage did not cause extensive weathering of the ferrous slags; weathering products, such as iron hydroxides and hematite, are limited to vesicles that were exposed to the atmosphere over the course of their burial or as rare grains in the slags. Figure 4.25, taken in plain light, shows an in-filling iron hydroxides lining a vesicle. These rinds are typically rust-colored in plain light and do not penetrate into the slag matrix more than a few millimeters around a vesicle. Vesicles that are internal, that is, were not exposed to the atmosphere for long periods of time, do not contain these weathering products.

Residual Ceramics: The presence of the ceramics was indicated by the reddish to black clay matrix and temper of quartz and/or calcite grains adhering to the grey-black, metallic slag. Mineral phases associated with residual ceramics consist primarily of quartz grains, ranging in size from a few microns to several millimeters, and clay and/or glass. The ceramic portions of the slags do not exhibit fayalite-wüstite mineralogy, but

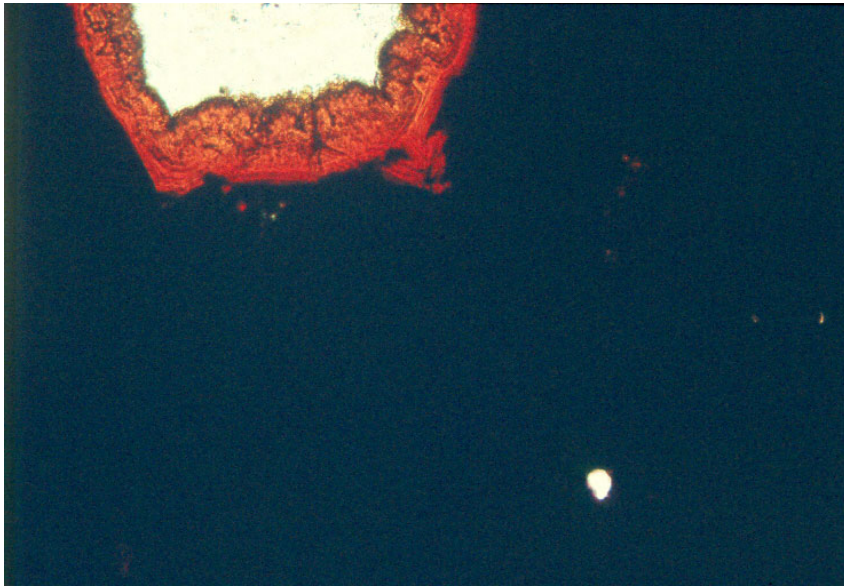


Figure 4.25
Photomicrograph of iron hydroxides (red) filling in a vesicle; tap slag
(Magnification: 10X, plain transmitted light), sample #2

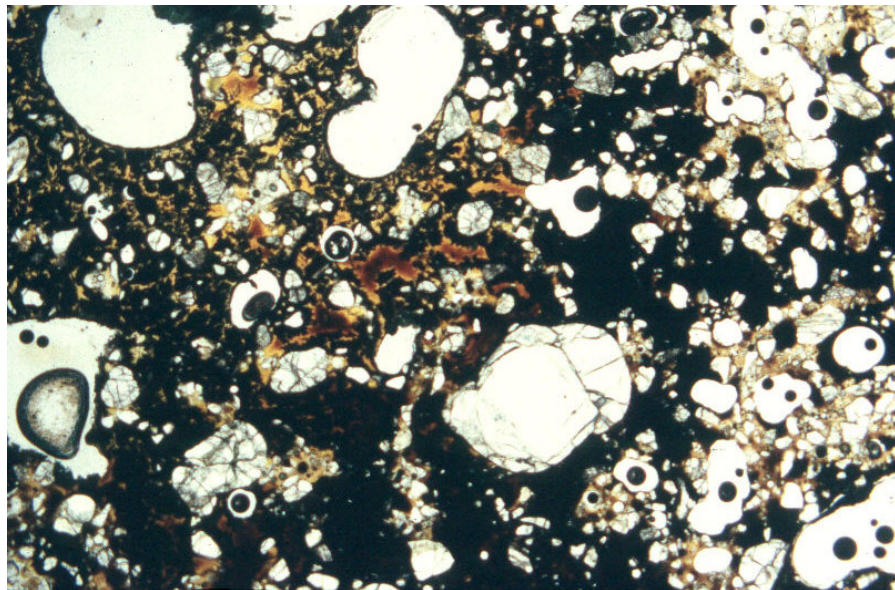


Figure 4.26
Photomicrograph of partially vitrified ceramic portion of slag; quartz
(fractured white grains), glass (reddish-yellow), slag (black), vesicles
(rounded white areas), (Magnification: 2.5X, plain transmitted light),
sample #13

rather amorphous anorthitic or iron-rich phases of varying degrees of vitrification. In plain light, these quartz rich glasses are reddish-yellow to brown in color and the abundance of quartz grains is clearly visible (See Figure 4.26). The clays are opaque in plain light, but polarized light reveals the un-vitrified clay-rich matrix and abundant quartz and calcite grains.

For sample numbers 13, 14, and 23, it was evident that ceramics were adhering to the slag only after the samples were cut for thin section. The friability of the ceramic resulted in detachment during cutting for thin sections. Therefore, no analytical data are available for the un-vitrified ceramics. Table 4.3 shows one analysis from the vitrified ceramic portion of sample #13. Elemental analysis revealed a chemical composition similar to other glasses in the iron slags, indicating the iron-rich melt permeated (and probably strengthened) the ceramic.

Discussion of iron slag petrography

The ferrous slags from the Yasmina site have a fairly concise mineralogy composed of fayalite and hedenbergite, wüstite and magnetite, iron, glass and iron hydroxides, along with varying amounts of vesicles and ceramic fragments adhering or incorporated into the slag. The minerals in the iron slags reflect three phases in the history of the slag as it cooled. At high temperatures, while the slag was still in the furnace, the slag was entirely molten except for bits of metallic iron. As the slag cooled slightly, fayalite started to grow. As the temperatures continued to decrease (in or out of the furnace), more fayalite along with pyroxene and iron oxides formed. As cooling continued, eventually lower temperature minerals, such as hedenbergite and iron oxides, crystallized from the glassy melt. Finally, after the slags had cooled completely and were

subsequently buried, weathering of the slags began, forming iron hydroxides and hematite. Quartz is present in some slags and seems to have been introduced to the system either from the slag collection pits outside the furnace, as in the case of tap slags, or from residual ceramic furnace fragments vitrified during the smelting process. Slags with portions of the furnace attached or incorporated via vitrification, tend to be more vesicular, less dense, and contain more quartz, than the tap or cake slags.

The four categories of iron slag types identified in the field classification were reassessed based on the information gained from the micro-analytical analysis, i.e. the field classifications of the slags were not always consistent with the petrographic analyses. After the petrographic survey of the slag, it was evident that there were five types of iron slag with distinct mineralogies, rather than the four (iron tap, iron cake, iron frothy and iron furnace fragments) identified in the field. Table 4.5 shows the original field classification and the re-classification of the iron slags based on the data collected from petrographic and electron microprobe analyses. As the table indicates, in some cases the type of metallurgy, i.e. iron versus copper, with which the slag was associated in the field, was not confirmed by petrographic analysis. Each of the five categories of iron slag outlined briefly on Table 4.5 are described below and accompanied by a photomicrograph and/or a backscattered electron image (BEI).

Iron tap slag: For the five iron tap slags analyzed, micro-analytical analyses confirmed the identifications made in the field. All five samples (#1, #2, #3, #4, #5) were primarily fayalitic in composition, with minimal interstitial glass of anorthitic composition and skeletal iron oxides. The ropey textured surfaces of these hand samples, interpreted as evidence of the slag being run out of a tap hole (Bachmann, 1982), is

Table 4.5

Iron Slag Re-categorization			Characteristics of Slag types:
Sample #	Original Designation (based on field obs.)	Re-categorization (based on petro/micro)	
1	iron tap slag	iron tap slag	<u>iron tap slag</u> : abundant euhedral fayalite, skeletal wustite, minimal interstitial glass of anorthitic composition, quartz adhering, boundaries between slag droplets evident, ropey texture on upper surface, "pocked" texture on lower surface, metallic grey in color, magnetic
2	iron tap slag	iron tap slag	
3	iron tap slag	iron tap slag	
4	iron tap slag	iron tap slag	
5	iron tap slag	iron tap slag	
6	iron cake slag	iron cake slag	
7	iron cake slag	iron cake slag	<u>iron cake slag</u> : abundant euhedral fayalite, skeletal wustite, minimal interstitial glass of anorthitic composition, quartz adhering, slightly concave upper surface, "pocked" lower surface - slightly convex in some cases, metallic grey in color, magnetic
8	iron cake slag	iron cake slag	
9	iron cake slag	iron cake slag	
10	iron cake slag	copper related slag	
11	iron furnace slag	weathered iron fragment	<u>iron furnace slag</u> : abundant euhedral fayalite, skeletal wustite, minimal interstitial glass of anorthitic composition, metallic iron prills surrounded by fayalite present (trace), slag phases fused to partially vitrified ceramic composed of clay, quartz, and calcite grains, magnetic
12*	iron furnace slag	iron furnace slag	
13	iron furnace slag	slagged ceramic (iron)	<u>iron furnace slag</u> : abundant euhedral fayalite, skeletal wustite, minimal interstitial glass of anorthitic composition, metallic iron prills surrounded by fayalite present (trace), slag phases fused to partially vitrified ceramic composed of clay, quartz, and calcite grains, magnetic
14*	iron furnace slag	slagged ceramic (iron)	
15	iron furnace slag	iron furnace slag	
16	iron frothy (dense)	iron cinder/bear	
17	iron frothy (dense)	iron cinder/bear	
18	iron frothy slag	iron furnace slag	
19	iron frothy slag	iron furnace slag	
20	iron frothy slag	iron cinder/bear	<u>slagged ceramic</u> : ceramic composed of clay and coarse grained calcite and quartz, slagged surface is magnetic, dark grey and vitreous in luster, distance slag penetrated into the ceramic is evident in cross-section
21	iron frothy slag	iron cinder/bear	
22	iron frothy slag	iron cinder/bear	
23	iron frothy slag	slagged ceramic (iron)	
*thin sections could not be made of these samples due to their friability; their reinterpretation is based on observations made after they were cleaned and cross-sectioned			<p><u>iron bear</u>: DEF: "material resulting from the reaction of molten smelting products with the refractory lining of the furnace hearth" (Bachmann, 1982)</p> <p>glass of variable composition, very fine grained ilmenite grains, plagioclase crystals, highly vesicular, magnetic</p> <p><u>iron cinder</u>: DEF: "cinders and slags are similar in their chemical composition (60-70%iron oxides and about 20% silica)...cinders are very porous, and often the shape of individual ore lumps can still be distinguished." (Bachmann, 1982)</p> <p>dark grey, grainy appearance, fine grained quartz and calcite in an unvitrified matrix, whole shell evident in cross section, no vesicles</p>

consistent with the presence of different cooling regimes evident within the slag (Figure 4.27). Iron oxide-rich boundaries formed between different droplets of slag as they poured out of the furnace and cooled in a lump outside. Quartz grains were rare, and if present, were adhering to the sample edges rather than incorporated into the slag matrix.

Iron cake slag: For the five iron cake slags analyzed, micro-analytical techniques confirmed that four of them were consistent with field identifications. Thin sections of samples #6, #7, #8, and #9 revealed abundant euhedral fayalite crystals, skeletal wüstite, and minimal interstitial glass of anorthitic composition (See Figure 4.28). Unlike the iron tap slags, the iron cake slags, do not exhibit flow textures or boundaries between droplets of slag. This category of slag is characterized by its large fayalite crystals whose morphology is indicative of slow cooling (Donaldson, 1976), perhaps in the furnace bottom as opposed to collecting outside the furnace as with the tap slag. Equally possible is that slag collected in the small slag pits commonly dug into the earth outside Roman smelting furnaces (See Figure 2.2) (Tylecote, 1962).

The occurrence of iron-magnetite-wüstite helps to define the conditions of the high temperature part of the process as well as some of the cooling history of the slag. As noted earlier, the presence of metallic iron in some of these slags is a result of the incorporation of iron in the molten silicate slag. As the slags cooled, wüstite and magnetite formed. According to Craddock's (1995) diagram (Figure 4.29) plotting temperature versus partial pressure of oxygen, the Yasmina tap and cake slags indicate operating temperatures in the range of 1100°C to 1200°C by the presence of magnetite and wüstite under reducing conditions ($-\log p_{O_2}$ around 20).

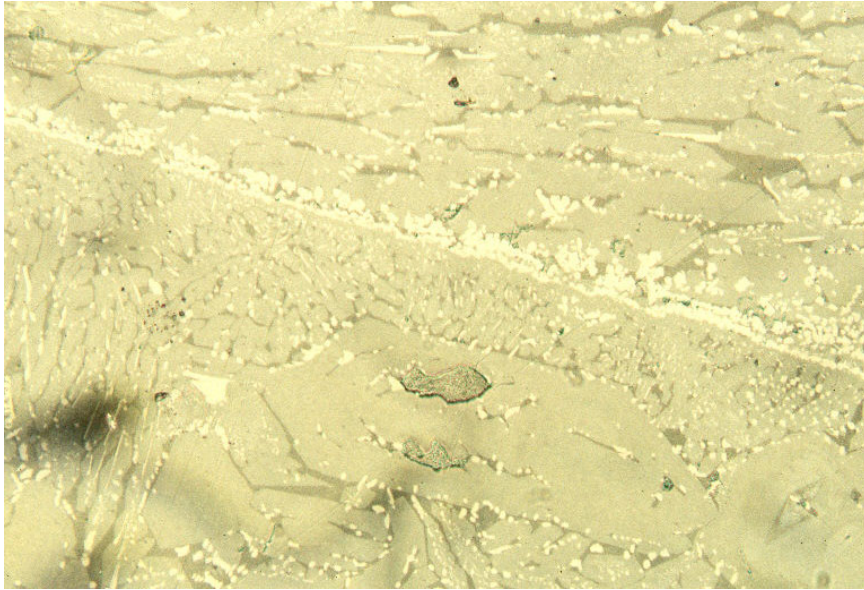


Figure 4.27
Photomicrograph of droplet boundary in iron tap slag, fayalite (light grey), iron oxides (white), and interstitial glass (dark grey), (Magnification: 20X, reflected light), sample #5

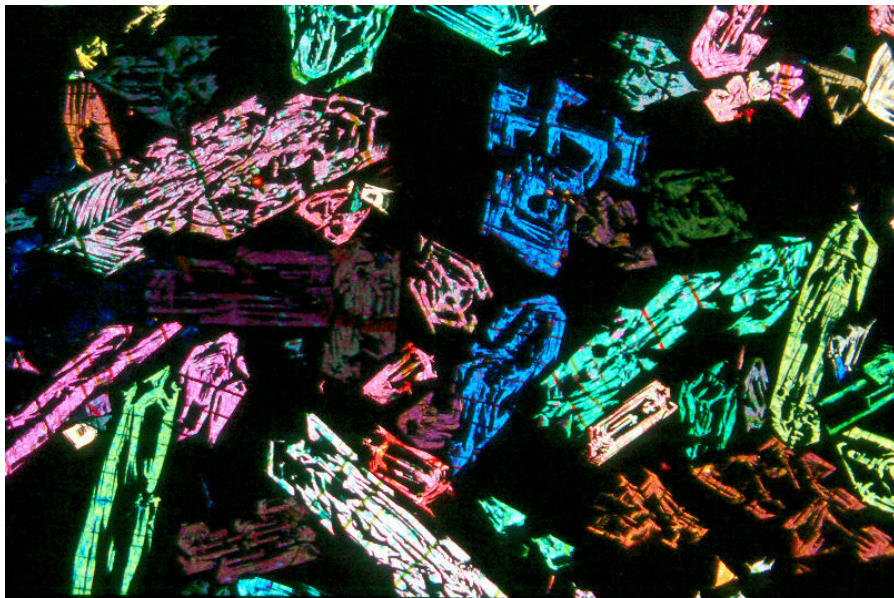


Figure 4.28
Photomicrograph of iron cake slag, fayalite (brightly colored crystals), iron oxides and glass (black), (Magnification: 2.5X, polarized transmitted light), sample #7

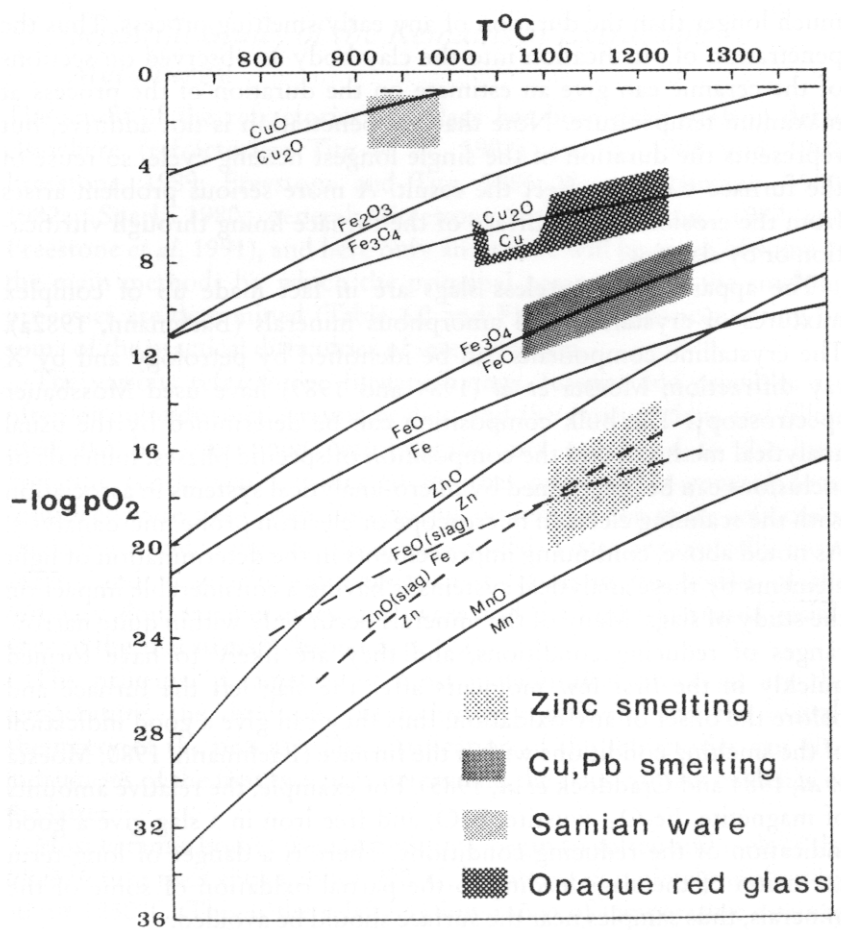
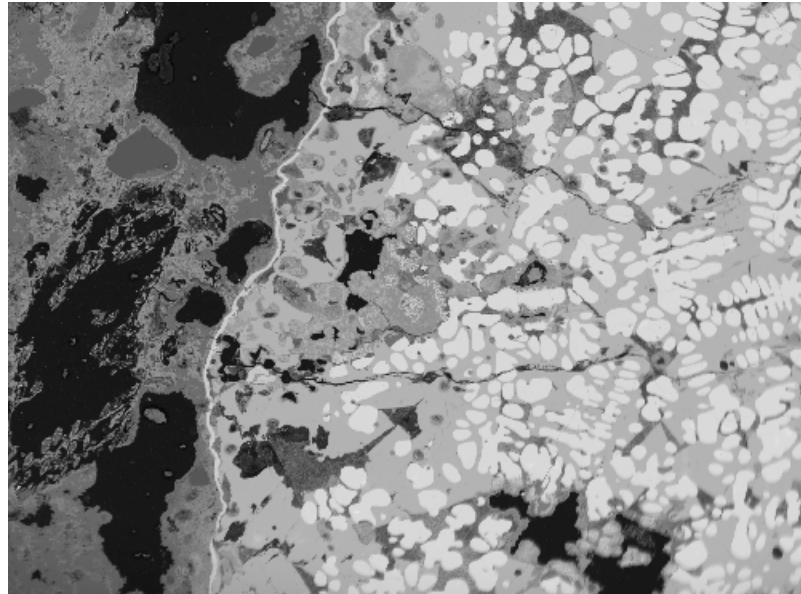


Figure 4.29
Plot of partial oxygen pressure against temperature. From study of the associated refractories and slags, the principal parameters of most metallurgical processes can be determined and represented as shown here. (Craddock, 1995).

Iron furnace slags: The variable mineralogy of the samples initially identified as “iron furnace slags” resulted in the re-classification of several of these samples. After petrographic and microprobe analyses, samples #12, #15, #18, and #19 were assigned to this category defined by the presence of slag compositionally similar to iron cake slags, but with the additional component of ceramic fused to the slag (See Figure 4.30). There is a distinctive clear break between the slag portion and the ceramic portion of the sample, as Figure 4.30 shows. The slag portion is composed of fayalite, iron oxides, and minimal interstitial glass, in addition to rare prills of metallic iron (See Figure 4.31). The metallic iron prills are on the order of only a few microns. These iron furnace slags are the only slags in which metallic iron was found. Analyses of the iron prills are shown in Table 4.3. The ceramic component fused to the slag clearly indicates that this portion of the slag remained in the furnace, rather than being tapped off as the iron tap slag.

Slagged ceramic: In addition to the iron furnace fragments, there were several samples that grouped together mineralogically that were distinct from any of the other categories of slag already mentioned. Samples #13, #14, and #23 were defined as slagged ceramics based on their distinct mineralogy consisting primarily of clay and coarse-grained quartz and calcite (See Figure 4.32). Some parts of the ceramics in these samples were completely vitrified, indicated by a reddish-yellow to brown glass. A layer of slag, generally less than a millimeter in thickness, adheres to the sample surface. The slagged surface is magnetic, with a typical fayalite-wüstite-glass mineralogy. Slag crystal sizes are on the order of a few microns, rather than the few millimeters evident in other slag types. Thin sections of the samples revealed slag penetrating into the ceramic along cracks as portions of the furnace melted during the smelting process.



BEI 15-2 boundary between two phases

Figure 4.30

Backscattered electron image of boundary between ceramic portion (left) and slag (right), sample #15

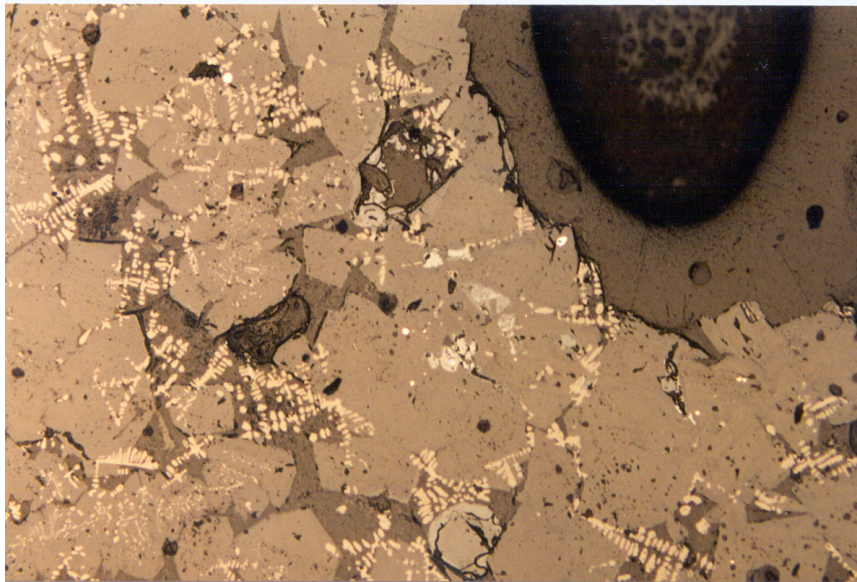


Figure 4.31

Photomicrograph of iron furnace slag with metallic iron prills (bright), fayalite (medium grey), and iron oxides (white dendrites) (Magnification: 10X, reflected light), sample #18

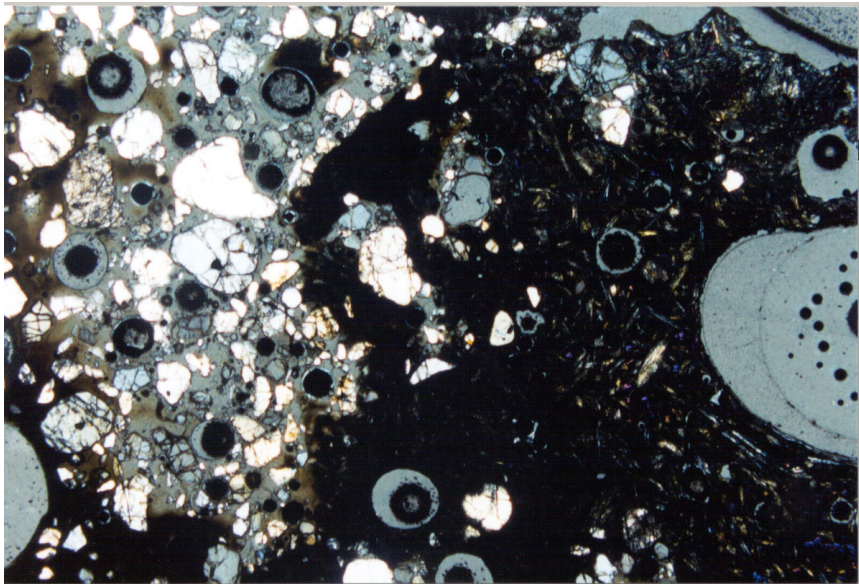
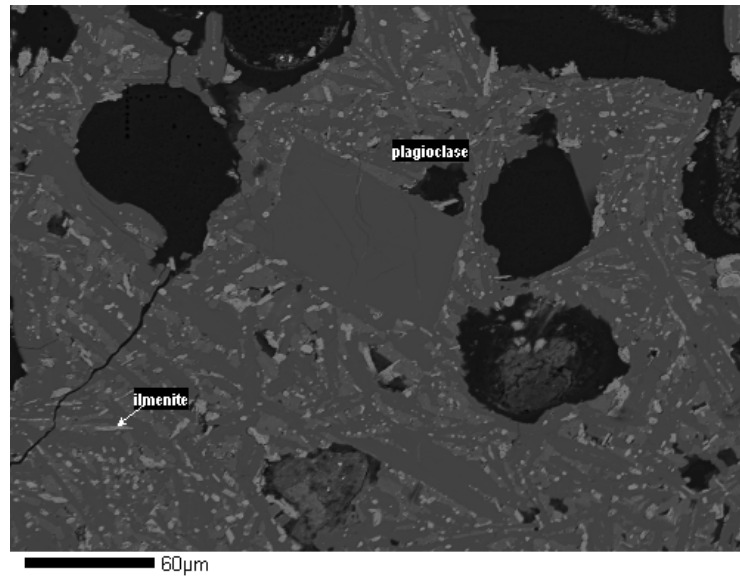


Figure 4.32
Photomicrograph of a iron slagged ceramic, fayalite slag to right, quartz and calcite-rich ceramic to left, (Magnification: 2.5X, polarized transmitted light), sample #13

According to Craddock (1995), most ceramic bodies (including furnaces) used in antiquity began to soften and melt at temperatures around 900°C and became completely molten by about 1250°C (1995). Therefore, it is possible that these varying degrees of ceramic vitrification represented in some of the ferrous slags, originated from the linings of the smelting furnace.

Iron cinders/bear: Samples #16, #17, # 20, #21 and #22 cannot be placed easily into any of the aforementioned iron slag categories. EDS analyses revealed glasses and/or clays of variable composition, dominated by iron, silica and calcium, and very fine grained iron oxides with a significant amount of titanium in them. Titanium-rich grains, were also evident in some areas of the partially vitrified ceramic portions. Iron hydroxide weathering rinds were surrounding some of the abundant vesicles and large euhedral plagioclase and calcium-rich pyroxene crystals were present in the some of the glass matrices. Additionally, residual magnesium-rich fragments of ore? or ceramic? were present and particularly visible in sample #17. There is compositional variation between these five samples, but all contain titanium-rich iron oxides and similarly composed glasses.

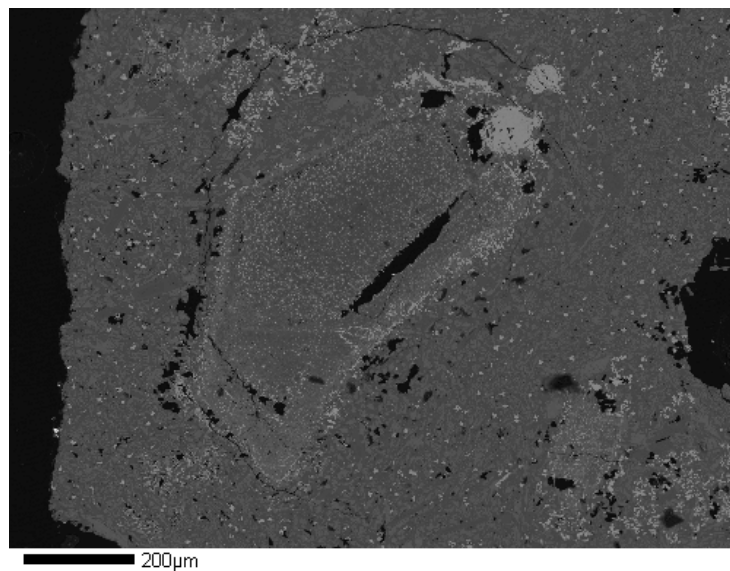
Figures 4.33, 4.34, and 4.35 show some of the variations of iron cinder from the Yasmina site. Figure 4.33 is a backscattered electron image of sample #20 showing the fine-grained titanium-bearing iron oxides and the larger plagioclase crystals. Another variation of iron cinder is shown in Figure 4.34, which exhibits the presence of a residual magnesium-rich lump. Finally, Figure 4.35 shows the abundant calcium-rich pyroxenes, glass, and titanium-bearing iron oxides typical of sample #16 and #17.



BEI #20, ilmenite and plagioclase

Figure 4.33

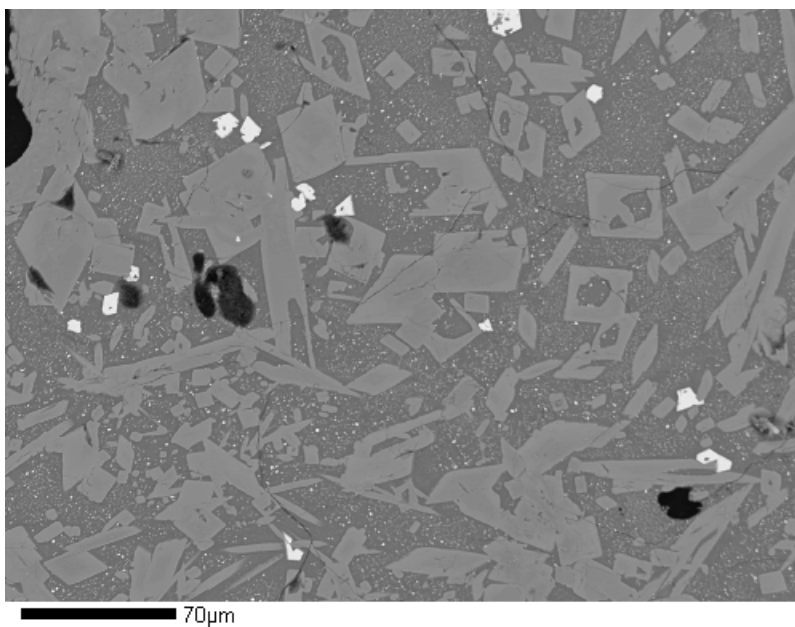
Backscattered electron image of “cinder,” sample #20



BEI 16-4 area with high Mg phase

Figure 4.34

Backscattered electron image of residual magnesium-rich phase (center), sample #16



BEI 16-3 view of sample w/pyroxene and FeO

Figure 4.35

Backscattered electron image of titanium oxides (white) and pyroxene crystals (light grey) in glass, sample #17

Bachmann defines cinders as similar to slags in composition [based on bulk analytical data], very porous, and often the shape of individual ore lumps can still be distinguished (1982). He defines bears as the result of the reactions of the molten smelting product with the refractory lining of the furnace (Bachmann, 1982). In general, cinders and bears are difficult to categorize chemically, since they result from the combination of so many aspects of the smelting materials that can vary from place to place and within the furnace itself (Tylecote, 1962). These five samples do contain mineral phases present elsewhere in the Yasmina iron slag sample suite, such as iron- and calcium-dominated glasses, but abundance of plagioclase, pyroxene and iron-titanium oxides distinguishes this group. Additionally, the presence of titanium grains in the un-vitrified ceramic portions and titanium-bearing iron oxides in the glassy portions, suggests a connection between furnace material and slagged material. These samples probably represent slag-modified furnace fragments where calcium from calcite and aluminum from clay reacted with the slag melt to form plagioclase and pyroxene.

Alternatively, the compositional similarity between some of these slags and the tap and cake slags, as well as their generally frothy morphology may be indicative of iron smithing. Iron smithing slags are often iron oxide and silicate rich, but with higher aluminum contents and of lower specific gravity than smelting slags (Bachmann, 1982). The glass analyses from Table 4.3 for sample #17 shows this higher aluminum content of the slag glass than for those tap or cake slags associated with smelting. The absence of fayalite in samples #16 and #17, however, may be indicative of another process altogether. Distinguishing between smelting and smithing slags is very difficult, as Tylecote (1962), Craddock (1995), and Bachmann (1982) have noted. “To determine

whether an iron slag came from primary smelting or smithing is much more difficult and requires more background information on the context and the quantities and nature of other associated materials and debris” (McDonnell, 1983). Without this contextual information – the Yasmina slags have clearly been moved from their original location – attributing many of the ferrous slags to one particular process is speculative. Slags of this variable composition and low-density that are still magnetic are equally strong candidates as slag cinders/bear and smithing slags.

In summary, the various iron slag morphologies represent various aspects of the iron smelting process. Figure 2.2 shows a representation of an iron shaft furnace from a Roman site in Norfolk in use during the second century CE. It is reasonable to assume that Roman Iron Age furnaces in Carthage would be generally similar to those in Roman Europe, and therefore we can use this furnace model to envision where these different slag morphologies were crystallized.

The iron tap slags demonstrate that the slag was indeed tapped from the furnace and collected in a slag pit outside the furnace walls. The ropery texture of the upper surfaces of some of the iron slags and the adhering sand grains, along with the previously identified mineralogy typical of iron tap slags described in the literature, led to the confirmation of the presence of iron tap slags at Yasmina. The so called iron cake slags demonstrate a slightly different mineralogy, consisting of essentially the same mineralogical composition as the iron tap slags, but with a different internal structure and ratio of iron silicate phases to iron oxide and glass phases. These may be the result of cooling inside the furnace or perhaps in the slag pits outside the furnace, as Tylecote’s terminology suggests.

Iron furnace fragments, slagged ceramics, and iron cinders are also present at Yasmina and represent varying degrees of interaction between the slag and the furnace materials. Fayalite-dominated slags adhering to or penetrating ceramics, i.e., furnace fragments, crystallized in the furnace. The only metallic iron found in the ferrous Yasmina slags occurred in association with furnace fragments, suggesting that these locations in the furnace where slag came into direct contact with the furnace walls was favorable for the entrapment of metallic iron. Slagged ceramics represent those furnace materials that were completely vitrified during the smelting process, composed primarily of glass and quartz grains. Finally, the varied group of iron cinders, represents the reaction of the furnace lining with the ferrous slag and the incorporation of relict ceramic and ore materials into the slag matrices. The compositional variations in these slags associated with furnace likely result from their crystallization in various portions of the shaft furnace as shown in Tylecote's diagram.

Although the composition and chemistry of the various slag categories identified at Yasmina suggest that they represent different portions of the smelting process, it is not implied here that they resulted from a single smelt. More likely these slags, collected from various excavation levels spanning hundreds of years, represent similar bloomery furnace operations over time and perhaps some iron smithing activity as well.

Additionally, the quantitative analyses of the various phases in the slags (Table 4.3) can provide some information about the types of fluxes or ores used in the smelting process. For example, iron slags with high calcium contents might suggest that some type of calcium-rich flux, such as calcite, was used (Craddock, 1995). Despite the local carbonaceous lithology in north Africa, calcite does not appear to have been used as a

flux in the iron processing represented by the Yasmina slags. The calcium content in the various slag phases analyzed are generally low (none above 24 oxide weight % for pyroxene). The fayalites and oxides do not contain calcium above 0.3 oxide weight % and the glasses, while variable, do not contain above 19.7 oxide weight % calcium. For systems that utilized calcium fluxes, one would expect much more consistent and abundant calcium present (Craddock, 1995).

Moreover, manganese and other trace elements in slags can sometimes be used to distinguish between ore sources; ores rich in manganese were sometimes intentionally exploited by ancient metallurgists as manganese silicates are fully mobile over a much wider range of pO_2 than iron silicates and therefore more easily formed low viscosity slags (Heimann, et al, 2001). However, in the Yasmina slags, manganese contents are consistently low (none above 2.7 oxide weight %) indicating that manganese-rich ores were not used for the iron smelting/smithing processes these slags represent.

Copper Slags

Twenty-five of the 48 samples selected for petrographic analysis were from the set labeled “copper slags” in the field based on hand sample characterization. As explained in the previous section, sample #10, originally identified as related to iron metallurgy, was subsequently determined using petrographic techniques to actually be related to copper metallurgy. Therefore, 26 of the 48 samples analyzed petrographically are related to one of the several types of copper metallurgy that have now been identified from Yasmina. The copper slags exhibit much greater heterogeneity than the iron slags, in terms of morphology, chemistry and mineral composition. The copper slags are mineralogically heterogeneous between samples as well as within different areas of a

single sample. The categories of copper tap, copper cake, copper furnace and copper frothy, initially identified in the field, were not supported by the mineralogical data obtained through petrographic and electron microprobe analyses. As glasses and metals were the most abundant phases of the slags, they were used to reclassify the copper slags into types according to the metallurgical process they likely represent.

Copper slags contain a variety of phases in a matrix of variable composition. A variety of copper, lead and tin alloys occur as metallic prills in either lead-silicate or calcium-silicate glasses. Occasionally, oxides and sulphides of these metals and iron sulphides also occur in the copper slags. A significant proportion of the copper slags appear to be ceramic in origin (both vitrified and un-vitrified); abundant weathering products such as copper, lead, and tin carbonates, hydroxides, and chlorides adhere to the sample surfaces. Identification of mineralogical phases were done using a combination of microscopic and electron microprobe techniques. Elemental analyses were performed on the metals, glasses, and pyroxene phases using the electron microprobe and are reported below and in the appendices. What follows is a description of the copper slag phases that are most relevant to the interpretation of metallurgical processes.

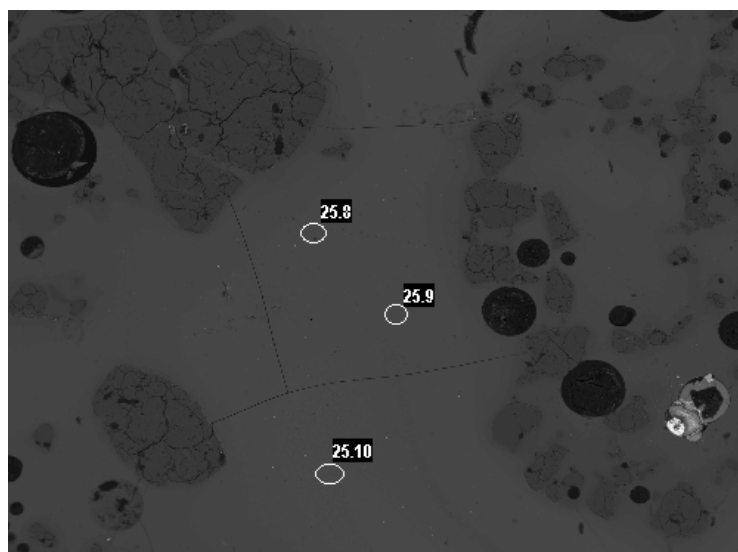
Glasses: Glass compositions of the copper-related slags are generally of two types: lead-silicate glasses and calcium-aluminum-silicate (anorthitic) glasses. Under the microscope in plain light, these glasses appear as transparent swirls of blue, yellow, or red glass. The glass represents a super-cooled melt phase that was cooled to a glass before crystallization of abundant minerals. Occasionally the glasses appear as grey-red-brown “feathery” areas in the slags. These feathery areas represent incipient crystallization of fine-grained dendrite crystals enclosed in glass and are compositionally

identical to the larger swirls of glass. The glasses are generally isotropic (dark) in polarized light. Glasses comprise a significant portion of the slag samples; in some cases, virtually the entire sample is glassy, with a few inclusions of metal or silicate minerals.

Electron microprobe analysis was used to determine the composition of the glasses. Backscattered electron images collected on the microprobe are particularly useful in examining the glasses and show their heterogeneous character. Lead-rich glasses appear very bright due to the high atomic weight of lead relative to silica (see data points 41.15 and 41.16, Table 4.6 and figure 4.40). Table 4.6 summarizes the analytical data collected from glass analyses in several copper slag samples. Figures 4.36 through 4.41 show the location of these analyses within sample numbers 25, 41, and 43. These samples were chosen for analysis because the glass phases were present in large enough pools to reasonably avoid contamination by other phases. Figures 4.36 and 4.37 are backscattered electron images of anorthitic glass from a copper slag. The mean data for the three points analyzed near the sample edge and again near the sample center reveal the glass is relatively homogeneous across this sample. Figure 4.38, 4.39, and 4.40 are backscattered electron images of various glassy portions of the same piece of copper slag. The brightness of the backscattered electron images of this glass is characteristic of lead-rich glasses, due to the high atomic weight of the lead. Comparison of these figures with the analytical data from Table 4.6 reveals that the lead glasses contain approximately 65% lead expressed as an oxide, while those glasses more closely associated with metallic prills or quartz (from the ceramic) contain only between 28% - 47% lead. Clearly there is a great deal of variability in glass compositions across this copper slag

Table 4.6

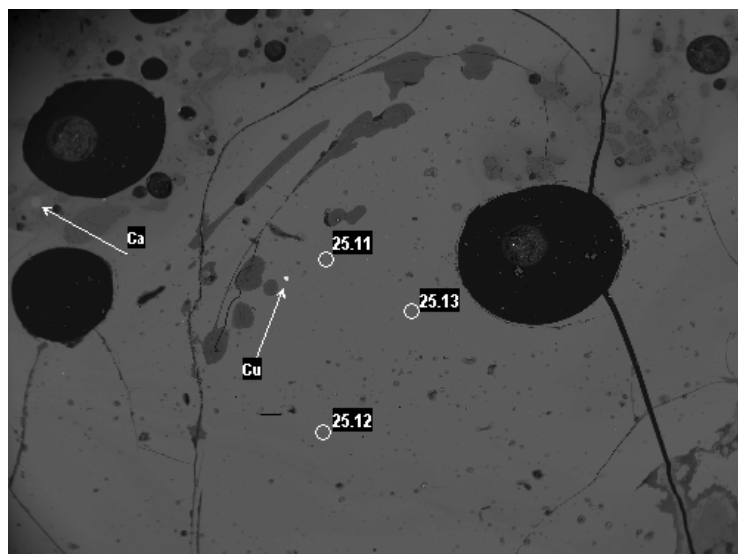
Copper Slag Glass Analyses				
Oxide	Sample #25			
	Mean of data points in Figure 4.36	Mean of data points in Figure 4.37		
SiO ₂	63.37	56.85		
Al ₂ O ₃	7.83	5.14		
FeO	3.95	2.4		
MgO	3.27	4.64		
CaO	13.96	22.08		
Na ₂ O	0.39	0.93		
K ₂ O	1.33	2.05		
CuO	0.08	0.27		
Sb ₂ O ₃	0.01	0.08		
SnO	0.01	0		
PbO	0	0		
SO ₂	0.01	0.05		
Oxide wt.% Total (Standard Deviation)	94.21 (1.71) <i>near sample edge</i>	94.49 (0.47) <i>near sample center</i>		
Sample # 41				
Oxide	Mean of data points in Figure 4.38	Mean of data points in Figure 4.39	data point 4.15 in Figure 4.40	data point 41.16 in Figure 4.40
SiO ₂	24.07	36.61	49.57	24.11
Al ₂ O ₃	3.27	4.90	8.55	3.43
FeO	0.48	0.72	1.12	0.50
MgO	3.13	3.78	1.77	2.61
CaO	0.38	1.29	3.54	0.10
Na ₂ O	0.13	0.45	0.36	0.07
K ₂ O	1.71	1.98	3.01	2.16
CuO	0.92	0.56	0.39	2.37
Sb ₂ O ₃	0.05	0.06	0.12	0.00
SnO	0.46	0.36	0.02	0.42
PbO	64.38	46.56	28.01	66.37
SO ₂	0.00	0.02	0.03	0.03
Oxide wt.% Total (Standard Deviation)	98.97 (1.78) <i>lead-rich glass</i>	97.30 (0.50) <i>glass near metal prill</i>	96.49 <i>glass with quartz</i>	102.15 <i>lead-rich glass</i>
Sample # 43 (Figure 4.41)				
Oxide	Mean of data points 43.4 - 43.7	Mean of data points 43.8 - 43.10	Mean of data points 43.11 - 43.13*	*43.13 is located just to left of the edge of the image (not shown here)
SiO ₂	26.25	48.31	54.32	
Al ₂ O ₃	3.58	10.40	17.65	
FeO	0.56	1.68	2.31	
MgO	3.47	4.02	5.02	
CaO	0.53	1.73	2.06	
Na ₂ O	0.16	0.43	0.34	
K ₂ O	1.46	4.77	6.64	
CuO	2.17	0.66	0.36	
Sb ₂ O ₃	0.01	0.09	0.14	
SnO	0.02	0.15	0.05	
PbO	59.20	26.20	8.24	
SO ₂	0.01	0.01	0.05	
Oxide wt.% Total (Standard Deviation)	97.42 (2.56) <i>lead-rich glass</i>	98.45 (1.44) <i>glass nearer quartz</i>	97.18 (1.93) <i>glass with quartz</i>	



SEI 25-2 glassy area near sample edge

Figure 4.36

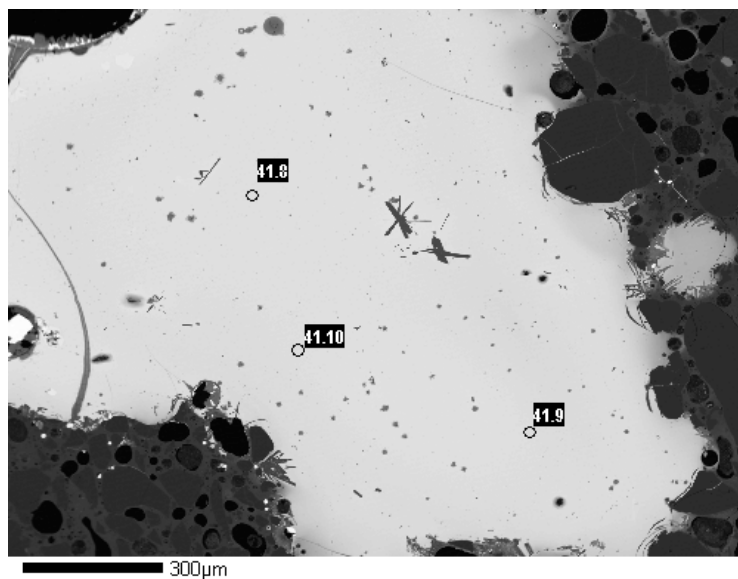
Backscattered electron image of glass analyses, sample #25



BEI 25-3 glassy area near sample center

Figure 4.37

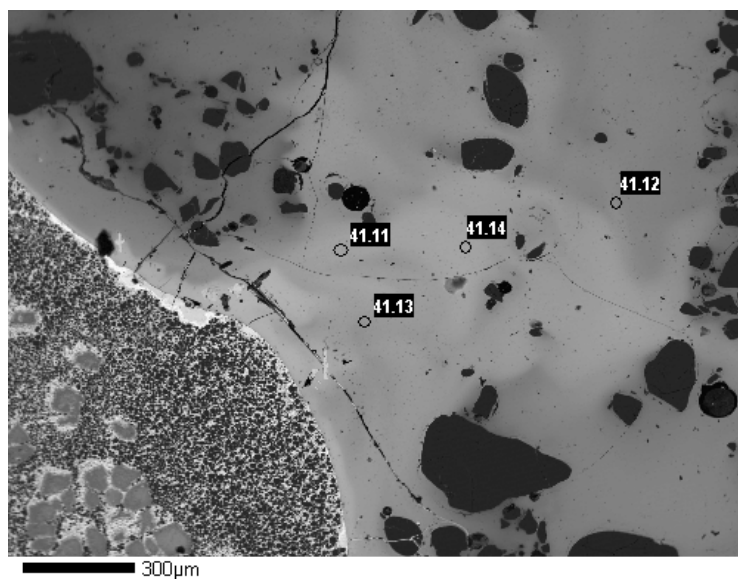
Backscattered electron image of glass analyses, sample #25



BEI 41-4 Pb-rich glassy area

Figure 4.38

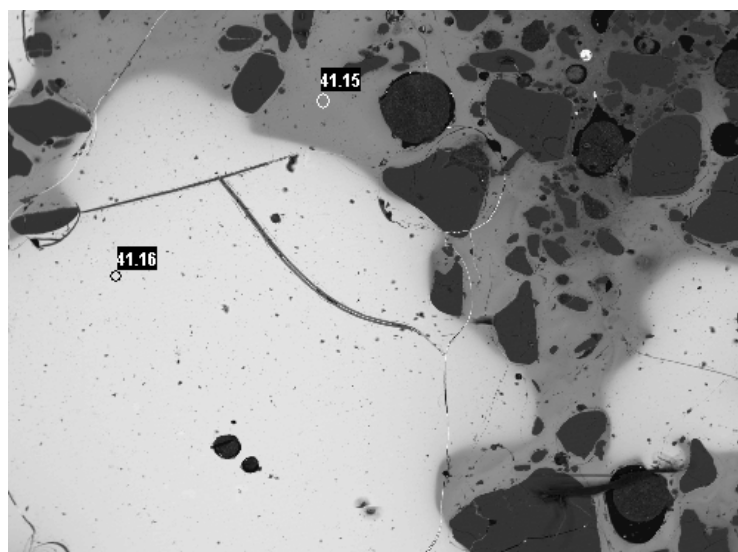
Backscattered electron image of glass analyses, sample #41



BEI 41-5 Pb-rich glass 2 (near Cu-Pb prill)

Figure 4.39

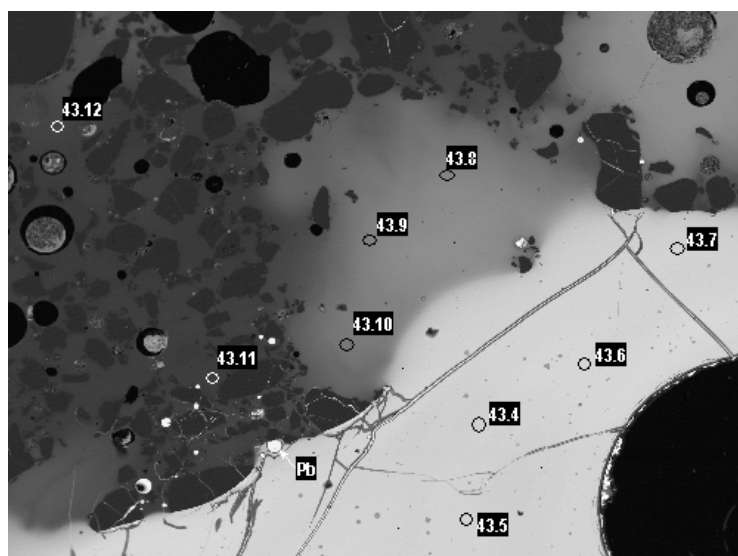
Backscattered electron image of glass analyses, sample #41



200µm
BEI 41-6 Pb rich glass

Figure 4.40

Backscattered electron image of glass analyses, sample #41



300µm
BEI 43-5 glassy area 1

Figure 4.41

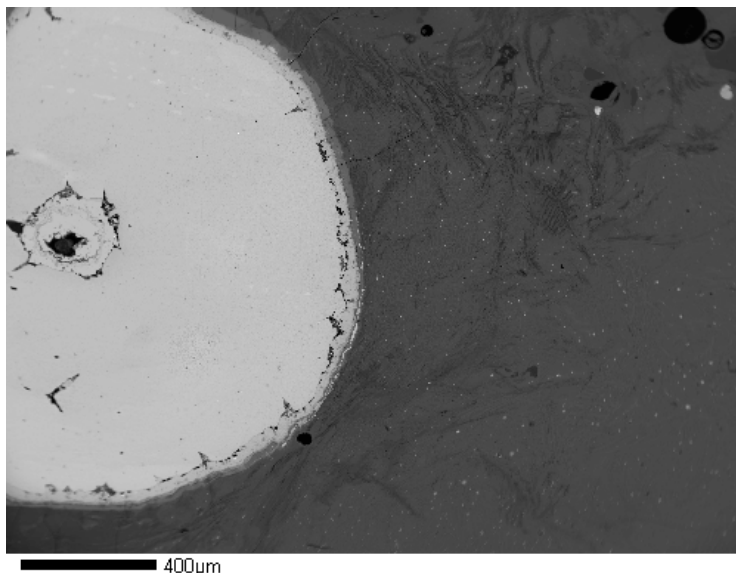
Backscattered electron image of glass analyses, sample #43

sample. Many of the copper slags that contain lead-rich glass display this same heterogeneity.

Figure 4.41 shows another glassy copper slag; the mean data for the analytical points shown here are summarized in Table 4.6. Again, the heterogeneity of the glasses within a single sample is evident. The vitrified portions of the ceramics in these slags clearly alter the chemistry of the lead-rich glasses by contributing elements such as aluminum, silica, iron, calcium, and potassium to the melt.

Metals: Metals in the copper slags generally occur as prills ranging in size from less than a micron to several millimeters in diameter. The metals occur as homogeneous phases composed of copper or lead, and as alloys, such as bronze or leaded copper, and as complex mixtures appearing as prills composed of visibly different phases. Samples #30, #32, and #43 contain massive copper (or its alloys) can be found – sample #30 contains a broad, curving band of bronze, sample #43 contains a mass of copper that comprises approximately 30% of the sample, and sample #32 is made entirely of a leaded bronze (copper with lead and stannite crystals (SnO_2) in the intergranular space between copper grains). In some cases, the metals occur in association with, silicate minerals, especially lead silicates, and oxides. Microprobe analyses often yielded low totals related to oxidation and hydration of the metal prills.

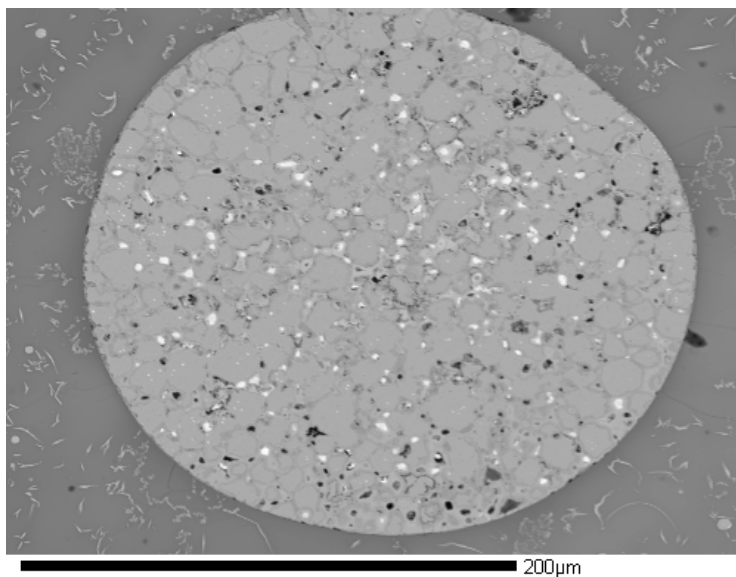
Figures 4.42 through 4.46 show some of the variety of metallic phases that occur in the copper slags. In all 26 of the copper samples analyzed, copper was present in either metallic form as pure copper or as an alloy of tin and/or lead. Weathering produced various copper oxides, carbonates, and sulfates in some samples.



BEI Cu bleb w/finely disseminated Cu

Figure 4.42

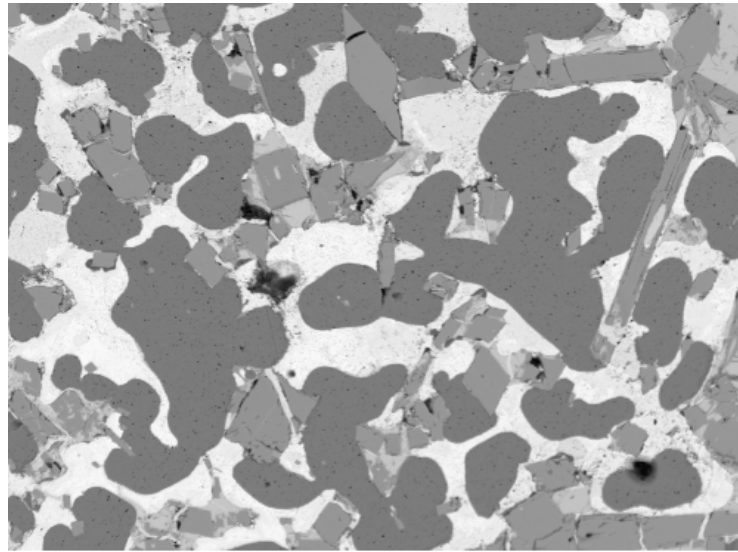
Backscattered electron image of “pure” copper prill in a partially crystallized “feathery” glass matrix, sample #29



BSI 31 Cu bleb w/ interstitial Sn and Pb-Si matrix

Figure 4.43

Backscattered electron image of leaded bronze prill with intergranular lead silicate (white) and stannite (light grey), in glass with stannite crystals, sample #31



BEI Massive Cu: Cu, Pb/Si, and Sn

Figure 4.44

Backscattered electron image of massive leaded bronze, copper (dark grey), stannite (light grey crystals), lead silicate mineral (white), sample #32

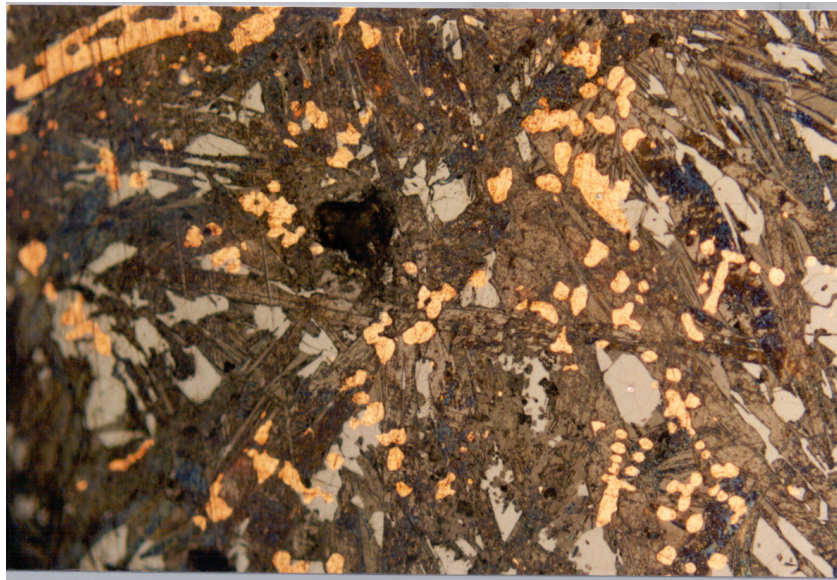


Figure 4.45

Photomicrograph of dendritic copper (gold) (contains 2+wt% Ag), lead/arsenic phase (blue), and copper silicate phase (grey), sample #30

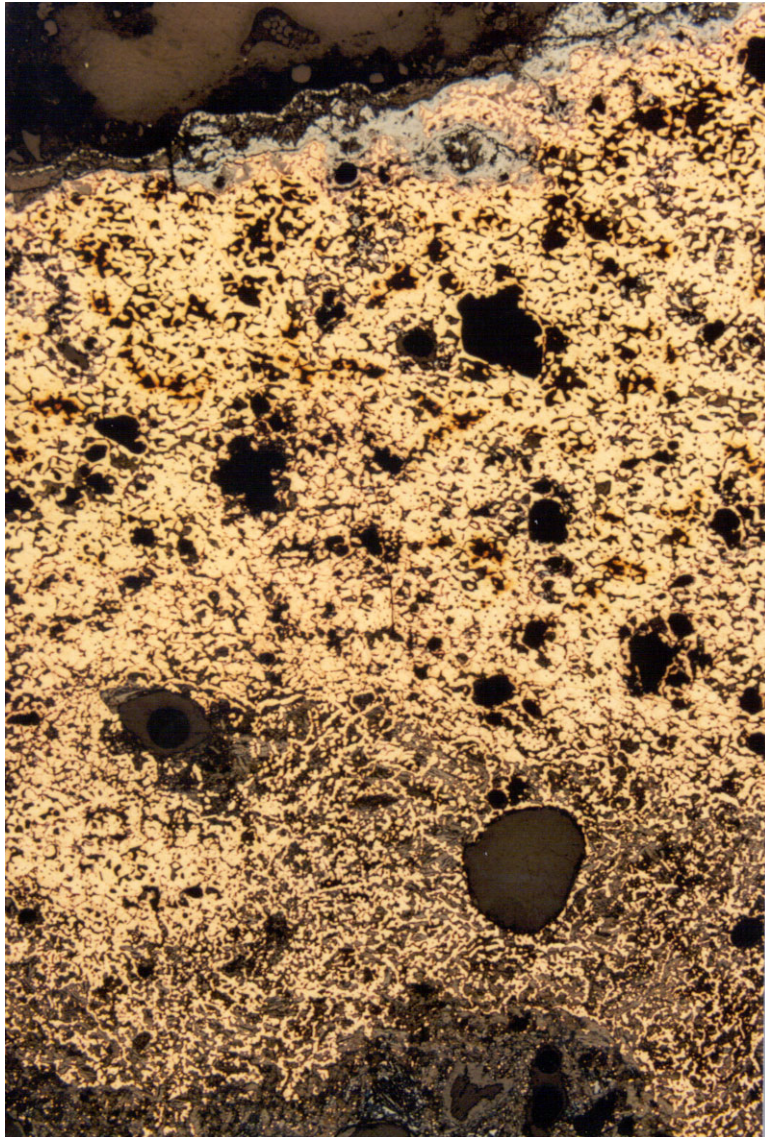


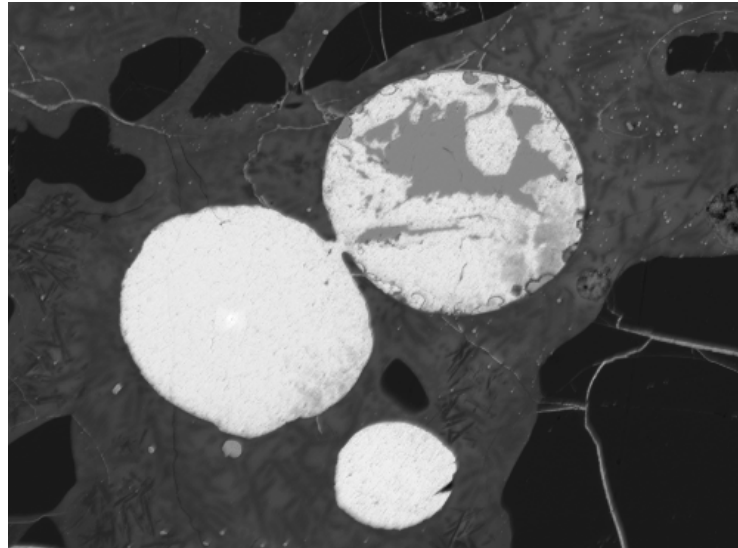
Figure 4.46
Photomicrograph of copper band with intergranular lead and tin phases,
sample #30

Microprobe analyses were done to distinguish between pure copper and copper alloys as there is no visible difference between them, even at high magnification in reflected light. Table 4.7 is a compilation of analyses of the metals in the copper slags and is referenced to the figures of the prills from which they came. The composition of the copper metals varies between samples and within different copper prills in the same sample. In sample #30 the relatively pure dendritic copper contains 2.7% silver, while other copper alloy prills contain much less silver (less than 1%). The amount of lead alloyed with the copper also varies; a copper–lead prill from sample #34 contains just over 2% lead, while the other coppers analyzed do not contain more than 1% lead. The percent tin also varies in the metallic copper. A bronze prill from #34 contains 15.71% tin; bronzes from sample #30 contain 3.32% and 4.18% tin. The various amounts of silver, lead, and tin alloyed with copper suggests that different copper alloys were being worked at Yasmina, ranging from bronzes to leaded coppers, to coppers with up to 2.7% silver. The copper metals analyses shown in Table 4.7 are from copper phases that appear homogeneous at high magnification; that is, these metals are alloys as opposed to mixtures, in which copper and other metal phases are visibly separate (see Figure 4.44). Metal alloy chemistry, particularly that of copper and tin, will be shown in the next section as useful indicators of process temperatures.

Oxides: Tin, copper, and lead oxides comprise a relatively small proportion of the phases in the copper slags. Lead oxides often initially appear as prills of copper or lead metal and only upon microprobe analysis does it become evident that they are oxidized. Figure 4.47 shows the small prills of lead oxide commonly found in lead-rich copper slags.

Table 4.7

Copper Slag Metals Analysis											
Sample #	Description	Figure #	Elements Analyzed								
			Cu	Sn	Sb	Pb	As	Fe	Ag	S	Total
	CMT Taylor Pyrite Standard		0.0	0.0	0.1	0.0	0.0	46.9	0.0	51.8	98.7
30	dendritic copper	Figure 4.45	93.8	0.0	0.0	0.3	0.0	0.0	2.7	0.0	96.9
30	massive bronze	Figure 4.46	92.6	3.3	0.0	0.3	0.0	0.0	0.2	0.0	96.4
30	bronze flecks		93.6	4.2	0.0	0.3	0.3	0.0	0.0	0.0	98.5
30	copper dendrites		94.2	0.0	0.0	0.9	0.4	0.0	0.8	0.1	96.3
34	copper within tin corona	Figure 4.50	95.7	0.0	0.0	0.3	0.0	0.0	0.2	0.1	96.4
34	leaded copper		91.6	0.6	0.8	2.1	0.9	0.0	0.0	0.3	96.3
34	bronze prill		78.8	15.7	0.2	0.3	1.0	0.1	0.0	0.7	96.8
			Cu	Sn	Zn	Pb	As	Fe			Total
44	leaded copper		99.3	0.4	0.0	0.2	0.1	0.0	N/A	N/A	100.0
32	massive copper	Figure 4.44	100.6	0.1	0.0	0.3	0.0	0.0	N/A	N/A	101.0



50µm
BEI Pb prills in silica/Pb matrix

Figure 4.47

Backscattered electron image of lead prills (white) in a copper slag, sample #37

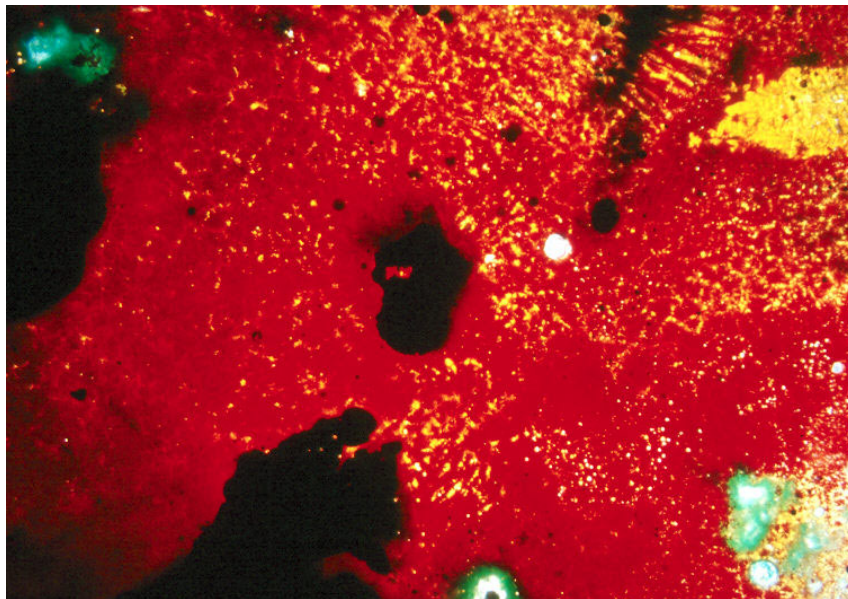


Figure 4.48

Photomicrograph of cuprite (red) dendrites in a copper slag, (Magnification: 20X, plain transmitted light), sample #44

Copper oxides, particularly cuprite, Cu_2O , appears as bright red dendrites either surrounding metallic prills or as an isolated phase in the glass matrix. Cuprite appears bright red in plain and polarized light. Figure 4.48 shows cuprite dendrites, typically found in association with copper prills in many of the Yasmina slags. Cuprite requires partly oxidizing conditions for its formation and is typically found in copper smelting slags, rather than in copper smelting slags (Bachmann, 1982).

Tin oxide, specifically stannite, SnO_2 , occurs in several crystal morphologies and in greater abundance than lead or copper oxides in the copper slags. Stannite occurs as euhedral crystals in the glass matrix of some slags (Figure 4.49), as elongate crystals in close association with copper metal (Figure 4.44), and as hollow euhedral crystals with cores of copper metal as shown in Figure 4.50.

Silicate minerals: Silicate minerals are relatively rare in the copper slags and are of two general types: plagioclase and pyroxene. Plagioclase (anorthite) typically occurs as euhedral crystals several microns in length in the calcium-rich lead glasses (Figure 4.51). These crystals were only visible with the electron microprobe; their chemistry was confirmed with the EDS detector.

The pyroxenes in the copper slags are calcium-rich with variable iron and magnesium contents. Table 4.8 is a summary of the pyroxene analyses obtained. The pyroxenes span a wide range of compositions and include augite (Ca, Fe, Mg), wollastonite (Ca), and a phase (essenite: Al, Ca, Fe, Mg) restricted to slags (Deare et al, 1996). Pyroxenes generally occur in close proximity to the ceramics portions of the slags, suggesting that their formation is, in part, due to the contribution of elements from the ceramic.

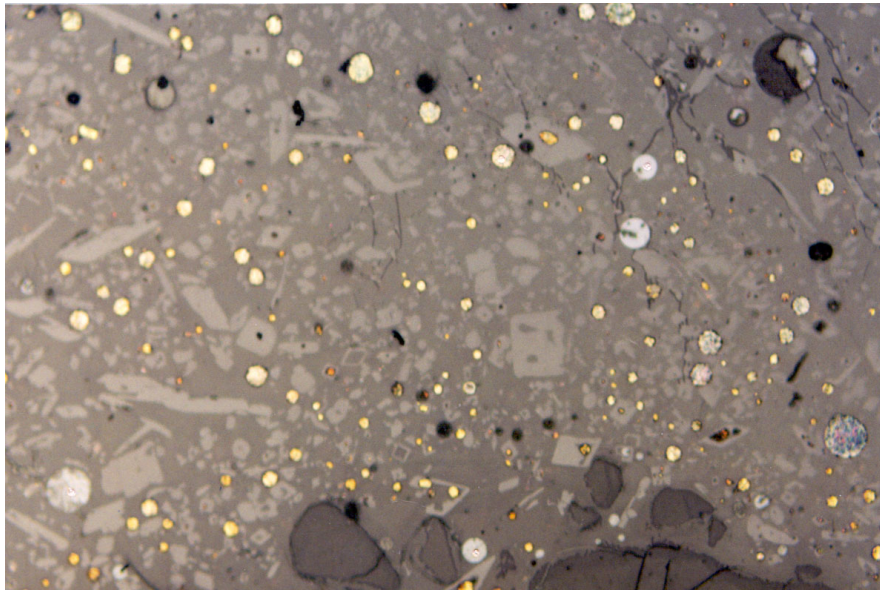


Figure 4.49

Photomicrograph of cassiterite (SnO_2) (light grey crystals) with copper and lead (blue-grey) prills, and quartz (dark grey – bottom), (Magnification: 10X, reflected light), sample #34

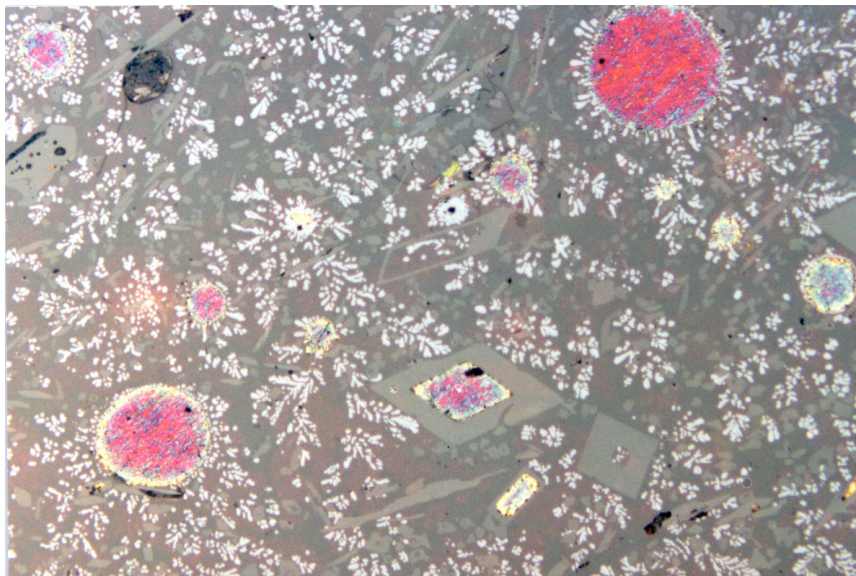
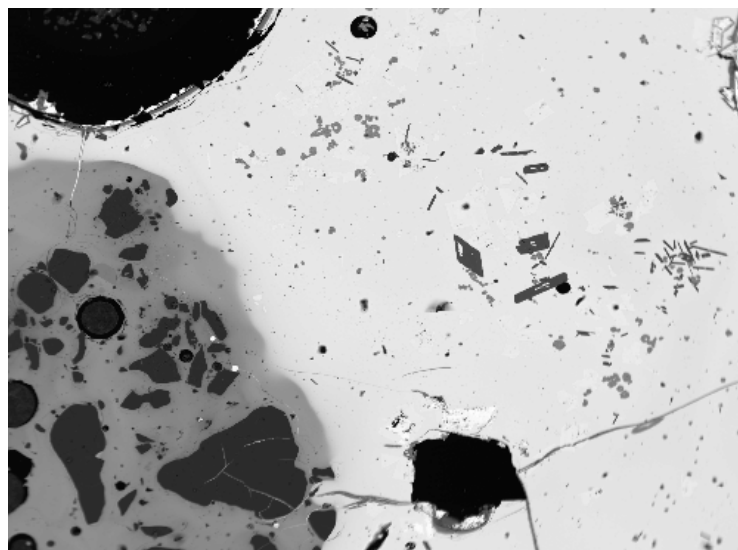


Figure 4.50
Photomicrograph of tin oxides (light grey) as coronas around metallic copper (pink), and cuprite dendrites (white), (Magnification: 20X, reflected light), sample #34



300µm
BEI Pb-rich blebs in Pb/Si matrix

Figure 4.51
Backscattered electron image of calcium silicate minerals (dark crystals) in lead-rich glass, sample #41

Table 4.8

Copper Slag Pyroxene Analyses		Oxide Weight %										
Sample #	Description	SiO2	TiO2	Al2O3	MgO	FeO	CaO	MnO	K2O	Na2O	Cr2O3	Total
Cr Augite	Std USNM	50.41	0.51	7.84	17.89	4.43	17.81	0.27	0.01	0.80	0.96	100.94
29	augite	60.48	0.42	6.04	11.56	2.46	17.69	2.37	0.58	0.53	0.00	102.13
29	augite	54.10	0.11	0.24	16.17	1.98	25.02	2.26	0.34	0.07	0.00	100.30
29	augite	52.13	0.32	0.39	16.67	2.57	24.91	1.92	0.07	0.07	0.00	99.05
29	augite	51.50	0.16	0.25	16.53	2.53	24.40	1.72	0.08	0.04	0.18	97.40
29	wollastonite	51.35	0.00	0.01	1.97	0.40	43.89	2.13	0.08	0.00	0.00	99.84
41	wollastonite	49.61	0.04	0.15	0.93	0.38	45.33	0.52	0.01	0.07	0.00	97.05
41	essenite	46.43	0.73	17.54	7.60	7.12	20.38	0.12	0.07	0.15	0.11	100.25
41	augite	44.35	0.88	6.49	9.41	10.38	24.66	0.11	0.01	0.01	0.08	96.39
43	wollastonite	50.76	0.04	0.04	0.00	0.03	47.75	0.00	0.00	0.00	0.01	98.64

Ceramic: Vitriified ceramics comprise a significant proportion of the copper slags analyzed. Quartz grains and residual clay materials indicate that ceramics have been incorporated into the lead-rich and anorthitic glasses previously discussed. Figure 4.52 shows the variable portions of these slags; the quartz-rich, lighter colored areas represent the ceramic portion that is infiltrated by the yellowish glass slag phases produced from metallurgical processing. Virtually every sample contains quartz grains of variable size and shape incorporated into the glassy matrix, the exception being sample #32 (Figure 4.44). Quartz grains range in size from several microns to several millimeters and are generally rounded. Un-melted ceramics were comprised of quartz grains and abundant calcite fragments in a clay matrix.

Weathering products: The copper slags contain a wide variety of weathering phases, particularly in association with the metallic phases in the slags. In addition to the copper chlorides, sulphates, and carbonates that form the green weathered surfaces of nearly all ancient copper slags (Bachmann, 1982), the Yasmina slags contain weathering products within the slag matrix, primarily in the form of copper chlorides and copper sulphates that have replaced portions of metallic phases.

Figure 4.53 shows a copper slag in plain transmitted light with the green weathered surfaces around the vesicle. Figures 4.54, 4.55, and 4.56 are backscattered electron images of prills in the copper slags that are variably oxidized with a complex mineralogy. Figure 4.54 shows a prill contained within an anorthitic glass with several phases including quartz, a lead silicate, crystals of a copper-iron mineral (no Sn, Cl, or Si), and a small mass chloride-rich copper. Analytical totals for this and the other weathered metallic prills in the copper slags were inconsistent, ranging from 30% to

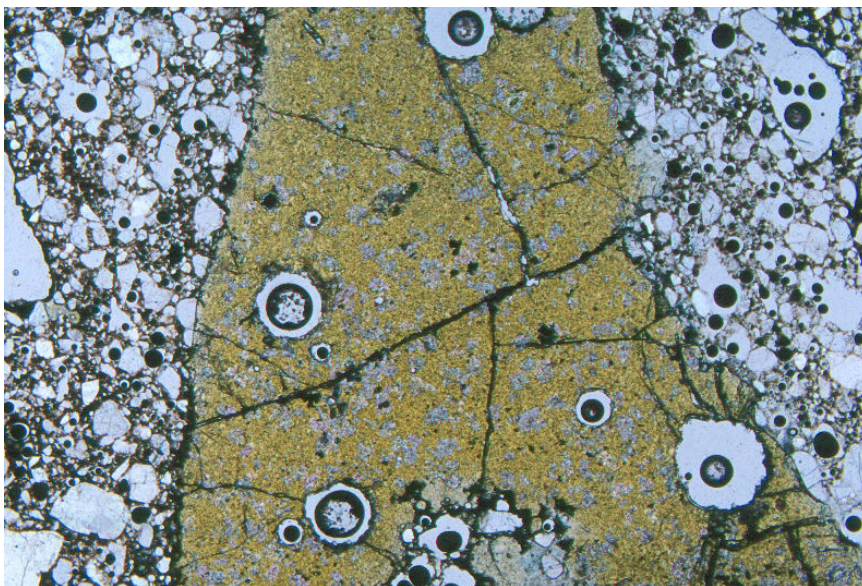


Figure 4.52
Photomicrograph of lead-rich copper slag (yellow) infiltrating quartz-rich ceramic (light), (Magnification: 2.5X, plain transmitted light), sample #44

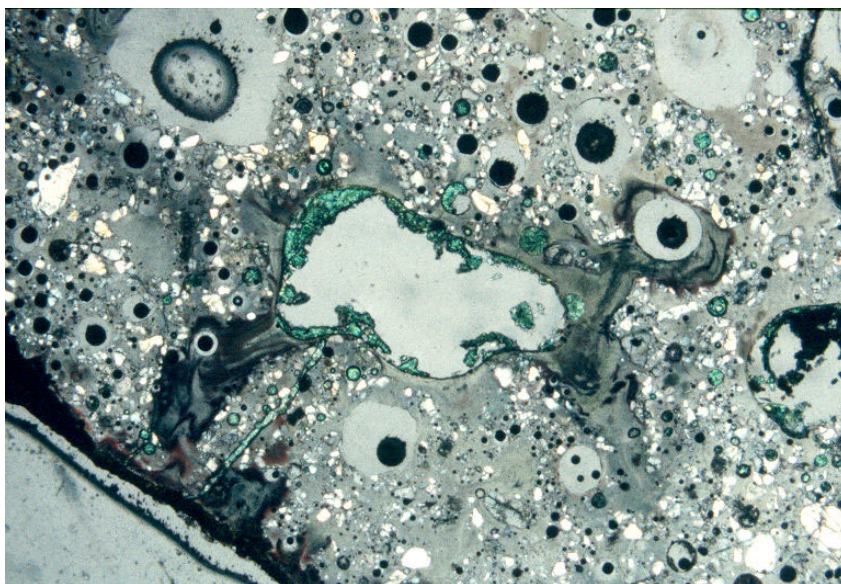
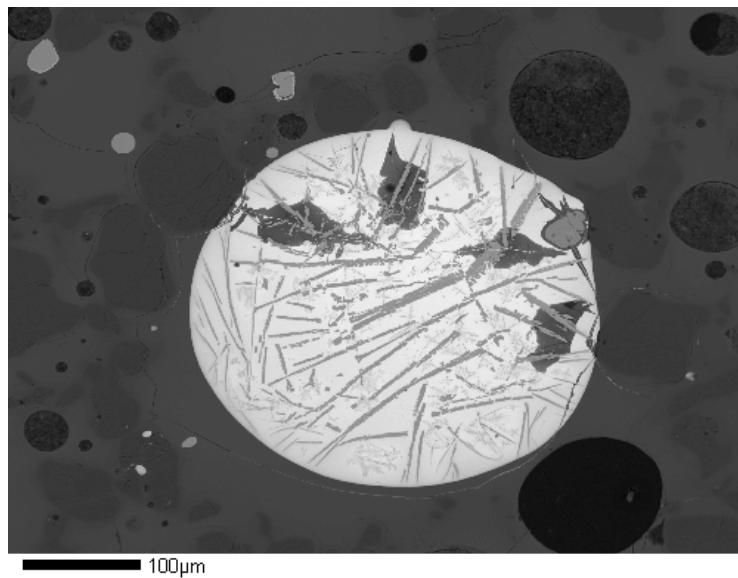


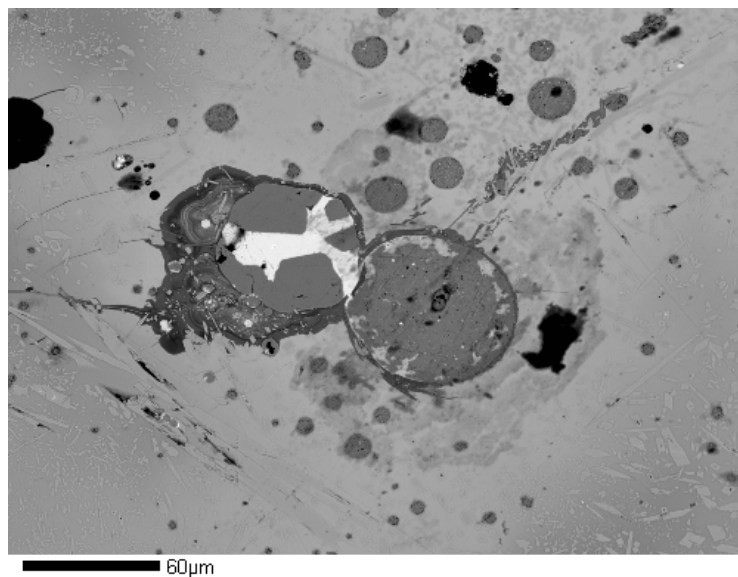
Figure 4.53
Photomicrograph of copper slag with green weathering rind inside a vesicle, (Magnification: 25.X, plain transmitted light), sample #28



BEI #28-1a

Figure 4.54

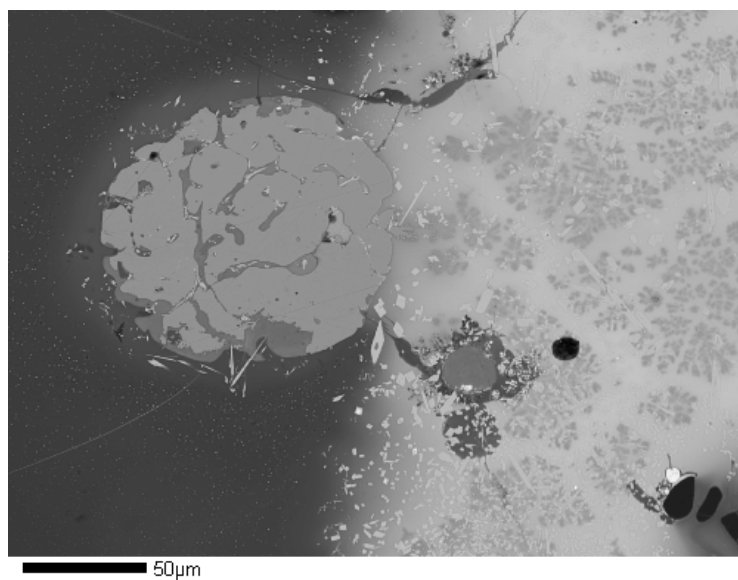
Backscattered electron image of complex weathering in copper slags; lead-rich phase w/ Cu, As, Si, Fe (white), copper-iron lathes (light grey), quartz (dark grey), and CuCl (medium grey), sample #28



BEI #28-2a

Figure 4.55

Backscattered electron image of complex weathering in copper slags; metallic copper prill (grey – right), copper mineral? (grey – left), and lead-arsenic (white), sample #28



BEI #28-3a

Figure 4.56

Backscattered electron image of complex weathering in copper slags; copper phase (medium grey) with CuCl (dark grey) infiltrating, to right are lead-rich glass and cuprite dendrites, sample #28

60%, depending on the analytical routine (elemental metals versus metal oxides) used. Similar totals were obtained for the weathered prills shown in Figures 4.55 and 4.56. Such low totals are difficult to reconcile with un-weathered metal compositions and weathering products should generally be avoided in slag phases analyses (Bachmann, 1982). These weathering products, however, do provide some evidence of the metals involved in the slag or prill.

Discussion of copper slag petrography

The variety and complexity of the phases associated with the Yasmina copper slags makes it difficult to associate any particular slag with any specific part of a copper smelting or smithing process. Therefore, it is possible to discuss only in a general sense the types of copper-related metallurgy represented by the Yasmina slags.

The abundance of ceramic materials in all of the copper slag samples suggests either crucibles or furnace linings were incorporated into these slags as they were forming. Residues of metallic copper intermixed with vitreous material have been interpreted at other archaeological sites as the result of high temperature crucible production/refining of metals, particularly copper and its alloys (Ryndia, 1999).

Additionally, there were no tap slags found in association with copper metallurgy. Copper tap slags are similar in appearance to iron tap slags, but chemical analysis will show the presence of copper in the glasses or silicate phases (Bachmann, 1982). The absence of this slag type at Yasmina does not rule out smelting of copper; however, the smelting of copper or its alloys cannot be confirmed in its absence. Therefore, the prominence of ceramic materials in these slags and the absence of any tap slags, suggests that the copper metallurgy represented at Yasmina is a secondary process, related to

crucible-based refining or recycling of metals. Moreover, the sizes of the slag pieces associated with copper metallurgy are generally no larger than 5-8 centimeters across (For comparison, the iron slags exhibited a much wider range of slag piece sizes, ranging from a few millimeters to 15-20 centimeters across). These small pieces may be the result of the slags having been broken after cooling as the metallurgists sorted through the slag for the metals of interest. Alternatively, the small size of the copper slag fragments may be related to small-scale crucible technology; Roman brass and bronze working crucibles are generally about fist-sized with 10 mm thick walls and a bag or pear shape (Rehren, 1999). Fragments of slags and ceramics from Yasmina are within this size range.

The metals present in the slags are variable between samples and within individual samples. For example, sample #28 contains metal prills of copper, bronze, iron sulphide and various weathering products associated with each. There are several samples that contain relatively pure copper prills and stannite dendrites in a lead-silicate glass (sample # 24, #29). These various combinations of metals and glasses suggest that several different metallurgical processes were being practiced.

Tin, and sometimes tin and lead, alloyed with the copper metals indicates that bronzes were being worked. In these alloys, the amount of tin does not exceed 3 wt%, lead in the alloys does not exceed 2 wt%. Roman bronzes did not contain tin in excess of 13.2 wt% (Cleere, 1976) and were generally considered to be low tin bronzes, with tin between 2 and 4 wt% (Ponting, 1998). Above 13.5 wt% tin, an intermetallic compound is formed upon cooling, resulting in a hard, but brittle alloy, unsuitable for cold working (Cleere, 1976). Lead was commonly added to bronzes for casting; lead around 2 wt%

lowers the alloy's melting point and improves fluidity, making a small amount of lead desirable in alloys intended for casting (Ponting, 1998). Above 30 wt% lead bronzes tend to separate into their constituent metal phases (Cleere, 1976), creating lead-rich "globules" within the copper alloy and structurally weakening the metal (Ponting, 1998). So, the amounts of tin and lead alloyed with the copper suggests the presence of bronze, rather than pure copper was being worked and the abundance of lead suggests a bronze casting technology.

The abundance of lead in the glasses of these bronze slags may be related to the refining of silver from bronzes. The abundance of tin and lead associated with relatively pure copper suggests recycling of bronze; the lead content in the intergranular phase is too high to have been contained in the copper-tin alloy and probably reflects the addition of a lead flux to the system or perhaps an attempt to concentrate silver. The process of liquation, described at the end of Chapter Two, was a method employed by metallurgists in antiquity to isolate silver from previously smelted metals, such as copper, or from partially roasted copper ores, called mattes or speiss (Craddock, 1995). The addition of lead to the metal or mixture of slag and copper matte/speiss takes up the silver and then, this lead/silver is cupelled. Cupellation, also outlined in Chapter Two, is the process by which lead is oxidized to litharge, PbO, leaving behind pure silver beads that collect in the cupellation furnace bottom (Craddock, 1987; 1995). The abundance of lead-rich glasses, copper prills and dendrites with elevated measurable silver content, and abundant tin oxides and occasional litharge (PbO) prills in the Yasmina copper slags suggest a complex processing of bronze with lead.

Sample #30, in particular, fits this model for the refining of silver from bronze. It contains dendrites of copper with up to 2.7 wt% silver, as well as a large band of massive bronze (3.3 wt% tin) with a modest (0.11 wt%) silver content. Lead-rich glasses as well as lead oxide phases and cassiterite crystals are present. The abundance of bronze, particularly in sample #30, suggests that these metals were not what the metallurgists were after; it is unlikely that Roman metallurgists, capable of extracting parts per thousand of silver out of lead and copper (Craddock, et al, 1996), were prone to processing errors that would leave behind slags with such an abundance of metals. It is more likely that these slags and chunks of metal were left behind because they were not the metal the metallurgist was after. Sample #32 (Figure 4.44) may be a product of such a separation and would explain why such a large chunk of metal (several hundred grams) was disregarded by the metallurgist. Despite an outward appearance as a metal, in actuality, sample #32 is composed of pure copper with intergranular stannite crystals in a lead silicate glass. The lead and copper separated in this sample due to the limited solubility of copper and lead discussed above; the presence of tin oxide in association with copper and lead oxides is widely observed in ancient bronze metallurgy and is the result of oxidation (Klein and Hauptmann, 1999). These unmixed metal phases precipitated from a homogeneous fully liquefied melt at the end of the melting process as a result of the use of open crucibles (Klein and Hauptmann, 1999). This phenomenon is widely observed throughout the Mediterranean from the first millennium BCE (Klein and Hauptmann, 1999).

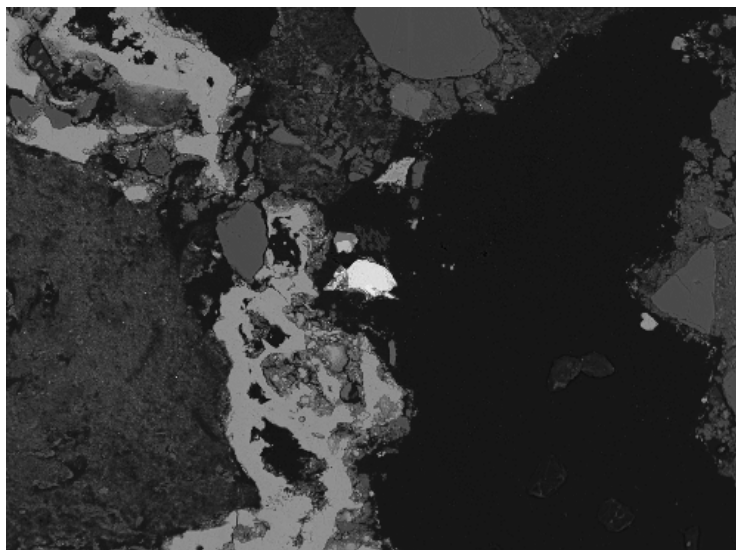
In addition to bronze working, there is evidence for the smelting/smithing of copper. Sample #29 contains only metallic prills of copper in an anorthitic glass matrix.

Quantitative analyses for this sample were not done due to the weathered state of the prills, but EDS analyses showed copper as the only metallic component. The absence of lead, tin, or silver indicates a different process from the recycling of bronzes suggested above. Only three of the 26 copper slags analyzed were of the same general type as sample #29 (anorthitic glasses, pure copper prills, absent lead phases).

At least two samples from the Yasmina slag sample suite had copper sulfide grains adhering to its surface. One sample in particular (Sample #11), composed of grains cemented together as they weathered, contains numerous and varied sulphide grains. Grains in sample #11 identified by EDS analysis on the microprobe include copper and silver sulfides. Figures 4.57, 4.58, and 4.59 show these various grains found adhering to slags and weathered sediments from the Yasmina sample suite. Although there is no direct evidence in the slags for the processing of sulphidic ores, the identification of rare sulphide grains attached to the slag samples suggests that copper and silver sulphides were in close proximity to the metallurgical site.

Bachmann notes that the presence of sulphides is an indication that sulphidic ores were smelted (1982). The location of these sulphide grains is suspect, as the chemistry of the samples with which they were found do not indicate either sulphidic ore smelting (no sulphide phases present) nor copper metallurgy (no copper phases present). The small size of these grains did not permit reliable quantitative data to be obtained regarding their elemental chemistry. Nevertheless, the presence of these grains in the slags sample suite is suggestive of some processing of sulfide ores.

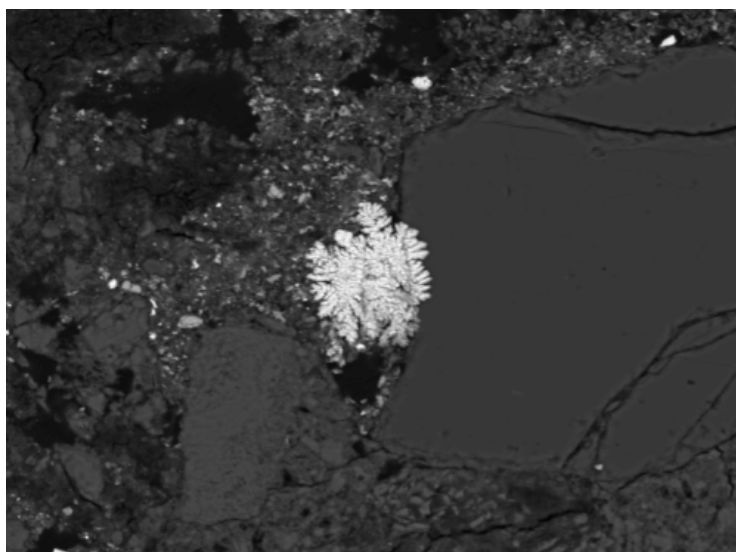
Estimating Working Temperatures: Estimates of working temperatures for the various metal-working processes can be made based on comparison of metal and glass



100µm
BEI Cu₂SAs₂ grain adhering to weathered Fe

Figure 4.57

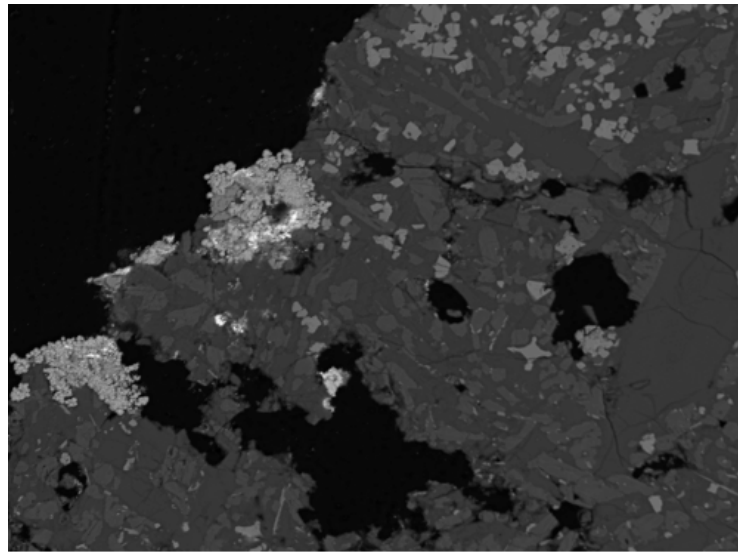
Backscattered electron image of a copper-sulphur-arsenic grain (bright white) adhering to a cemented mass of sediments, sample #11



30µm
BEI Ag₂S grain in matrix of SiO₂ and Pb

Figure 4.58

Backscattered electron image of a silver-sulphide grain (white) adhering to a cemented mass of sediments, sample #11



40µm
BEI 16-6 copper sulphide grains

Figure 4.59

Backscattered electron image of copper sulphides (light grey/white) adhering to an iron slag, sample #16

compositions to phase diagrams. The phase diagrams represent compositional variations as a function of temperature and are based on laboratory experiments. In the experiments, care is taken to be sure the results are equilibrium results, that is, that the reactions under study have reached a steady-state and show no further tendency to change with time. Clearly the dynamic situation of furnaces or hearths seldom reach such equilibrium conditions and the application of such equilibrium experiments to the products (slags, metal prills) of such dynamic processes is problematic.

Another concern in applying phase diagrams to complex systems is the limited number of chemical components typically represented in phase diagrams. Experimentalists limit the number of chemical species in a particular experiment in an effort to reduce the level of variability. This makes application of the experimental results (phase diagrams) to polycrystalline slag or metal systems difficult. For example, iron slags are composed of major amounts of silica, iron, oxygen, and variable amounts of calcium and aluminum. Representation of each of the variables (chemical components, temperature, oxygen content or oxygen fugacity) typically uses one graphical dimension, so a system with five chemical components and temperature as variables is a challenge. There are some graphical “shortcuts” (that will be used here), such as combining chemical components (for example, copper and tin, see Appendix) rather than the more realistic, but graphically challenging $\text{Cu}+\text{Pb}+\text{Sn}+\text{O}+\text{S}$ system.

The glass analyses (Table 4.6 and appendix) can also be used to interpret process temperatures using ternary phase diagrams. Copper slags contain a variety of chemical components including Si, Ca, Al, Pb, O, Na, K, Cu, plus a number of less important components (Bachmann, 1982). Two different systems, $\text{SiO}_2\text{-FeO-anorthite}$ and PbO-

SiO₂-Na₂O (reproduced in the appendices) can be used to represent some of the chemical variation, but obviously some components are not represented by these simplified systems. The anorthitic glasses from sample #25 and #29 plot on the ternary phase diagram (anorthite, SiO₂, FeO) at liquidus temperatures ranging from 1200°C to 1400°C. At first this seems unlikely, as Bachmann states that ancient metallurgists could not achieve temperatures above 1300°C to 1400°C, and generally operated at much lower temperatures (1982). The association of these high temperature glasses, however, with the vitrified ceramic portions of the slags, may indeed corroborate Bachmann's statement; these slags likely represent the failure (i.e., vitrification) of the ceramic at 1200°C to 1400°C, supporting the idea proposed by Bachmann (1982) and others (Craddock, 1995; Tylecote, 1980) that it was the inability of the furnace to withstand higher temperatures that limited the temperatures that could be obtained. The Yasmina anorthitic copper slag glasses indicate melting temperatures coincident with those associated with ceramic failure.

It is also worth mentioning that the iron slag glasses (Table 4.4) also plot in this same temperature range (~1350°C), indicating that the Yasmina metallurgists produced furnaces that could withstand such high temperature ranges (sample #7 shows no evidence of ceramics incorporated into the slag).

The lead-rich glasses indicate yet another aspect of copper metallurgy. Analytical data from Table 4.6, sample #41 and #43, were also plotted on a ternary phase diagram (PbO, SiO₂, Na₂O) and indicate minimum temperatures between 700°C and 800°C. These temperatures are the minimum temperatures required to produce these glasses;

actual temperatures may have been much higher. However, these temperatures probably represent the target range for the process.

The addition of lead to these systems significantly lowered the melting temperatures of the melt (Craddock, 1995); even a few percent of lead in these systems could lower the melting temperature by 100-200°C. The large amount of lead in these systems is the likely the result of its purposeful addition (for example, as part of a liquation process) as the amount of lead in these glasses is much greater than what would have come from a copper-lead alloy (Ponting, 1999). These lead-rich, low temperature glasses suggest a different metallurgical process, perhaps related to silver recovery, than the high temperature anorthitic glasses that are probably related to failure of ceramic crucibles and/or furnaces.

Phase diagrams of bulk slag chemistries can also be used to distinguish slags that have accumulated over time from different metallurgical stages, but caution should be used in selecting the appropriate diagram (Herz and Garrison, 199). For example, studies of slag heaps in Jordan that contain copper slags from the Early Bronze Age through the Roman period, were analyzed and plotted on the ternary system CaO-(+BaO)-MnO(+FeO)-SiO₂ (Weisgerber and Hauptmann, 1986). Slags from different metallurgical periods plotted together and were relatively distinct from one another. The Roman age copper slags, in particular, were distinguishable based on their high manganese content. As mentioned in reference to the iron slags, manganese-rich ores were sometimes exploited to facilitate the formation of slag, and in this case, it seems, to prevent the formation of metallic iron during the copper smelting process. The Yasmina copper slags, however, do not contain significant amounts of manganese (none in

pyroxenes above 2.4 oxide weight %; Table 4.8). Therefore, the Romans at Carthage were not exploiting the same manganese-rich copper ores as those from Jordan, nor were they adding manganese-rich fluxes to the copper processing at Carthage. Since manganese contents in all the Yasmina slags were low, it was not a useful parameter to use to distinguish these slags from one another.

In summary, the copper slags from Yasmina represent a variety of copper related metallurgical processes including bronze refining for silver, copper smelting/refining for casting, and the possible use of copper and silver sulfide ores. The abundance of vitrified ceramics in the slags suggests that either furnaces linings or crucibles were incorporated and routinely melted. As most of the evidence from the metals and glasses in the slags indicates, it is likely that copper metallurgy here was primarily related to refining or recycling of metals and alloys. Therefore, it is reasonable to suppose that the ceramic portions of the slags come from crucibles, rather than from the lining of primary copper smelting furnaces. Crucible technology is also consistent with the relatively small volume of slag from the site.

The Yasmina slags are typical of Roman technology in terms of the metals smelted and refined and were produced on a scale typical of a metallurgical site on the edge of a residential area, i.e., there are no large slag heaps on the scale of 1000's of kilograms as one would expect at a primary production center, but rather slag on the order of several hundred kilograms, suggestive of a smaller-scale operation. Another way to confirm that these slags are indeed typical of Roman metals technology is to ascertain something about the temperatures at which these furnaces operated. The metals and glasses present in the slags can be used to estimate the temperatures at which some of

those processes likely occurred. Craddock's plot of partial pressures of oxygen against temperature, reproduced here in Figure 4.29, shows the types of phases one should expect to find in slags that were formed at certain oxygen pressures and temperatures.

For the iron slags, the presence of both metallic iron (Fe) and iron oxides, wüstite (FeO) and magnetite (Fe₃O₄) in the samples allows us to estimate that the temperature of formation of these slags occurred roughly between 1000°C and 1250°C. The fact that magnetite is the primary iron oxide present in the crystalline fayalite slags suggests that the temperature of formation was usually on the higher end of this temperature range and in a fairly reducing atmosphere of $-\log p_{O_2}$ 20. Those slags with metallic iron present formed under even more reducing conditions. For the copper slags, those with cuprite (Cu₂O) and metallic copper (Cu), can be used to estimate temperatures in a range from 1050°C to 1250°C. These slags indicate that conditions were more oxidizing for the copper metallurgy, with a $-\log p_{O_2}$ of around 11. It is generally accepted that furnace operating temperatures in antiquity did not exceed 1300°C-1400°C (Bachmann, 1982). The phases in the iron and copper slags here fall well below this maximum. The different reducing conditions that the phases from the iron versus the copper slags, $-\log p_{O_2}$ of 20 and $-\log p_{O_2}$ of 11, respectively, indicate supports the notion that the iron metallurgy was primarily a smelting operation, requiring more reducing conditions, while the copper processing occurred under more oxidizing, typical of refining and recycling metallurgy.

CHAPTER FIVE

CONCLUSIONS AND RECOMMENDATIONS

The use of micro-analytical techniques, rather than bulk chemical analyses of the slags, proved to be a useful method for characterizing and interpreting the metallurgical slags from the Yasmina cemetery. In the absence of any contextual evidence, i.e. furnace remains, hearths, or tuyeres, micro-analytical techniques provided more detailed information, particularly about metallic phases and processes than bulk chemical analyses. Preliminary characterizations of small numbers of slag samples using micro-analytical techniques, such as petrography and the electron microprobe, is an effective method for determining the metals involved and the processes by which they were processed. To answer more specific questions about process temperatures or reducing conditions, bulk chemical methods may be more appropriate.

The metallurgical slags excavated from the fill at the Yasmina cemetery are indicative of two distinct types of metallurgy: iron and copper. The morphology and chemistry of the iron slags indicates the primary smelting of iron ores as part of the bloomery process, typical of Roman iron metallurgy. The copper slags exhibit a much greater morphological and chemical variety and cannot be attributed to a single metallurgical process. The nature of the metals and glasses in the slags suggests a variety of processes, including several versions of metal recycling, specifically, the recycling of bronzes (presumably for their silver) and the addition of lead to copper and bronzes,

presumably to improve casting quality. Additionally, there is some evidence for the primary production of copper and the use of sulphidic copper ores.

The evidence in the slags of metal recycling is particularly interesting in light of the discovery on the Byrsa of Punic metallurgical sites that produced evidence of copper metal working (Lancel, 1982). As the Phoenicians were clearly producing copper and perhaps copper alloys as well, it is reasonable that the Romans may have been recycling the Phoenician metals for their own use. The recycling evident at Yasmina could also involve Roman coinage, made of silver, bronze and copper, as coinage was devalued over time and also changed frequently with changes of the emperor. Attributing the recycling to coinage specifically would require further study of the metallography of the coins removed from Yasmina as well as more specific chemical analyses of the metals in the Yasmina slags. The evidence of recycling could be attributed simply to the general recycling of the abundant bronze and copper pieces used widely throughout the Roman empire.

Canadian excavations at Carthage in the area just north of the theater recovered numerous metallic objects. Most of these objects are copper alloys and show a wide range of compositions, from bronzes to brasses (Unglik, 1991). The work by Unglik used both bulk analyses (using energy dispersive techniques and X-ray fluorescence on the metal objects) and microanalytical techniques to analyze the metal objects. The bulk analyses provide an “average” composition for the metal objects by integrating the various exsolved metal phases into a single bulk composition. These bulk analyses are not directly comparable to the microanalyses reported in this study. Only integration of

the various metal phases in the prills into a single analysis will provide “bulk” analyses for these samples.

Several of the smaller metal objects, fasteners of various sorts, were relatively pure copper. This is similar to the relatively pure copper prills from the copper slags in this study. The pure copper was soft and easier to bend than copper alloys; this explains its use in fasteners.

The bronzes are high in copper, but have lead contents that range up to 25% lead, but generally less than 10% tin (Unglik, 1991). These high lead, low tin bronzes are consistent with the results from the slag analyses. Unglik concludes the high lead content of the bronzes was to promote the casting of the bronzes and several of the objects he examined are statuary that must have been cast. He examined one sample of “nonferrous” that is clearly related to copper processing. A bulk composition showed major amounts of calcium, silica, copper, tin, and lead, similar to the copper slags in this study.

Unglik (1991) also cited some earlier work he had done on some iron objects from Carthage and some iron slag. He concluded iron was smelted at Carthage (as evidenced by the slag) using a low efficiency bloomery process.

One does not get a sense of the relative abundance of the various metal types from Unglik’s 1991 study. He reports on data for 41 copper alloys (about half of them brass) and on 21 iron objects. However, he states these samples are a subset of the total collection and does not offer any information on the proportion of various metal types in the entire collection.

Although brass was a major part of Unglik's collection, none of the slags examined in this study show any zinc and thus do not document the production of brass at Carthage. Perhaps brass was imported from another source. Alternatively, maybe sampling procedures used at the Yasmina cemetery inadvertently omitted the brass-making slags from the sample suite. This second explanation does not seem likely in light of how well the slags document the rest of the metal suite documented by Unglik; therefore, the importation of brass to Carthage seems the most likely explanation.

Alternatively, the slags from Yasmina may represent the actual Phoenician metallurgical processes, rather than Roman metallurgy. Careful comparison of the chemistry and morphology of the slags from Yasmina with those recovered from the Byrsa excavations would be required to test this hypothesis. Small numbers of Punic artifacts, however, have been recovered from the fill layers at the Yasmina cemetery and may support the notion that the Yasmina slags are Punic in origin. It is reasonable to suggest that the Romans collected fill material from nearby areas that contained remains from the Punic civilization that once thrived in Carthage.

The amount of metallurgical slags excavated from the cemetery is small compared to the enormous slag heaps usually associated with the primary smelting of metals (Craddock, 1995; Bachmann 1982). Admittedly, these slags were not in situ and presumably there is a metallurgical site in close proximity to the Yasmina cemetery that has not yet been discovered. Regardless, the variety of slags from Yasmina suggests that the metallurgical operation was equipped to process an assortment of metals, including copper, bronze, silver, and iron. Unlike major smelting centers typically located near the mine sites and producing enormous slag heaps (Craddock, 1995), the Yasmina slags

indicate a much smaller scale metallurgy capable of processing various metals and alloys. Evidence for small-scale processing is supported by the appearance of droplet boundaries within a single slag piece, as demonstrated with the iron tap slags, or the measure of various compositions of metal prills within a single copper slag sample. That we are able to observe individual droplets of tap slag as it was removed from the furnace suggests that the furnace operation was producing small quantities of slag at any given time. This type of small-scale and varied production is typical of metallurgical sites nearer village or cities, such as metallurgical sites located near the Carthaginian port complex (Hurst, 1974); in general, during Roman times, major smelting occurred away from civilization centers near the ore source (Forbes, 1955).

The types of ores utilized for the iron and copper processes represented in the Yasmina slags could not be determined. The presence of sulphides in the slag matrices would indicate that sulphidic ores were exploited, but these phases are absent altogether in the both the iron and the copper slags. The variety of metal sulphide grains adhering to several of the slag samples cannot be correlated directly with any of the Yasmina slags, but certainly raise more questions about the copper metallurgy represented here.

Determining the ores sources for these slags is similarly confounded by the fact that Roman Carthage was a major trading port for the Roman empire. As such, its metallurgists had access to virtually any metal exploited or any metal produced in the extensive Roman empire at the time through the long-standing trade networks throughout the Mediterranean. It is possible that metal ingots of lead, copper, bronze, and iron were used as ballasts on the numerous ships that frequented the port city of Roman Carthage and were traded to the metallurgists of the city for local use. The absence of pieces of ore

from the Yasmina fill and the evidence of recycling, rather than the primary smelting of metals, suggests that the slags at Yasmina represent the secondary refining of metals. Where those metals came from would be difficult to determine, as the Roman trade networks were extensive

Romans obtained tin from Britain and eastern Europe (Healy, 1978). Roman lead came from sources in Spain, Greece, and the eastern Mediterranean basin (Healy, 1978). Iron ores could be obtained virtually anywhere, although there is abundant evidence of its exploitation in Spain, Gaul, and Britain (Healy, 1978). Finally, evidence of copper exploitation is particularly abundant in Cypriot and Sardinia (Healy, 1978). Additionally, local copper ores in northeastern Tunisia were known during the Roman era (Sainfeld, 1955; Tylecote, 1976) and could have been exploited as well.

In summary, the iron and copper slags from the Yasmina cemetery are indicative of small-scale iron, copper, and bronze metallurgy practiced on the outskirts of a major civilization center. The metallurgical processes themselves are not unusual for Roman metallurgy, with the possible exception of the recycling of bronze with lead, evidence for which has not been cited elsewhere. The types of slags suggest a focus on the refining of copper and its alloys and the limited working/refining of iron. The recycling of the copper alloys was likely in an attempt to recover the more valuable metal, silver. Iron may have been produced on such a small-scale for tools on site, as has been seen at other smithing sites throughout the Roman empire (Healy, 1978). The variety of metallurgical processes at work also suggests production for local use, rather than production for export, which one would expect to be on a much greater scale and further removed from

the city proper nearer the mine sites, as we see at Rio Tinto, for example (Craddock, 1995).

The preliminary characterization of the metallurgical slag from the Yasmina cemetery was able to answer basic archaeological and metallurgical questions: what types of metals were being smelted? What processes were being used to obtain the metals? What are some of the details of the metallurgical processes at work? What type of metallurgical site do these slags indicate may be present near by? Are these processes typical of Roman metals technology (i.e. what does the lack of evidence for brass production at this site suggest)? The answers to these questions and the additional data collected regarding these slags, can be used answer the many questions that this characterization study raised. Suggestions for further study include:

1. Locating the origin of these slags, i.e., determining the location of the site at which they were smelted. The magnetic character of the slags, as well as the magnetic signals generated by hearths and furnaces, suggests the use of geophysical techniques, particularly a magnetometer, to locate this site. As the slags at Yasmina were excavated as part of fill materials used by the Romans to level the cemetery for its next stage of use, it is unlikely that they brought sediments for such a purpose from any great distance. A geophysical survey to locate the site and determine its spatial extent and organization would be helpful in assessing the actual scale of metallurgical production.
2. Determining possible ore sources using lead isotope analytical techniques. The abundance of lead in the copper slag samples could be used to determine possible ore source throughout the Mediterranean. Metallurgists in Roman

Carthage would have had access to virtually any metal produced in the empire, as the trade networks were so extensive and Carthage was a major port city in the Mediterranean basin. Lead isotopic signatures for a variety of ore sources throughout this region have been used in other lead isotope studies on Carthaginian materials (Pintozzi, 1991). Ore sources for the lead used in the refining of the copper and its alloys may be useful in establishing metals trade routes during the Roman empire.

3. Determining more specifics about the processes, particularly the copper metallurgical processes, represented by the Yasmina slags. While the iron metallurgy proved to be straight-forward, the interpretation of the complex copper slags must remain general without further analytical work on the metals, ceramics, and glass phases, including trace element analysis. Detailed analysis of all of these phases was beyond the scope of this study, but the techniques employed here have proven very useful in providing information about metallurgical processes. Further work with these slags using micro-analytical techniques will be necessary to answer more detailed questions regarding the copper metallurgy. Trace element analysis (using ICP-MS) of metal prills and possibly glass might help to understand what was being processed. Sulfur isotope studies would constrain the possible sources of the sulfide phases.
4. Comparison of the chemistry and morphology of the Yasmina slags with the high temperature remains excavated from the Punic layers on the Byrsa to determine if the Yasmina slags may indeed be Phoenician in origin, rather

than Roman. Trace element analyses would also be useful in determining if any correlation exists between these two suites of metallurgical remains.

5. Bulk analysis of representative samples from the Yasmina sample suite would be useful in comparing the characteristics of these slags with others in the Roman empire during the Roman Iron Age. The majority of published data are from bulk chemical analyses. Correlating the bulk analytical data with the microscopic data will provide a clearer and more meaningful picture of the Yasmina slags in the context of the Roman Iron Age. However, the relatively small size and heterogeneity of the slag samples will make it difficult to obtain representative samples for analysis.
6. Analysis of the abundant ceramic portions of the Yasmina slags and comparison with the crucible fragments that have been excavated from the Yasmina site to determine the types of structures and processes used to produce the Yasmina slags.
7. Search excavated slags for non-ceramic copper slags that may be related to primary copper production as opposed to secondary or refining processes.
8. Examination of “crucibles” also excavated from the Yasmina site but not included with the metallurgical remains examined here. These “crucibles” may relate to the metallurgical processing represented by the Yasmina slags.

REFERENCES

- Bachmann, Hans-Gert, 1982, *The Identification of Slags from Archaeological Sites*. Occasional Publication No. 6. London: Institute of Archaeology.
- Blair, Carl, 1999, *The Iron Men of Rome*. Edited by Mary R. Demaine and Rabun M. Taylor. *Life of the Average Roman: A Symposium*. Bear Lake, Minnesota: PZA Publishing.
- Bullard, Reuben G., 1975, *Excavations at Carthage 1975 Conducted by the University Of Michigan*. Edited by J.H. Humphrey. *The Environmental Geology of Roman Carthage*. Ann Arbor: The University of Michigan.
- Carmichael, I.S.E., 1967, The iron-titanium oxides of silic volcanic rocks and their associated Ferromagnetism silicates. *Contributions to Mineralogy and Petrology* 14, 36.
- Cleere, Henry, 1976, *Roman Crafts*. Edited by Donald Strong and David Brown. *Ironmaking*. New York: New York University Press.
- Craddock, Paul T. I.C. Freestone and M. Hunt Ortiz, 1987, "Recovery of Silver from Speiss at Rio Tinto (SW Spain)." IAMS Newsletter, October 11.
- Craddock, Paul T., 1989, *Scientific Analysis in Archaeology*. Edited by Julian Henderson. *The scientific investigation of early mining and metallurgy*. Oxford: Oxford University Committee for Archaeology and individual authors.
- Craddock, Paul T., 1995, *Early Metal Mining and Production*. Washington, D.C.: Smithsonian Institution Press.
- Craddock, Paul T., I.C. Freestone, N.H. Gale, et al., 1996, "The Investigation of a small Heap of silver smelting debris from Rio Tinto, Huevla, Sapin." In *Furnaces and Smelting Technology in Antiquity*. Edited by P.T. Craddock and M. J Hughes. British Museum Occasional Paper No. 48, 199-217.
- Deer, W.A., R.A. Howie, and J. Zussman, 1966, *An Introduction to Rock-forming Minerals*. New York: John Wiley & Sons.
- Donaldson, Colin H., 1976, "An Experimental Investigation of Olivine Morphology." *Contributions to Mineralogy and Petrology*, 57, 187-213.

- Ettler, Vojtech, Olivier Legendre, and Françoise Bodenan, et al., 2001, "Primary Phases And Natural Weathering of Old Lead-Zinc Pyrometallurgical Slag from Pribram, Czech Republic." *The Canadian Mineralogist*, 39, 873-888.
- Forbes, R.J., 1955, *Studies in Ancient Technology. Vol. 3*. Leiden: E.J. Brill.
- Girgia, Monir S., 1987, *Mediterranean Africa*. New York: University of Press of America.
- Gruen, Erich S., 1970, *Imperialism in the Roman Republic*. New York: Holt, Rinehart, and Winston.
- Healy, John F., 1978, *Mining and Metallurgy in the Greek and Roman World*. London: Thames and Hudson.
- Heimann, R.B., U. Kreher, I. Spazier, and G. Wetzels, 2001, "Mineralogical and Chemical Investigations of Bloomery Slags from Prehistoric (8th century BC to 4th century AD) Iron Production sites in Upper and Lower Lusatia, Germany." In *Archaeometry*, 43, 2, 227-252.
- Herz, Norman and Ervan Garrison, 1998, *Geological Methods for Archaeology*. New York: Oxford University Press.
- Humphrey, John H., 1980, *New Light on Ancient Carthage*. Edited by John Griffiths Pedley. *Vandal and Byzantine Carthage: Some New Archaeological Evidence*. Ann Arbor: The University of Michigan Press.
- Hurst, Henry, 1974, "Excavations at Carthage, 1974: First Interim Report." In *Antiquaries Journal*, LV. New York: Oxford University Press.
- Hurst, Henry, and Lawrence Stager, 1978, "A Metropolitan Landscape: The Late Punic Port of Carthage." *World Archaeology*, 9, 3, 334-346.
- Hurst, Henry, 1984, *Excavations at Carthage: The British Mission. Vol. II, 1*. Oxford: Oxford University Press for the British Academy.
- Hurst, H. P., and S.P. Roskams, 1984, *Excavations at Carthage: The British Mission. Vol I, 1*. Huddersfield, Great Britain: H. Charlesworth, Ltd. For the British Academy.
- Kassianidou, Vasiliki, 1995, "Ores, Slags, Refractories and other finds relating to ancient Metallurgy." In *The Practical Impact of Science on Field Archaeology: Maintaining Long-term Analytical Options: A Workshop on Cyprus, 22 & 23 July, 1995*. Sponsored by The Society for Archaeological Sciences, The Institute For Aegean Prehistory, and The Samuel H. Kress Foundation.

- Khader, Aicha Ben Abed Ben, and David Soren, ed., 1987, *Carthage: A Mosaic of Ancient Tunisia*. New York: W.W. Norton & Company.
- Klein, Sabine and Andreas Hauptmann, 1999, "Iron Age Leaded Tin Bronzes from Khirbet Edh-Dharih, Jordan." *Journal of Archaeological Science*, 26, 1075-1082.
- Kolstrup, Else, 1995, *Africa Proconsularis: Regional Studies in the Segermes Valley Of Northern Tunisia*. Edited by Soren Dietz, Laila Ladjimi Sebai, and Habib Ben Hassen. *Holocene Vegetational Records from the Segermes Valley, NE Tunisia with Special Reference to the Roman Period*. Copenhagen: The Carlsburg Foundation and The Danish Research Council for Humanities.
- Lancel, Serge, 1995, *Carthage: A History*. Trans. By Antonia Nevill. Cambridge: Basil Blackwell, Ltd.
- Lancel, Serge, 1982, "Byrsa II: Rapports preliminaires sur les fouilles 1977-1978: Niveaux et vestiges puniques." In *Mission Archeologique Francaise A Carthage*. Palais Farnese: Ecole Francaise De Rome.
- McDonnell, G., 1983, "Iron and its alloys in the fifth to eleventh centuries AD in England." *World Archaeology*, 20, 3, 373-381.
- Niemeyer, Hans Georg, *Greek Colonists and Native Populations*. Edited by Jean-Paul Descoedres. *The Phoenicians in the Mediterranean: A Non-Greek Model for Expansion and Settlement in Antiquity*, 468-489. New York: Clarendon Press.
- Norman, Naomi J., and Anne E. Haeckl, 1992, "The Yasmina Necropolis at Carthage, 1992." *Journal of Roman Archaeology*, 238-250.
- Norman, Naomi J. <http://classics.uga.edu> (Web address)
- Nriagu, Jerome O., 1983, *Lead and Lead Poisoning in Antiquity*. United States: John Wiley & Sons.
- Purdy, Judy, 1995, "Ancient Voices Speak Again." In Research Reporter, Winter 1995, Vol. 25, No. 2. Research Communications Division, The University of Georgia.
- Peacock, D.P.S., and R. Tomber, 1991, "Roman amphora kilns in the Sahel of Tunisia: Petrographic investigation of kiln material from a sedimentary environment." In *Recent Developments in Ceramic Petrology*. Edited by A. Middleton and I. Freestone. British Museum Occasional Paper, no. 81, 289-301.
- Pintozzi, Lisa Anne, 1991, "Testing the Metal of the Gods: A Study of Defixiones from The University of Georgia Excavations at Carthage." Masters Thesis. University Of Georgia.

- Ponting, Matthew J., 1999, "East Meets West in Post-Classical Bet She'an: The Archaeometallurgy of Culture Change." *Journal of Archaeological Science*, 26, 1311-1321.
- Rakob, Friedrich, 2000, "The Making of Augustan Carthage." In *Romanization and the City: Creation, Transformation, and Failures: Proceedings of a conference held at the American Academy in Rome to celebrate the 50th anniversary of the excavation at Cosa, 14-16, May, 1998*, edited by Elizabeth Fentress, 76-82. Journal of Roman Archaeology: Portsmouth, Rhode Island.
- Raven, Susan, 1984, *Roma in Africa*. New York: Longman Group, Ltd.
- Rehren, Thilo, 1999, "Small Size, Large Scale Roman Brass Production in Germania Inferior." *Journal of Archaeological Science*, 26, 1083-1087.
- Ryndina, Natalja, 1999, "Copper Production from Polymetallic Sulphide Ores in the Northeastern Balkan Eneolithic Culture." *Journal of Archaeological Science*, 26, 1059-1068.
- Sainfeld, Paul, 1955, "The Lead-Zinc-Bearing Deposits of Tunisia." *Economic Geology and the Bulletin of the Society of Economic Geologists*, 51, 150-77.
- Salter, Chris J., and J. Peter Northover, 1992, "Metalworking at Hengistbury Head, Dorset, and the Durotrigan Coinage: A Reinterpretation of an Iron Age and Roman Industrial Site." *Materials Research Society Symposium Proceedings, Vol, 267*.
- Sherlock, David, 1976, *Roman Crafts*. Edited by Donald Strong and David Brown. *Silver and Silversmithing*. New York: New York University Press.
- Snodgrass, Anthony M., 1980, *The Coming of the Age of Iron*. Edited by Theodore A. Wertime and James D. Muhly. *Iron and Early Metallurgy in the Mediterranean*. New Haven: Yale University Press.
- Soren, David, Aicha Ben Abed Ben Khader, and Hedi Slim, 1990, *Carthage: Uncovering the Mysteries and Splendors of Tunisia*. New York: Simon and Schuster.
- Tylecote, R.F., 1980, *The Coming of the Age of Iron*. Edited by Theodore A. Wertime and James D. Muhly. *Furnaces, Crucibles, and Slags*. New Haven: Yale University Press.
- Tylecote, R.F., 1962, *Metallurgy in Archaeology*. London: Edward Arnold Publishers, Ltd.
- Tylecote, R.F., 1976, *A History of Metallurgy*. London: Metals Society.

Unglik, Henry, 1991, "Structure, Composition, and Technology of Late Roman Copper Alloy Artifacts from the Canadian Excavations at Carthage." *Archaeomaterials*, 5, 91-110.

Weisberger, Gerd and Andreas Hauptmann, 1986, "Early Copper Mining and Smelting in Palestine." Edited by R. Maddin. *The Beginnings of the Use of Metals and Alloys*. Cambridge: MIT Press.

Wightman, Edith Mary, 1980, *New Light on Ancient Carthage*, Edited by John Griffiths Pedley. *The Plan of Roman Carthage: Practicalities and Politics*. Ann Arbor: The University of Michigan Press.

Wilson, A.J., 1994, *The Living Rock*. Cambridge: Woodhead Publishing, Ltd.

Ancient Sources:

Appian, *Libyca*, 134.

Corripus, VI, 60.

Chronica Gallica, a. ccccxv

Polybius, III, 22.

APPENDICES

Appendix: Sample List				
	Registry #	Square #	Locus #	Field description of slag
1	92.14.38	4		IRON TAP
2	92.14.25	4		IRON CAKE
3	92.14.22	4		IRON FURNACE FRAGMENT
4	92.14.55	4		IRON FROTHY
5	92.14.24	4		COPPER OTHER (ORE?)
6	92.14.24	4		TIN OTHER (ORE?)
7	92.14.259	unknown		IRON TAP
8	92.14.81	unknown		IRON CAKE
9	92.14.90	unknown		IRON FROTHY (LIGHT)
10	92.14.235	unknown		IRON FORTHY (DENSE)
11	92.14.268	unknown		COPPER TAP
12	92.14.248	unknown		COPPER FURNACE
13	92.14.238	unknown		COPPER FROTHY (LIGHT)
14	92.14.78	unknown		COPPER FROTHY (DENSE)
15	92.14.270	unknown		COPPER ORE?
16	92.14.107	unknown		COPPER ORE?
17	92.14.90	unknown		TIN OTHER?? (REDDISH FROTHY)
18	93.16.0148	10	10002	IRON TAP
19	93.16.0150	10	10004	IRON CAKE
20	93.16.0184	8	8030	IRON FROTHY
21	93.16.0048	5	5031	COPPER TAP
22	93.16.0066	5	5026	COPPER CAKE
23	93.16.0265	5	5064	COPPER FURNACE
24	93.16.0048	5	5031	COPPER ORE?
25	93.16.0249	7	7096	IRON TAP
26	93.16.0170	7	7025	IRON CAKE
27	93.16.0022	7	7022	IRON FURNACE
28	93.16.0022	7	7022	IRON FROTHY (LIGHT)
29	93.16.0107	7	7011	IRON FROTHY (DENSE)
30	93.16.0081	7	7035	COPPER TAP/CAKE?
31	93.16.0017	7	7012	TIN OTHER?? (REDDISH FROTHY)
32	93.16.0126	7	7071	IRON FROTHY DENSE
33	93.16.0142	6	6034	IRON CAKE
34	93.16.0061	6	6006	IRON FROTHY (DENSE)
35	93.16.0118	6	6053	IRON FROTHY (LIGHT)
36	93.16.0072	6	6003	IRON FROTHY (DENSE)
37	93.16.0011	6	6024	COPPER TAP
38	93.16.0011	6	6024	COPPER ORE?
39	93.16.0009	6	6011	PARTIALLY VITRIFIED ASHLAR?
40	94.16.0043	15	15044	IRON CAKE
41	94.16.0188	15	13043	IRON FURNACE
42	94.16.0086	15	15049	IRON FROTHY

43	94.16.0126	13	13031	COPPER CAKE
44	94.16.0185	13	13043	COPPER TAP
45	94.16.0185	13	13043	COPPER FURNACE
46	94.09.0175	6	6173	IRON TAP
47	94.16.0055	6	6127	IRON FURNACE/FROTHY
48	94.16.0039	6	6121	IRON FROTHY (DENSE)
49	94.16.0002	6	6080	COPPER TAP
50	95.16.0114	7	7350	IRON TAP
51	95.16.0030	7	7304	IRON TAP
52	95.16.0068	7	7320	COPPER CAKE
53	95.16.0030	7	7304	COPPER FROTHY
54	95.16.0134	7	7361	OTHER (REDDISH FROTHY)
55	95.16.0154	7	7129	OTHER (NON-MAGNETIC METALLIC)
56	95.16.0154	7	7129	OTHER (FROTHY, NON-MAGNETIC)
57	95.16.0133	13	13069	IRON TAP
58	95.16.0224	13	13099	IRON CAKE
59	95.16.0079	13	13048	IRON FURNACE
60	95.16.0001	16	16018	IRON TAP
61	95.16.0122	13	13069	COPPER CAKE
62	95.16.0224	13	13099	COPPER TAP
63	95.16.0190	13	13093	COPPER FURNACE
64	95.16.0058	8	8028	COPPER CAKE
65	95.16.0075	16	16014	OTHER (SANDY STONE??)
66	95.16.0042	16	16026	IRON FURNACE
67	95.16.0227	8	8144	IRON CAKE
68	95.16.0019	6	6196	IRON TAP
69	95.16.0185	6	6226	IRON FROTHY
70	95.16.0210	6	6242	OTHER (NON-MAGENTIC FROTHY)
71	95.16.0034	6	6175	IRON FURNACE
72	95.16.0006	6	6172	OTHER (NON-MAGNETIC TAP)
73	95.16.0074	6	6193	COPPER TAP
74	97.14.6	6		IRON TAP
75	97.16.0164	6	6330	IRON CAKE
76	?????	6		OTHER (NON-MAGNETIC FROTHY)
77	97.16.0047	7	7506	IRON FROTHY
78	97.16.0031	7	7515	IRON TAP
79	97.16.0036	7	7525	COPPER FROTHY
80	97.16.0051	7	7528	COPPER ORE?
81	97.16.0059	7	7545	COPPER FURNACE
82	97.16.0037	8	8152	COPPER TAP
83	97.16.0046	8	8160	COPPER CAKE/TAP
84	97.16.0103	8	8195	COPPER FURNACE
85	97.16.0108	8	8205	COPPER/CARBON ORE??
86	97.16.0128	8	8217	IRON FROTHY
87	97.16.0093	8	8191	COPPER FROTHY

Appendix: Iron and Copper Slag Phase Data

*Sample # is indicated by the digits preceding the decimal, e.g 25.2 is the second analytical data point for sample #25

Iron Slag Phase Analyses

GLASSES

Analysis/Description	Analytical Routine (elements or oxides analyzed)										
Sample #7	SiO2	Al2O3	FeO	MnO	MgO	CaO	Na2O	K2O	Total	Cr	Total
York 76-C-150 glass standard	56.28	4.37	0.256	0.21	6.5	21.9	9.85	1.542	100.92		
7.1 interstitial glass	47.41	5.96	37.6	0.1	0	3.09	0.5355	2.417	97.11		
7.2 interstitial glass	45.63	6.17	36.26	0	0	1.75	0.9159	2.817	93.54		
7.4 interstitial dark phase	47.67	5.97	36.42	0.067	0.011	3.43	0.2176	2.604	96.38		
7.6 interstitial glass	48.2	6.25	36.21	0.134	0	2.73	0.4448	3.12	97.08		
Sample #9	SiO2	Al2O3	FeO	MnO	MgO	CaO	Na2O	K2O	Total	Cr	Total
9.23 glass interstitial to fayalite	52.38	14.42	16.38	0	0.036	7.95	1.5007	3.47	96.15		
9.24 glass interstitial to fayalite	55.08	14.79	11.24	0.199	0	10.2	1.7907	3.62	96.92		
Sample #17	SiO2	TiO2	Al2O3	MgO	FeO	CaO	MnO	K2O	Na2O	Cr	Total
9.14 glassy area near sample edge	48.78	0.172	4.22	1.417	31.44	11.4	0.3442	1.393	0.567	0	99.73
Sample #17	SiO2	TiO2	Al2O3	MgO	FeO	CaO	MnO	K2O	Na2O	Cr	Total
17.7 glass	43.12	0	35	0.031	1.656	19.7	0	0.045	0.551	0.009	100.1

METALS

Analysis/Description	Analytical Routine (elements or oxides analyzed)										
Sample # 18	Cu	Sn	Sb	Pb	As	Fe	Ag	S	Total	Cr	Total
CMTaylor Pyrite Std.	0	0	0.05	0	0	46.9	0.048	51.75	98.73		
iron prill	0.05	0	0.004	0.022	0	97.9	0.0119	0.04	97.98		
iron prill	0.05	0	0.008	0	0.029	96	0	0.01	96.13		
Sample #19	Cu	Sn	Sb	Pb	As	Fe	Ag	S	Total	Cr	Total
iron prill	0.141	0	0	0.066	0	96.8	0	0.011	97.05		
PYROXENES	Analytical Routine (elements or oxides analyzed)										
Sample #9	SiO2	TiO2	Al2O3	MgO	FeO	CaO	MnO	K2O	Na2O	Cr2O3	Total

CR augite std USNM	50.41	0.508	7.84	17.89	4.43	17.8	0.2713	0.014	0.8045	0.957	100.9
9.1 hedenbergite	45.63	0.07	2.037	0.504	31.59	19.9	0.2184	0.041	0.1685	0	100.1
9.7 hedenbergite	44.82	0.112	2.422	0.865	29.57	21	0.2458	0.012	0.0747	0	99.12
Sample #13	SiO2	TiO2	Al2O3	MgO	FeO	CaO	MnO	K2O	Na2O	Cr2O3	Total
13.3 hedenbergite	49.31	0.054	0.051	2.858	28.1	16.1	2.6553	0.061	0.0037	0	99.17
Sample #17	SiO2	TiO2	Al2O3	MgO	FeO	CaO	MnO	K2O	Na2O	Cr2O3	Total
17.5 pyroxene	45.64	0.792	6.5	11.71	10.33	24.2	0.2371	0.109	0.3561	0.104	100

OXIDES

Analysis/Description	Analytical Routine (elements or oxides analyzed)																			
	SiO2	TiO2	Al2O3	MgO	FeO	CaO	MnO	Cr2O3	Total	SiO2	TiO2	Al2O3	MgO	FeO	CaO	MnO	Cr2O3	Total		
Sample #9																				
Hematite std (CMT)	0	0	0	0	0.29	61.8	0.053	0.016	62.18											
Magnetite std USNM	0.03	0	0.02	0	0.19	64.5	0	0.008	64.76											
9.4.1 wustite	0.205	0.071	0.243	0.044	100.2	0.01	0.008	0	100.75											
9.8 magnetite	1.316	2.386	6.03	0	84.46	0.03	0.1455	0.106	94.48											
9.11 magnetite	0.692	1.699	5.18	0.075	87.81	0.04	0.0725	0.044	95.61											
9.4 wustite	77.52	0	0	0.07	0.002	22.3	99.85													
Sample #16																				
16.2 iron oxide	0	0	0.002	0	0	54.6	0.0532	0.005	54.63											
Sample #17																				
17.9 iron oxide	0	0	0	0	0	55	0.0177	0.002	54.98											
Sample #18																				
18.4 iron oxide	0	0	0	0	0	65	0.0416	0.15	65.21											
Sample #19																				
19.4.2 iron oxide	0.027	0	0	0.044	0	65.1	0.0059	0	65.17											
OLIVINES																				
Analysis/Description	Analytical Routine (elements or oxides analyzed)																			

Sample #7	SiO2	Al2O3	MgO	FeO	CaO	Ni	Mn	Cr	Ti	Total	
<i>olivine 5 std large grain</i>	39.4	0.003	44.3	17.02	0.01	0	0.234	0.031	0	100.9	
7.3 fayalite	29.22	0	0.523	67.89	0.349	0.02	0.2125	0	0.0021	98.22	
Sample #9	SiO2	Al2O3	MgO	FeO	CaO	Ni	Mn	Cr	Ti	Total	
9.9.1 fayalite	28.94	0.072	1.026	68.45	0.312	0	0.1936	0.007	0.016	99.02	
9.10 fayalite	28.81	0.081	1.022	68.77	0.279	0	0.187	0.045	0	99.19	
CR augite Std USNM	SiO2	TiO2	Al2O3	MgO	FeO	CaO	MnO	K2O	Na2O	Cr2O3	Total
9.9 fayalite	50.4	0.508	7.84	17.89	4.43	17.8	0.271	0.014	0.8045	0.957	100.9
	29.94	0.007	0.098	1.606	66.88	1.15	0.5253	0.002	0.0508	0	100.3

Copper Slag Phase Analyses
GLASSES

Analysis/Description	Analytical Routine (elements or oxides analyzed)												
	SiO2	Al2O3	MgO	CaO	K2O	Na2O	FeO	CuO	Sb2O5	SnO	PbO	SO2	Total
Sample #25													
25.8 glassy area near sample edge (pt. 1)	64.62	8.1	3.05	13.47	1.393	0.42	3.96	0.047	0.0089	0	0	0	95.05
25.9 glassy area (see 25.8)	62.19	7.92	3.22	12.83	1.258	0.34	4.41	0.056	0	0	0	0.024	92.24
25.10 glassy area (see 25.8, 25.9)	63.29	7.48	3.55	15.59	1.331	0.41	3.49	0.121	0.0268	0.02	0	0.024	95.33
AVERAGE	63.37	7.83	3.27	13.96	1.33	0.39	3.95	0.07	0.01	0.01	0.00	0.02	94.21
STANDARD DEVIATION	1.22	0.32	0.25	1.44	0.07	0.04	0.46	0.04	0.01	0.01	0.00	0.01	1.71
25.11 glassy area near sample center	57.84	5.26	4.45	21.15	2.367	0.94	2.1551	0.065	0.0401	0	0	0.071	94.34
25.12 glassy area (see 25.11)	56.8	5.23	4.48	22.41	1.872	0.85	2.7898	0.466	0.0711	0	0	0.036	95.01
25.13 glassy area (see 25.11, 25.12)	55.91	4.92	5	22.67	1.916	1	2.2523	0.28	0.1333	0	0	0.036	94.11
AVERAGE	56.85	5.14	4.64	22.08	2.05	0.93	2.40	0.27	0.08	0.00	0.00	0.05	94.49
STANDARD DEVIATION	0.97	0.19	0.31	0.81	0.27	0.07	0.34	0.20	0.05	0.00	0.00	0.02	0.47
Sample #29													
29.3 glassy area near Cu prill	57.06	3.15	4.16	26.48	3.17	0.41	1.2686	0.763	0.1595	0	0	0.059	96.68
29.4 glassy area (see 29.3)	63.11	5.24	1.872	5.09	6.46	2.2	4.1	3.44	0.2492	0.1	0	0	91.87
29.5 glassy area (see 29.3, 29.4)	57.9	4.59	4.7	9.43	3.77	0.94	1.8448	14.27	0.1766	0	0	0.084	97.7
29.6 glassy area nearer sample edge	59.55	4.08	4.02	26.38	2.812	0.59	1.5602	0	0.1244	0	0	0	99.11
29.7 glassy area (see 29.6)	58.58	4.03	3.73	23.3	3.87	0.66	1.6799	0.252	0.1688	0	0	0.012	96.28
29.8 glassy area (see 29.6, 29.7)	59.99	5.03	3.87	19.48	3.87	0.68	1.9024	0.056	0.1336	0.068	0	0	95.09
Sample #41													
	SiO2	Al2O3	MgO	CaO	K2O	Na2O	FeO	CuO	Sb2O5	SnO	PbO	SO2	Total

41.8 pt 1 in Pb rich glass *	23.56	3.1	0.384	3.25	0.378	0.19	1.4447	1.334	0	0.56	62.88	0	97.07
41.9 pt 2 in Pb rich glassy area	24.38	3.44	0.489	2.839	0.311	0.1	1.2848	0.881	0.0686	0.367	65.33	0	99.49
41.10 pt 3 in Pb rich glass	23.99	3.34	0.463	3.23	0.393	0.25	2.2088	0.582	0.1255	0.346	66.26	0	101.2
41.10 pt 3 in Pb rich glass (replicate)	24.34	3.18	0.57	3.22	0.438	0	1.9002	0.886	0	0.55	63.03	0	98.12
AVERAGE	24.1	3.265	0.48	3.135	0.38	0.13	1.71	0.921	0.0485	0.456	64.38	0	98.97
STANDARD DEVIATION	0.38	0.154	0.08	0.198	0.05	0.11	0.423	0.31	0.0607	0.115	1.684	0	1.782
41.11 pt 1 in Pb rich glass near Cu prill	35.34	4.7	0.678	4.35	1.096	0.46	2.2562	0.468	0	0.534	47.41	0.054	97.35
41.12 pt 2 in Pb rich glass near Cu prill	42.79	6.52	0.728	2.675	1.942	0.48	2.0799	0.3	0	0.248	38.9	0	96.67
41.13 pt 3 in Pb rich glass (near Cu prill)	35.95	4.51	0.724	4.27	1.328	0.64	1.9444	0.684	0.0802	0.38	47.39	0	97.9
41.14 pt 4 in Pb rich glass (near Cu prill)	32.36	3.85	0.731	3.84	0.813	0.21	1.6458	0.772	0.1716	0.287	52.55	0.027	97.26
AVERAGE	36.6	4.895	0.72	3.784	1.29	0.45	1.982	0.556	0.063	0.362	46.56	0.02	97.3
STANDARD DEVIATION	4.41	1.143	0.02	0.772	0.48	0.18	0.258	0.213	0.0817	0.127	5.656	0.026	0.504
41.15 glassy area 3	49.53	8.46	1.107	1.74	3.48	0.36	2.9887	0.394	0.1152	0.021	27.12	0.029	95.34
41.15 glassy area 3 (replicate)	49.61	8.63	1.135	1.796	3.6	0.37	3.04	0.395	0.122	0.022	28.89	0.029	97.64
AVERAGE	49.6	8.545	1.12	1.768	3.54	0.36	3.014	0.395	0.1186	0.021	28.01	0.029	96.49
STANDARD DEVIATION	0.06	0.12	0.02	0.04	0.08	0.01	0.036	0.001	0.0048	8E-04	1.252	4E-04	1.626
41.16 glassy area 3	24.11	3.43	0.495	2.611	0.101	0.07	2.1556	2.373	0	0.417	66.37	0.026	102.2

Sample #43

	SiO2	Al2O3	MgO	CaO	K2O	Na2O	FeO	CuO	Sb2O5	SnO	PbO	SO2	Total
43.4 Pb rich glassy area pt 1	26.43	3.78	0.499	3.24	0.573	0.14	1.5651	1.882	0.0571	0.02	55.53	0	93.72
43.5 Pb rich glassy area pt 2	26.14	3.38	0.601	4	0.595	0.14	1.6924	2.325	0	0	60.6	0.052	99.52
43.6 Pb rich glassy area pt 3	24.86	3.49	0.619	3.09	0.483	0.2	1.522	2.069	0	0	61.5	0	97.84
43.7 Pb rich glassy area pt. 4	27.57	3.65	0.516	3.56	0.47	0.14	1.0594	2.412	0	0.062	59.16	0	98.6
AVERAGE	26.3	3.575	0.56	3.473	0.53	0.16	1.46	2.172	0.0143	0.02	59.2	0.013	97.42
STANDARD DEVIATION	1.11	0.176	0.06	0.403	0.06	0.03	0.277	0.242	0.0286	0.029	2.628	0.026	2.561
43.8 glass near Pb rich area pt 1	47.15	8.49	1.506	3.34	1.127	0.42	4.01	0.6	0.2193	0.156	32.96	0	99.98
43.9 glass near Pb rich area pt 2	46.14	11.59	1.845	4.8	1.159	0.47	4.85	0.755	0	0.115	26.51	0.029	98.25
43.10 glass near Pb rich area pt 3	51.65	11.13	1.683	3.93	2.891	0.41	5.44	0.614	0.0577	0.167	19.14	0	97.12
AVERAGE	48.3	10.4	1.68	4.023	1.73	0.43	4.767	0.656	0.0923	0.146	26.2	0.01	98.45
STANDARD DEVIATION	2.93	1.673	0.17	0.734	1.01	0.03	0.719	0.085	0.1137	0.028	6.915	0.017	1.44
43.11 glass interstitial to quartz	57.49	19.23	2.328	5.69	2.573	0.48	6.36	0.31	0	0.042	0.829	0.063	95.39
43.12 glass interstitial to quartz pt 2	55.67	18.92	2.267	5.23	2.1	0.34	7.61	0.721	0.1154	0.105	3.8	0.062	96.94
43.13 glass interstitial to quartz	49.81	14.8	2.348	4.14	1.496	0.21	5.96	0.041	0.3116	0	20.08	0.03	99.22
AVERAGE	54.3	17.65	2.31	5.02	2.06	0.34	6.643	0.357	0.1423	0.049	8.236	0.051	97.18
STANDARD DEVIATION	4.01	2.473	0.04	0.796	0.54	0.14	0.861	0.342	0.1575	0.053	10.36	0.019	1.927

METALS

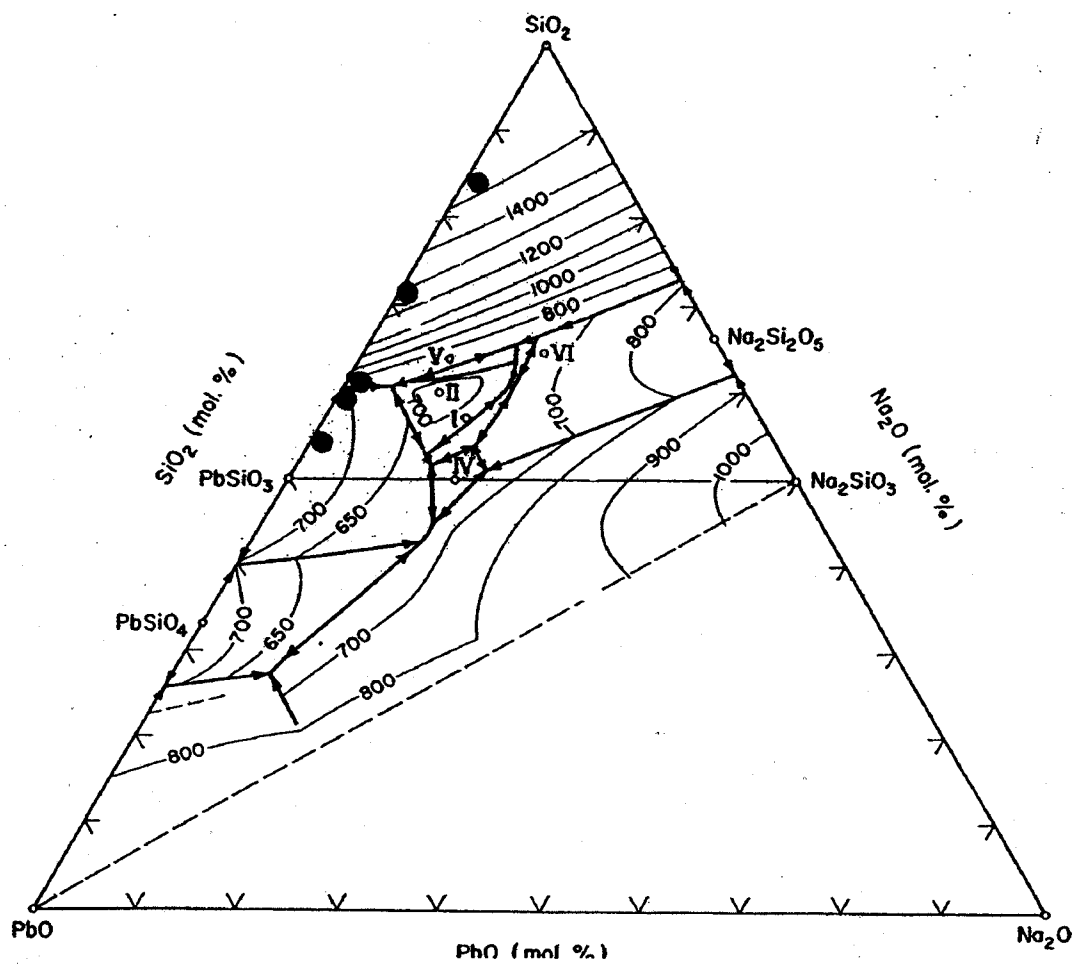
Analysis/Description		Analytical Routine (elements or oxides analyzed)									
		Cu	Sn	Sb	Pb	As	Fe	Ag	S	Total	
Sample #30		93.79	0	0.037	0.328	0	0	2.7058	0	96.86	
	#30, pt. 1.2 (dendritic copper)	92.57	3.32	0	0.281	0	0.04	0.1723	0.003	96.38	
	#30, pt. 2.2 (massive copper)	93.61	4.18	0.018	0.305	0.313	0.02	0.0308	0.007	98.48	
	#30, pt. 4 (bronze flecks)	94.18	0	0	0.918	0.359	0	0.7571	0.087	96.31	
	#30, pt. 3 (copper dendrites)										
Sample #32		Cu	Sn	Zn	Pb	As	Fe	Total			
	#32.1, massive copper	100.6	0.101	0	0.254	0	0.05	101.04			
Sample #34		Cu	Sn	Sb	Pb	As	Fe	Ag	S	Total	
	#34, pt. 4 (copper within tin corona)	95.73	0.043	0.004	0.282	0	0	0.2411	0.092	96.39	
	#34, pt. 1.3 (copper/lead prill)	91.58	0.599	0.793	2.128	0.855	0.01	0.0186	0.317	96.3	
	#34, pt. 2 (bronze prill)	78.76	15.71	0.184	0.32	0.99	0.05	0	0.749	96.77	
Sample #44		Cu	Sn	Zn	Pb	As	Fe	Total			
	#44.1, copper prill with lead inclusions	99.27	0.391	0	0.228	0.103	0	99.99			

PYROXENES

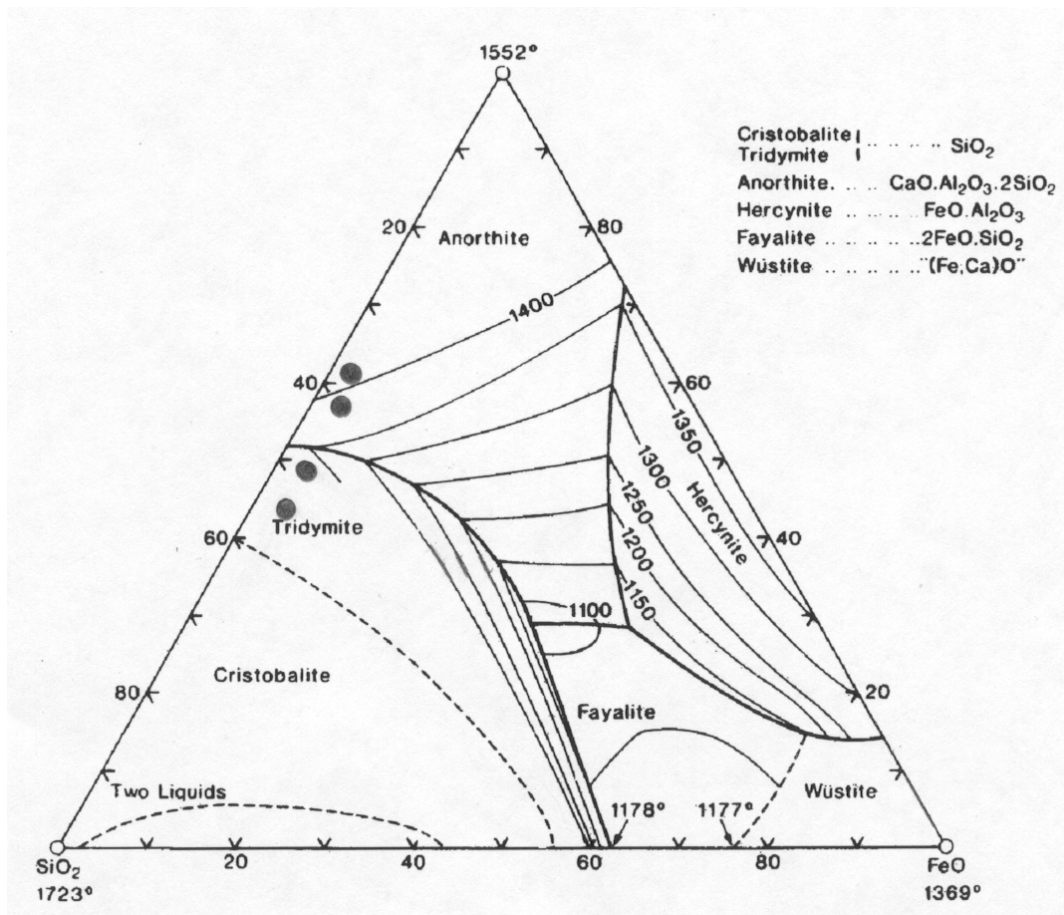
Analysis/Description		Analytical Routine (elements or oxides analyzed)										
		SiO2	TiO2	Al2O3	MgO	FeO	CaO	MnO	K2O	Na2O	Cr2O3	Total
Sample #29		60.48	0.421	6.04	11.56	2.463	17.7	2.3694	0.576	0.5346	0	102.1
	#29, pt. 1	54.1	0.109	0.244	16.17	1.978	25	2.264	0.342	0.0689	0	100.3
	#29, pt. 2	71.89	0.481	4.81	1.749	1.869	9.78	1.8394	1.657	0.343	0	94.42
	#29, pt. 3	52.13	0.322	0.393	16.67	2.569	24.9	1.9191	0.069	0.0711	0	99.05
	#29, pt. 4	51.5	0.157	0.253	16.53	2.532	24.4	1.7201	0.084	0.0439	0.183	97.4
	#29, pt. 5	46.91	1.673	6.19	2.011	14.55	14.7	4.07	3.47	0.1439	0.012	93.7
	#29, pt. 6	51.35	0	0.012	1.974	0.397	43.9	2.1332	0.075	0	0	99.84
Sample #41		SiO2	TiO2	Al2O3	MgO	FeO	CaO	MnO	K2O	Na2O	Cr2O3	Total
	#41, pt. 1	49.61	0.045	0.148	0.926	0.383	45.3	0.5187	0.01	0.0746	0	97.05
	#41, pt. 2	46.43	0.734	17.54	7.6	7.12	20.4	0.1171	0.067	0.1489	0.108	100.3
	#41, pt. 3	44.35	0.882	6.49	9.41	10.38	24.7	0.1079	0.015	0.0134	0.084	96.39

#41, pt. 4 47.79 0.119 20.93 0.259 1.112 2.02 0.0634 5.08 1.6387 0 79.01

Sample #43
#43, pt. 1 SiO2 TiO2 Al2O3 MgO FeO CaO MnO K2O Na2O Cr2O3 Total
50.76 0.039 0.042 0 0.03 47.8 0 0 0.0044 0.012 98.64

Appendix: PbO-SiO₂-Na₂O phase diagram

Points plotted for Samples #41 and #43

Appendix: FeO-SiO₂-anorthite phase diagram

Points plotted for Samples #25 and #29